PacificSPIN 2026

The 13th Circum-Pan-Pacific Symposium on High Energy Spin Physics

Jefferson Lab
Exploring the Nature of Matter

clas
CEBAF Large Acceptance Spectrometer

DVCS with & BEYOND CLAS12

- DVCS off free proton
- DVCS off bound proton in Deuterium
- Double-DVCS
  - μCLAS12
  - EIC
- And a bit more …

Adam HOBALLAH

IJCLab
Irène Joliot-Curie
Laboratoire de Physique des 2 Infinis

cnrs

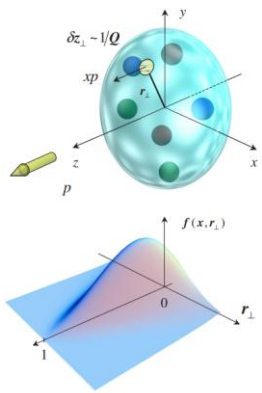
université PARIS-SACLAY

Generalized Parton Distributions - GPDs

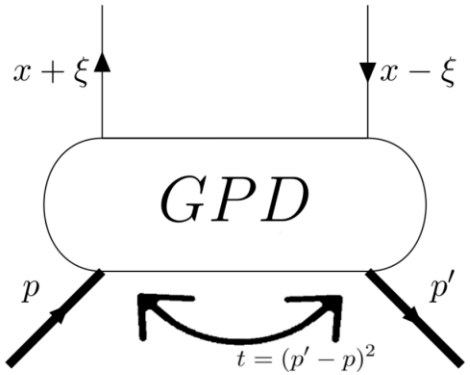
Belitsky, Radyushkin, Physics Reports, 2005

- Nucleon structure studies: QCD at low energies, a non-perturbative regime
  - Need structure functions to describe the nucleon

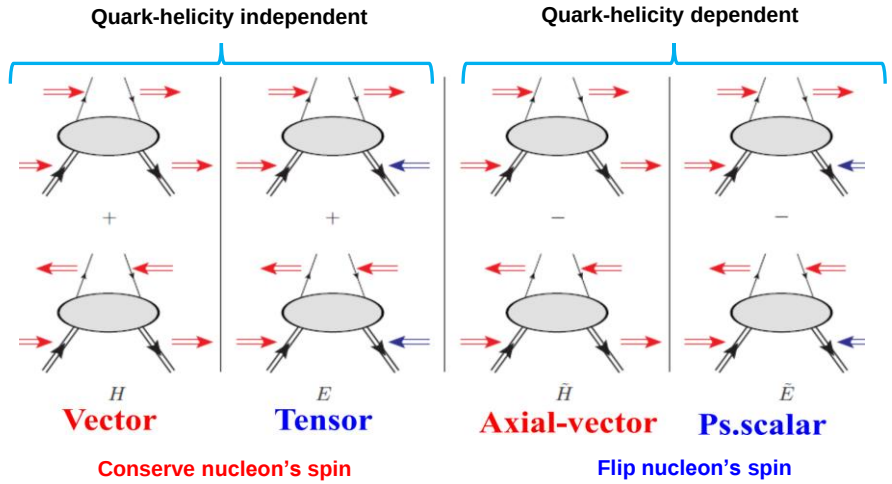
GPDs quantify correlations of transverse position and longitudinal momentum of partons in a hadron



- For the nucleon, there are 8 GPDs at leading-twist that describe the various combinations between nucleon/quark helicity states
- At leading order QCD, chiral-even (quark helicity is conserved), quark sector: 4 GPDs for each quark flavor $H, \tilde{H}, E$ and $\tilde{E}$
- GPDs can be accessed through exclusive leptoproduction reactions
- GPDs depend on x, ξ and t = (p' − p) ^{2}



Nucleon Polarization	Quark Polarization: Unpolarized (U)	Longitudinally Polarized (L)	Transversely Polarized (T)
U	H		$2\tilde{H}_T + E_T$
L		$\tilde{H}$	$\tilde{E}_T$
T	E	$\tilde{E}$	$H_T, \tilde{H}_T$



Properties of GPDs and Why they are important?

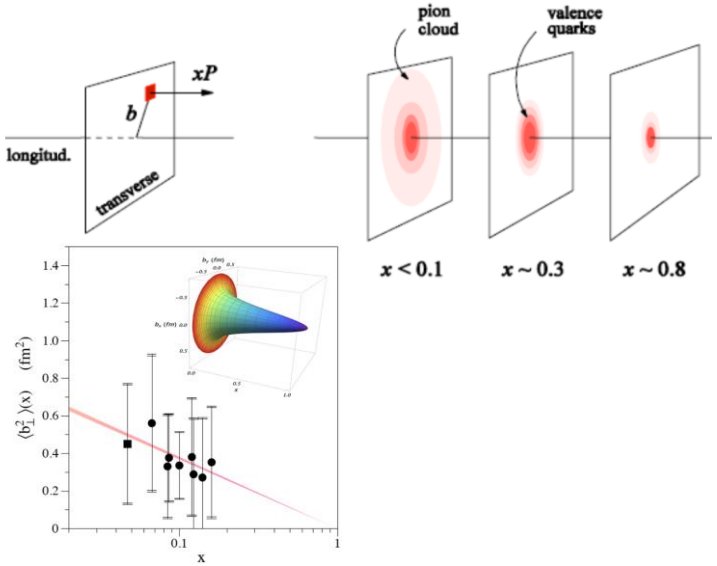
- GPDs are well-constrained functions: Fourier transforms of non-local, non-diagonal QCD operators
- They are universal: The same GPDs parametrize different processes: DVCS, DVMP, DDVCS, TCS

Nucleon tomography

M. Burkardt, PRD 62, 71503 (2000)

$$q(x,\mathrm{b}_\perp) = \int_0^\infty \frac{d^2\Delta_\perp}{(2\pi)^2} e^{i\Delta_\perp \mathrm{b}_\perp} H(x,0,-\Delta_\perp^2)$$

$$\Delta q(x,\mathrm{b}_\perp) = \int_0^\infty \frac{d^2\Delta_\perp}{(2\pi)^2} e^{i\Delta_\perp \mathrm{b}_\perp} \widetilde{H}(x,0,-\Delta_\perp^2)$$



R. Dupré, M. Guidal, M.Vanderhaeghen, PRD95, 011501 (2017)

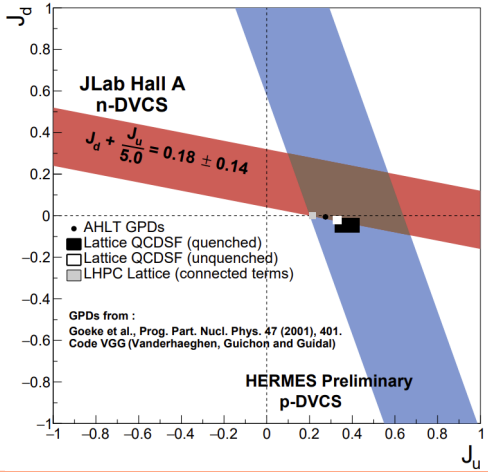
Quark angular momentum

X. Ji, Phy.Rev.Lett.78,610(1997)

$$\frac{1}{2}\int_{-1}^{1} x dx (H(x,\xi,t=0) + E(x,\xi,t=0)) = J = \frac{1}{2}\Delta\Sigma + \Delta L$$

Nucleon spin: $\frac{1}{2} = \frac{1}{2}\Delta\Sigma + \Delta L + \Delta G$

GPDs: quantify the contribution of orbital angular momentum of quarks to the nucleon spin

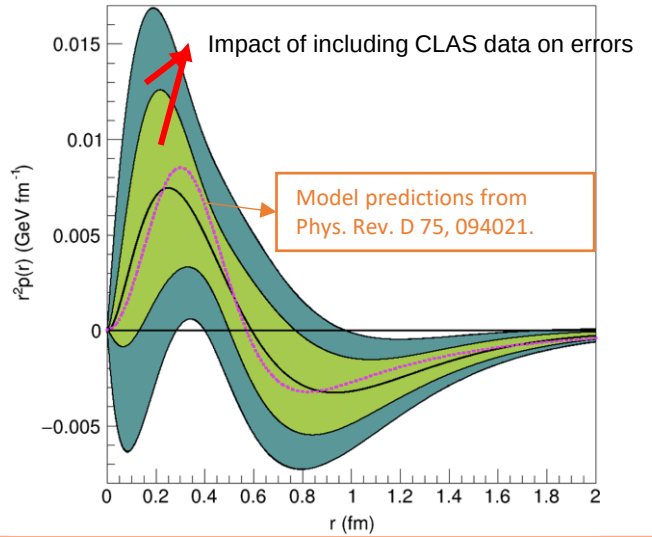


The pressure distribution inside proton

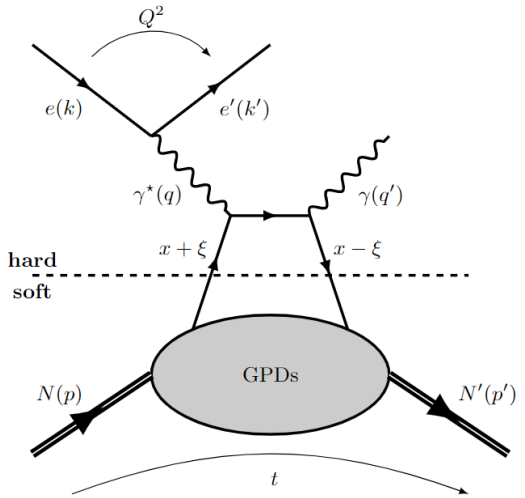
V. Burkert, L. Elouadrhiri, F.X. Girod, Nature 557, 396-399 (2018)

To be read in parallel with
Kumerički, K. *Nature* 570, E1–E2 (2019)
H.Dutrieux et al EPJC (2021) 81:300
Rev. Mod. Phys. 95, 041002 (2023)

- Gravitational form factor
  - $\int xH(x,\xi,t)dx = M_2(t) + \frac{4}{5}\xi^2 d_1(t)$
  - $d_1(t) \propto \int \frac{j_0(r\sqrt{-t})}{2t}\rho(r)d^3r$



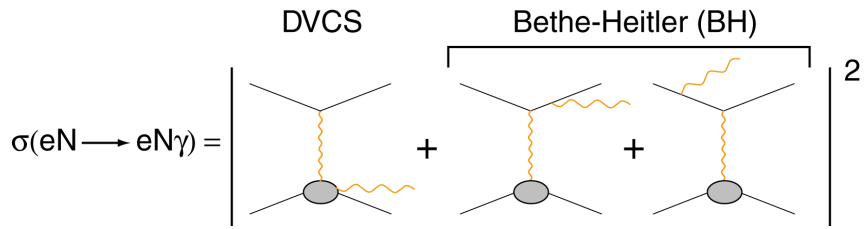
Deeply Virtual Compton Scattering of leptons off nucleons



- DVCS allows access to 4 complex GPDs-related quantities (only helicity-conserved terms are considered):
  - Compton Form Factors (x, ξ, t) (CFFs)

$$\mathcal{H} = \sum_q e_q^2 \left\{ i\,\pi\,[H^q(\xi,\xi,t) - H^q(-\xi,\xi,t)] + \mathcal{P}\int_{-1}^{1} dx H^q(x,\xi,t)\left[\frac{1}{\xi-x} - \frac{1}{\xi+x}\right] \right\}$$

- x cannot be accessed experimentally by DVCS: Models needed to map the x dependence



BH is purely electromagnetic and parametrised by FFs

- The DVCS-BH interference term (linear in CFFs)
  - Access the phase of the DVCS amplitude: isolate imaginary and real parts of CFFs.

➢ Experimentally measured observables: Access to a combinations of CFFs

➢ Separation of CFFs: measurement of several observables

➢ Proton or Neutron: different sensitivity to the CFFs (GPDs)

➢ Flavor separation of GPDs: need measurements on both nucleons

$$(H,E)_u(\xi,\xi,t) = \tfrac{9}{15}\left[4(H,E)_p(\xi,\xi,t) - (H,E)_n(\xi,\xi,t)\right]$$
$$(H,E)_d(\xi,\xi,t) = \tfrac{9}{15}\left[4(H,E)_n(\xi,\xi,t) - (H,E)_p(\xi,\xi,t)\right]$$

Deeply Virtual Compton Scattering: physics observables and their link to CFFs

Belitsky, Müller, Kirner, Nuc. Phys. B 629 (2002)

Polarized beam, unpolarized taget

$$\Delta\sigma_{LU} \sim \sin(\phi)\, \Im\{F_1 \boldsymbol{H} + \xi(F_1 + F_2)\widetilde{\boldsymbol{H}} - k\, F_2 \boldsymbol{E} + \ldots\}$$

Unpolarized beam, polarized target

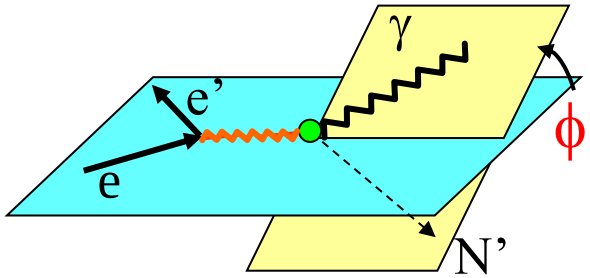
$$\Delta\sigma_{UL} \sim \sin(\phi)\, \Im\left\{F_1\, \widetilde{\boldsymbol{H}} + \xi(F_1 + F_2)\left(\boldsymbol{H} + \frac{x_b}{2}\boldsymbol{E}\right) - \xi k\, F_2 \widetilde{\boldsymbol{E}}\right\}$$

polarized beam, longitudinal polarized target

$$\Delta\sigma_{LL} \sim (A + B\cos(\phi))\, \Re\{F_1\, \widetilde{\boldsymbol{H}} + \xi(F_1 + F_2)\left(\boldsymbol{H} + \frac{x_b}{2}\boldsymbol{E}\right) + \ldots\}$$

unpolarized beam, transverse polarized target

$$\Delta\sigma_{UT} \sim \cos(\phi)\, \sin(\phi_s - \phi)\, \Im\{k(F_2\, \boldsymbol{H} - F_1 \boldsymbol{E}) + \ldots\}$$



Different contributions from F_1 and F_2 for the different nucleons

Observable	Proton	Neutron
$\Delta\sigma_{LU}$	$\Im\{\boldsymbol{H_p}, \widetilde{H}_p, E_p\}$	$\Im\{H_n, \widetilde{H}_n, \boldsymbol{E_n}\}$
$\Delta\sigma_{UL}$	$\Im\{\boldsymbol{H_p}, \widetilde{\boldsymbol{H}}_{\boldsymbol{p}}\}$	$\Im\{\boldsymbol{H_n}, E_n\}$
$\Delta\sigma_{LL}$	$\Re\{\boldsymbol{H_p}, \widetilde{\boldsymbol{H}}_{\boldsymbol{p}}\}$	$\Re\{\boldsymbol{H_n}, E_n\}$
$\Delta\sigma_{UT}$	$\Im\{\boldsymbol{H_p}, \boldsymbol{E_p}\}$	$\Im\{\boldsymbol{H_n}\}$

e.g. (in experiment):

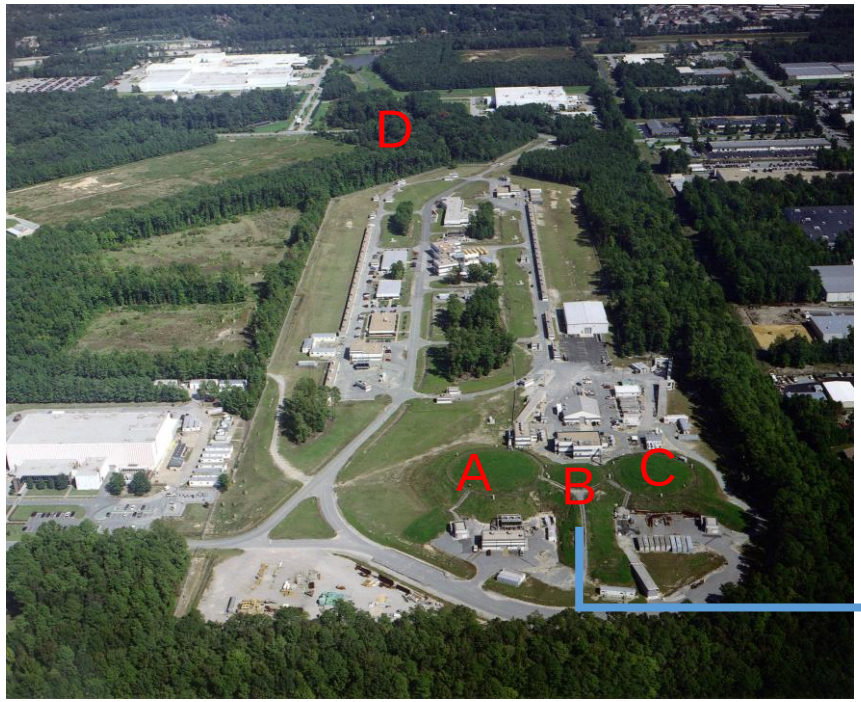
$$\Delta\sigma_{LU} = \frac{1}{Pol.} \times \frac{N^+ - N^-}{N^+ + N^-} \sim \frac{a_1 \sin(\phi)}{1 + a_2 \cos(\phi)}$$

Computed as a function of the angle ϕ

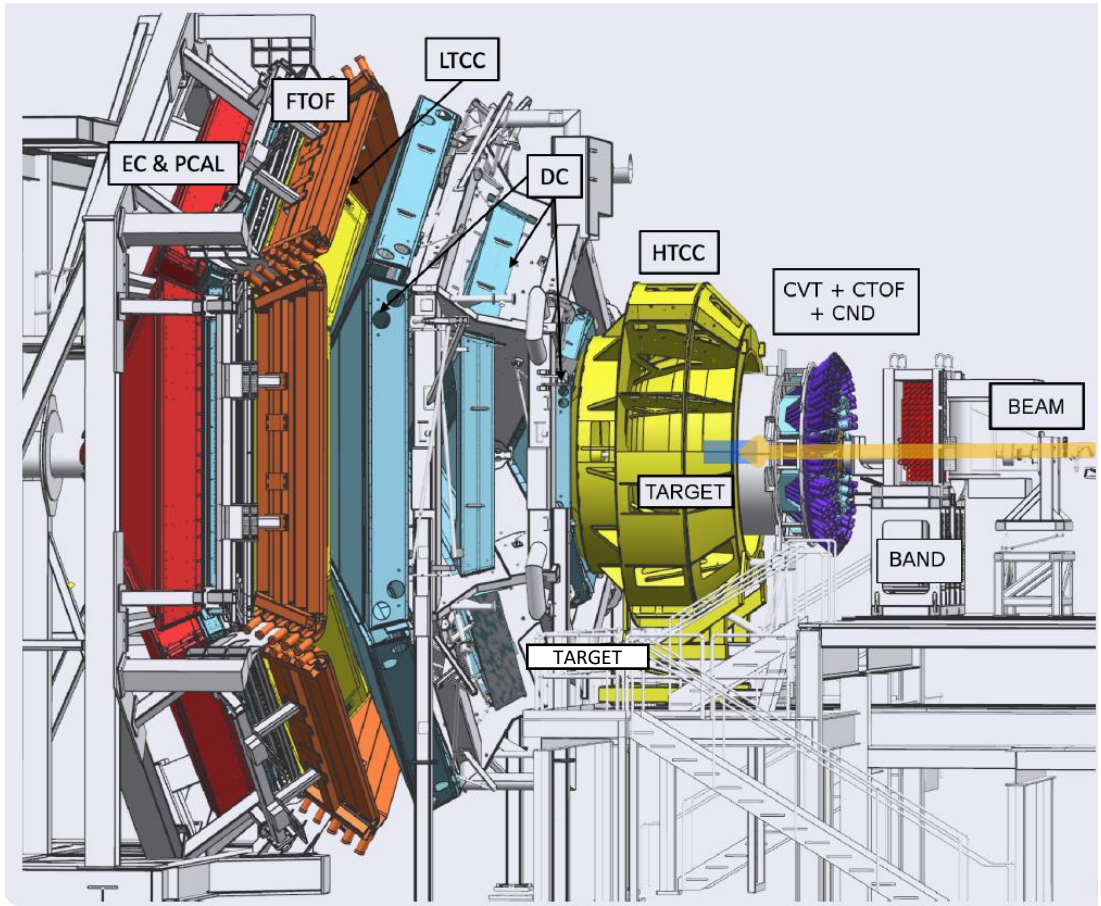
The CEBAF and CLAS at Jefferson Laboratory

Continuos Electron Beam Accelerator Facility

- Up to 12 GeV electrons
- Two anti-parallel linacs, with recirculating arcs on both ends
- 4 experimental halls



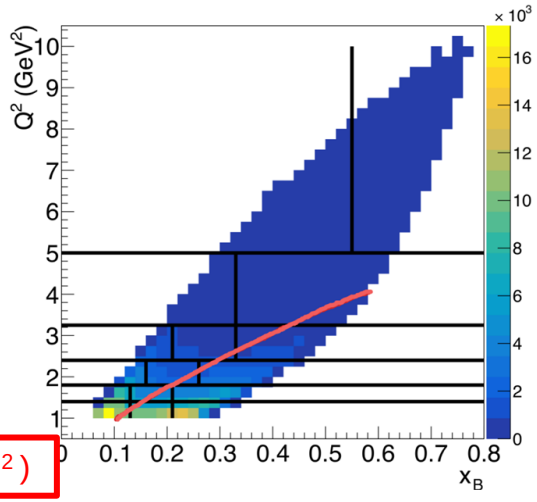
CLAS12



DVCS off proton BSA

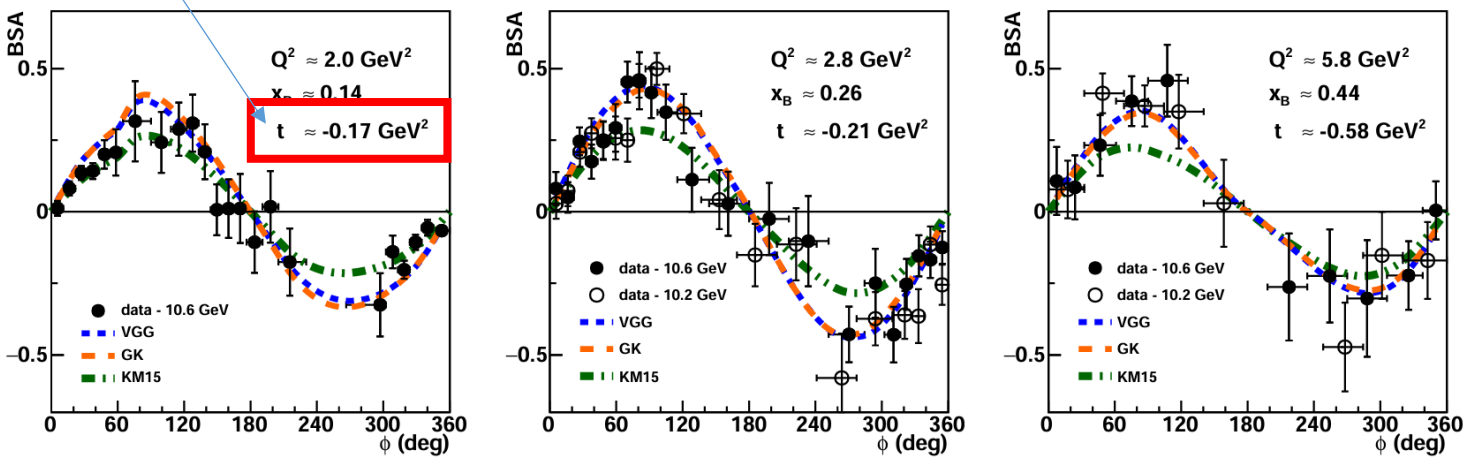
Phys. Rev. Lett. 130 (21) 211902 (2023)

- **Extended kinematical coverage wrt CLAS**
  - Polarised beam (86%) with energy 10.6 GeV
  - Unpolarised LH2 target
  - 64 (Q^2, x_b, t) kinematical bins



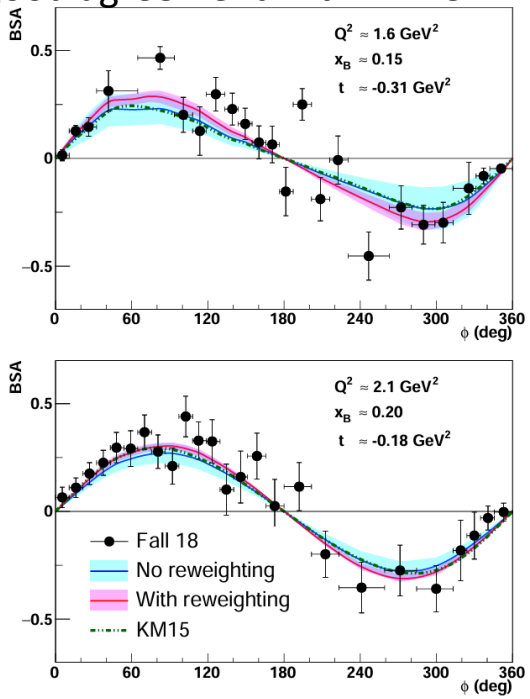
Kumericki, Kresimir and M uller, Dieter, EPJ Web of Conferences 112, 01012 (2016).
S. V. Goloskokov and P. Kroll, EPJC 65, 10.1140 (2009)
M. Vanderhaeghen, P. A. Guichon, and M. Guidal, Phys.Rev. D60, 094017 (1999)

Smallest t value reached with this approach (bin edge 0.12 GeV^2)



H. Moutarde, P. Sznajder, and J. Wagner, EPJC 79, 614 (2019)

- Deriving the mean and standard deviation of a 100 ANN-predictions produced by a global fit (PARTONS)
- The new data are shown to be in good agreement with KM15



DVCS Beam Spin Asymmetry at small t: update Credits: Sebastian Alvarado

Access to Gravitational Form Factors.

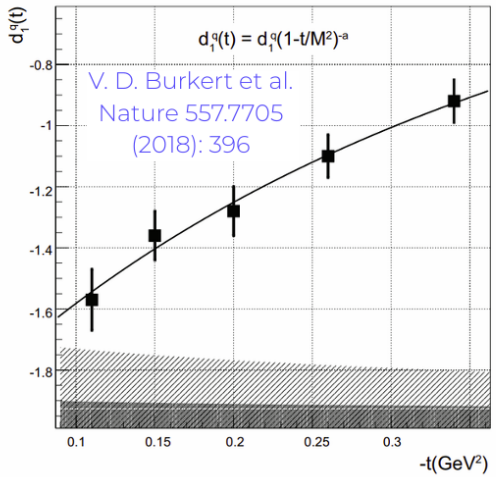
H. Dutrieux *et al.*, Eur. Phys. J. C 81 (2021) 4, 300

The proton internal pressure distribution can be accessed through Δ(t)

$$\Delta(t) = \mathfrak{Re}[\mathcal{H}(\xi,t)] - \frac{1}{\pi}\int_0^1 d\xi' \, \mathfrak{Im}[\mathcal{H}(\xi',t)] \left(\frac{1}{\xi-\xi'} - \frac{1}{\xi+\xi'}\right)$$

Sensitive to the extrapolation to t=0

$$\Delta(t) \equiv \Delta(t=0) f_1(t)$$



$$ep \to e'p'\gamma$$

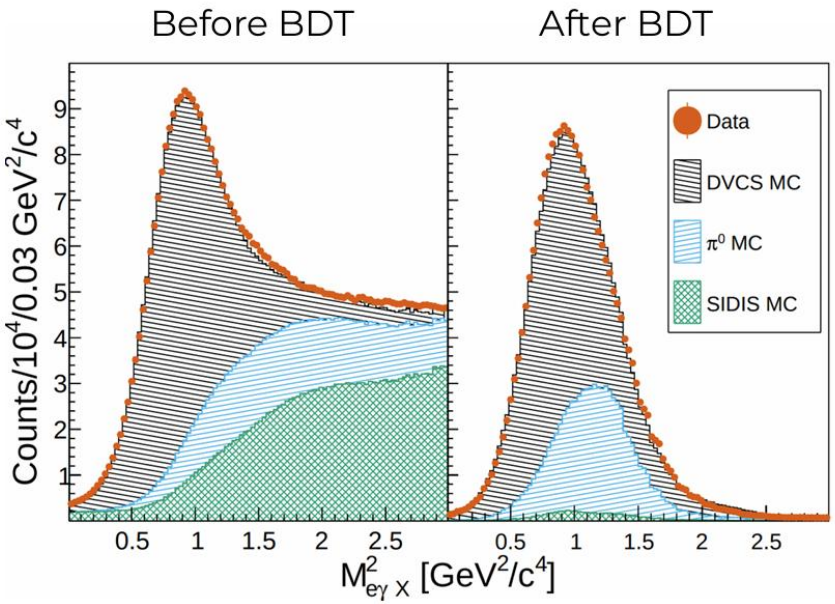
$$t(p' = 0.35) = 0.1225 \text{ GeV}^2$$

- In the CLAS12 context, detecting the proton ensures exclusivity of the reaction, but limits the |t| coverage
- Not requiring proton detection: |t| coverage down to |t|=0.022 GeV²
  - precise t=0 extrapolation
- However there is less information to constrain event selection hence increased background
  - Use of ML algorithms for channel selection (Boosted Decision Trees, **BDT**)

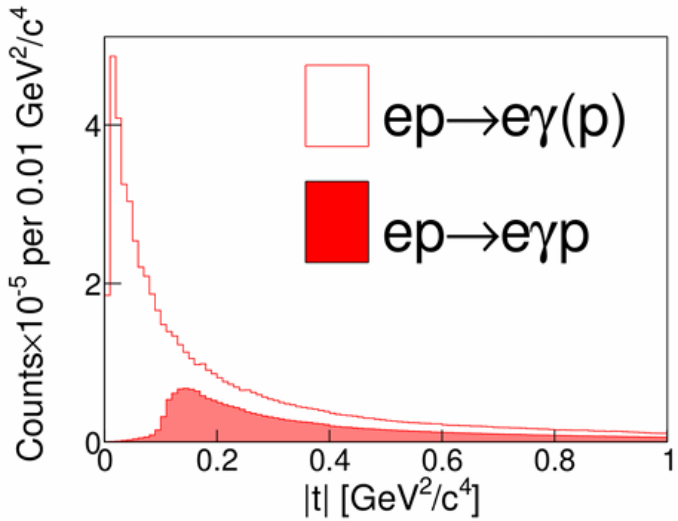
DVCS Beam Spin Asymmetry at small t: update Credits: Sebastian Alvarado

Missing proton mass distribution

$M_{e\gamma X}^2 = (e + p - e' - \gamma)^2$



Without requiring proton detection, there is contamination from **inclusive** π^0 production from SIDIS



By not detecting the proton

- Small |t| access is granted
  - Down to 0.02 GeV²
- Boost in statistics

Irreducible background from partially reconstructed π^0 decays is subtracted using simulations

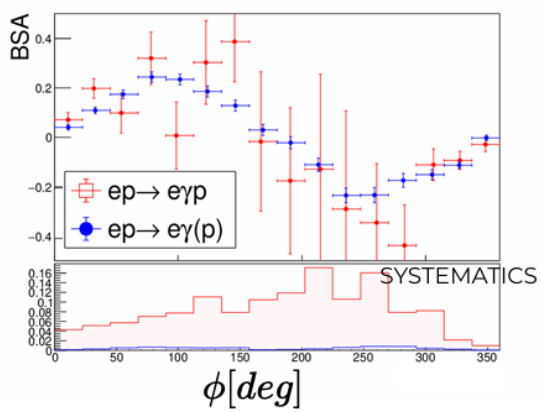
DVCS Beam Spin Asymmetry at small t: update Credits: Sebastian Alvarado

- The results constraint both the Im[CFF] and Re[CFF]
- Results are in reasonable agreement with the KM15 model
- Smaller systematic error than when requiring the detection of the proton
  - Proton related systematic errors are discarded

The smaller the t, the better the interpretation in terms of GPDs

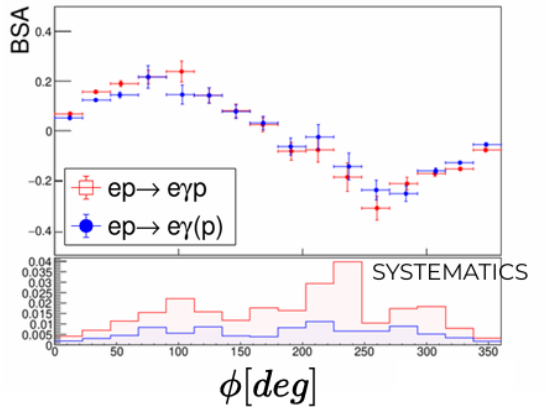
$2.4 < Q^2[\mathrm{GeV}^2] < 3.25, 0.17 < x_B < 0.27$

$0.07 < -t[\mathrm{GeV}^2] < 0.12$



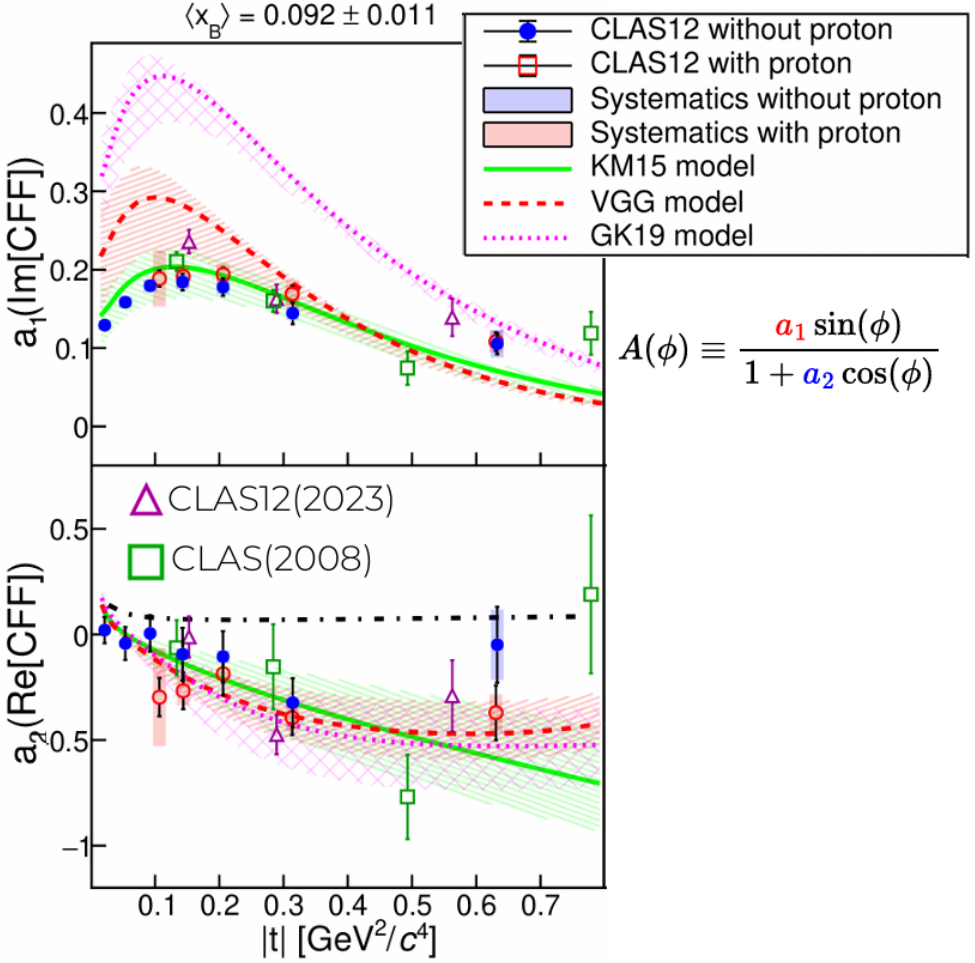
$1.6 < Q^2[\mathrm{GeV}^2] < 2.4, 0.12 < x_B < 0.17$

$0.25 < -t[\mathrm{GeV}^2] < 0.4$



$\langle Q^2 \rangle = 1.246 \pm 0.108\ \mathrm{GeV}^2/c^4$

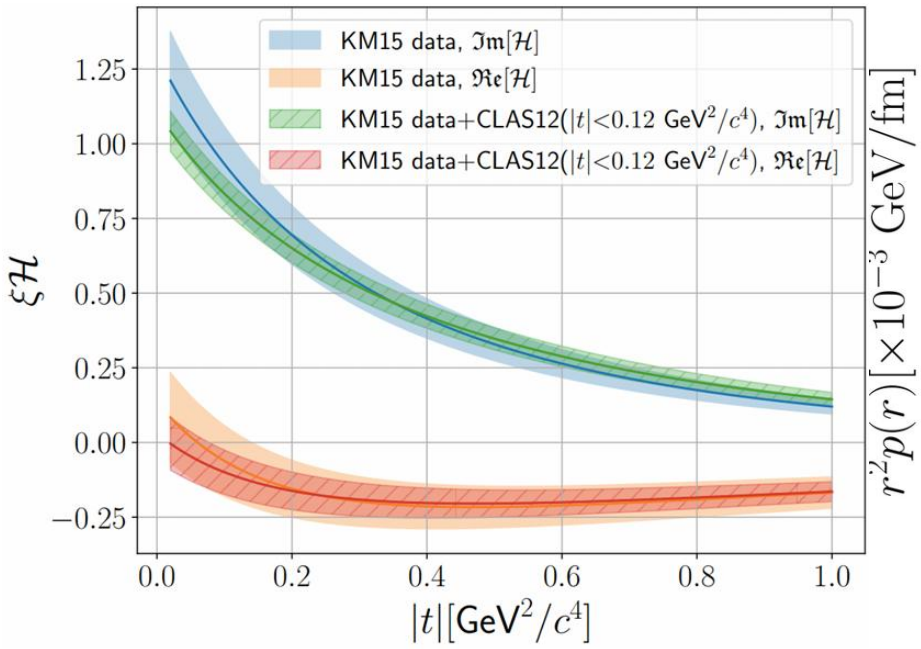
$\langle x_B \rangle = 0.092 \pm 0.011$

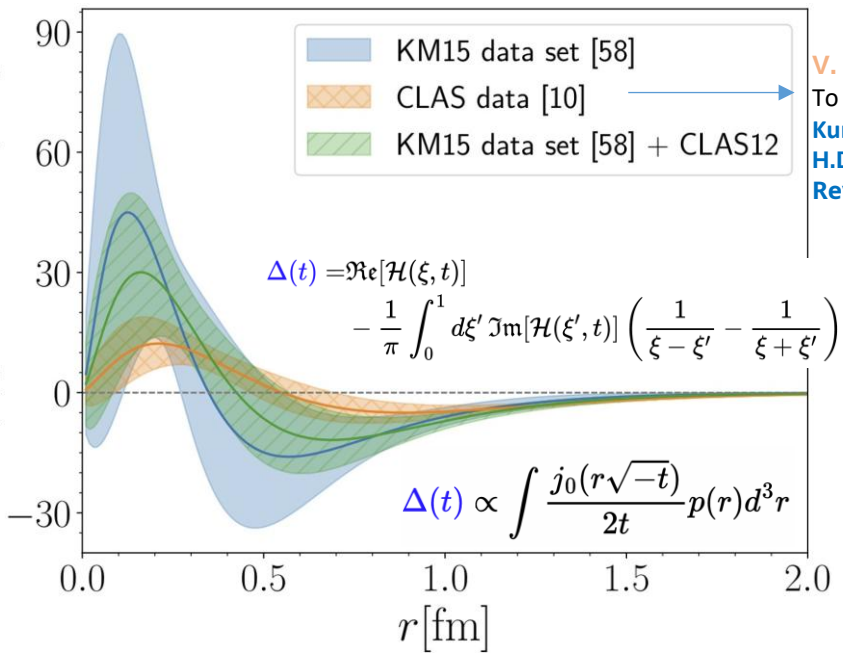


$$A(\phi) \equiv \frac{a_1 \sin(\phi)}{1 + a_2 \cos(\phi)}$$

DVCS Beam Spin Asymmetry at small t: update Credits: Sebastian Alvarado

K. Kumerički and D. Müller. Nucl. Phys. B 841, 1–58 (2010)





V. Burkert et al. Nature 557.7705 (2018)
To be read in parallel with
Kumerički, K. *Nature* 570, E1–E2 (2019)
H.Dutrieux et al EPJC (2021) 81:300
Rev. Mod. Phys. 95, 041002 (2023)

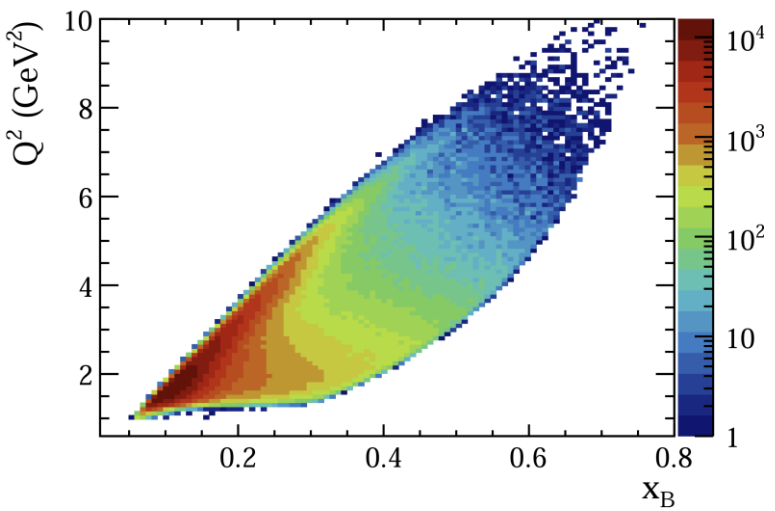
$$\Delta(t) \equiv \frac{C}{\left(1-\frac{t}{M^2}\right)^3}$$

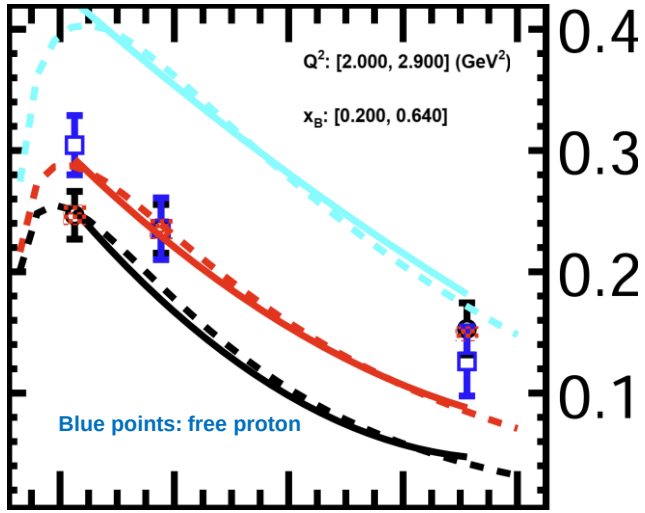
- Global fit of DVCS measurements to the KM15 parametrization
- Improved precision on CFF extraction
- Improved model-dependent proton internal pressure extraction
  - Tripole model for the subtraction constant was assumed.

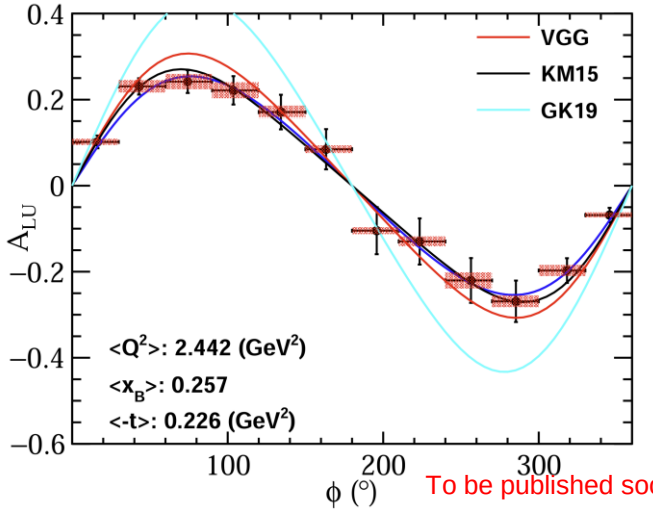
pDVCS BSA and t-profile of the $\sin(\phi)$ moment

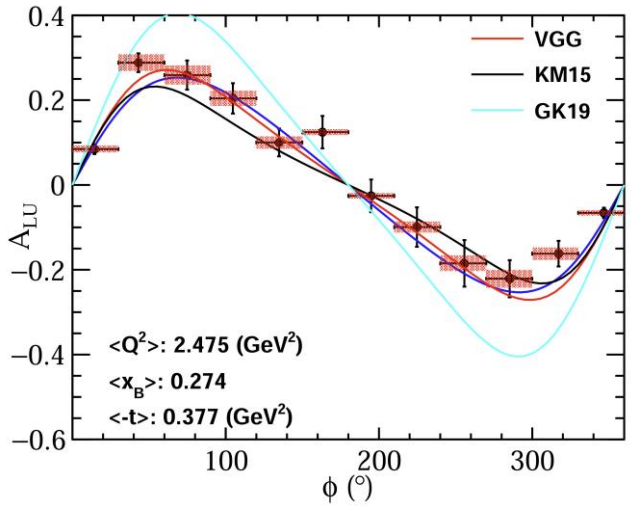
- Incoherent pDVCS on deuteron
  - Quantify medium effects on GPDs: Comparison with BSA from free proton
    - Clearly, medium effects in deuterium are negligible (as expected)
- More to understand with results from data taken on nuclear targets at CLAS12
  - Currenty being analyzed

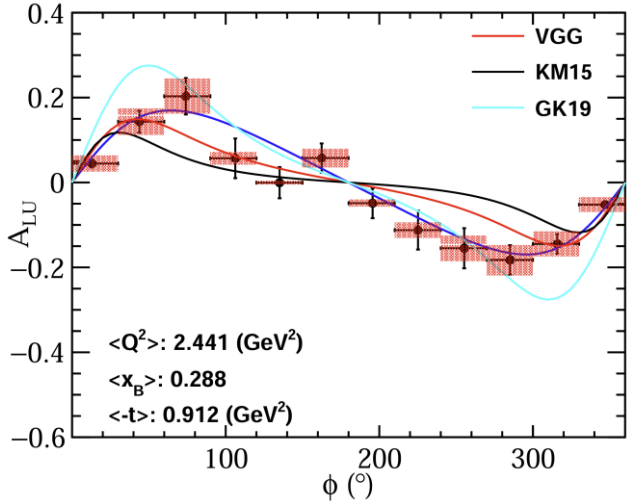
$$f = \frac{A_{LU}\,\sin(\phi)}{1 + b\,\cos(\phi)}$$











To be published soon.

Double DVCS: better understand the nucleon structure

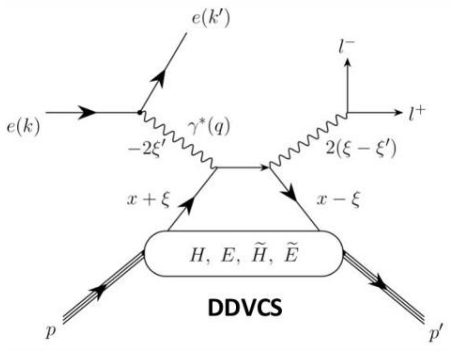
- DVCS is limited to x=+-ξ — Check: Extracting GPDs from data: status and perspectives
  - Limits available data to constrain the extraction
- GPDs extraction from CFF is not unique
  - Inverse problem: several class of functions that can be used to make the extraction.

$$\mathcal{H} = \sum_q e_q^2 \left\{ i\,\pi\,[H^q(\xi,\xi,t) - H^q(-\xi,\xi,t)] \; + \; \mathcal{P}\int_{-1}^{1} dx H^q(x,\xi,t)\left[\frac{1}{\xi-x} - \frac{1}{\xi+x}\right] \right\}$$

- With this problematic appear **Shadow GPDs (SGPD)**
  - **GPD with null CFF and null forward limit**
  - Can be added to any solution without altering data

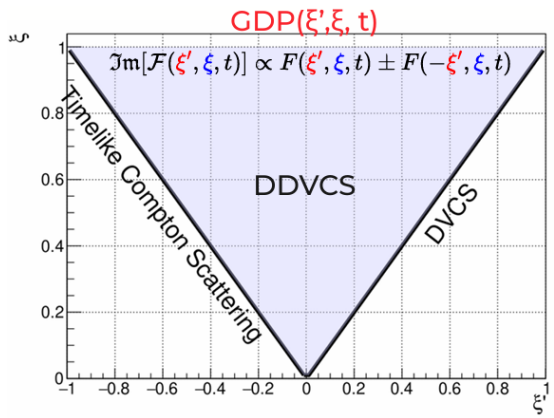
Are they just a mathematical construct?

- Double-DVCS: use virtuality to make the full scan



$$\xi = -\xi' \frac{Q^2 + Q'^2}{Q^2 - Q'^2 + t/2}$$

$$\xi' = x_B \frac{Q^2 - Q'^2 + t/2}{(2 - x_B)\,Q^2 - x_B\,(Q'^2 - t)}$$



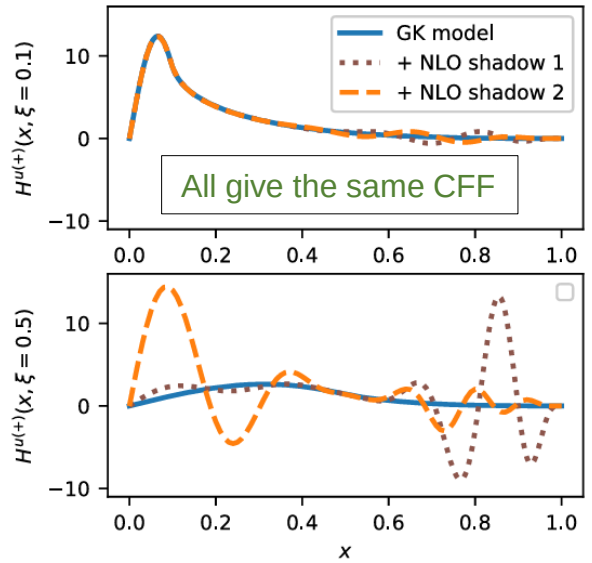
PHYSICAL REVIEW D **103,** 114019 (2021)

Deconvolution problem of deeply virtual Compton scattering

V. Bertone,[1,*] H. Dutrieux,[1,†] C. Mezrag,[1,‡] H. Moutarde,[1,§] and P. Sznajder[2,‖]
[1]*IRFU, CEA, Université Paris-Saclay, F-91191 Gif-sur-Yvette, France*
[2]*National Centre for Nuclear Research (NCBJ), Pasteura 7, 02-093 Warsaw, Poland*

(Received 16 April 2021; accepted 20 May 2021; published 22 June 2021)

Generalized parton distributions are instrumental to study both the three-dimensional structure and the energy-momentum tensor of the nucleon, and motivate numerous experimental programs involving hard exclusive measurements. Based on a next-to-leading order analysis and a careful study of evolution effects, we exhibit nontrivial generalized parton distributions with arbitrarily small imprints on deeply virtual Compton scattering observables. This means that in practice the reconstruction of generalized parton distributions from measurements, known as the deconvolution problem, does not possess a unique solution for this channel. In this paper we discuss the consequences on the extraction of generalized parton distributions from data and advocate for a multichannel analysis.



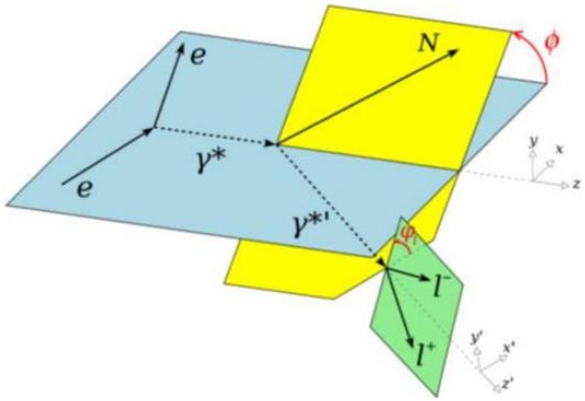
Double DVCS: μCLAS12

S. Stepanyan et al., LOI12-16- 004 (2016)
J.S. Alvarado et al. Eur. Phys. J. A 62, 157 (2026).

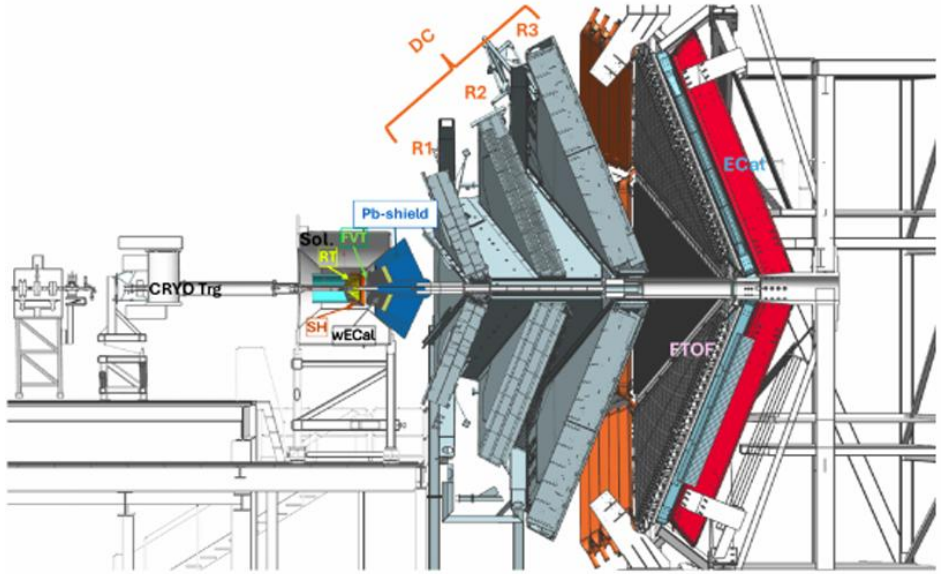
- Proposed in 2003: never measure. Cross section 3 orders of magnitude smaller than that of DVCS
- Require a muon-pair in the final state (even smaller cross section)
  - design of muon detectors **(avoid electron antisymmetrization)** and a high luminosity upgrade **(need $\mathcal{L} \geq 10^{37}$ cm^{-2}s^{-1})**
- **Measure BSA (integrate over lepton decay angles)**
  - Scan in both **timelike** (Q2 < Q'2) **and spacelike** (Q2 > Q'2) regions
  - Sign change of BSA: test of factorization

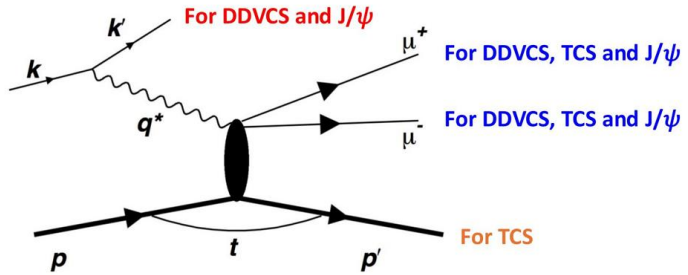
$$\Delta\sigma_{LU} \propto \mathrm{Im}[\boldsymbol{F_1\mathcal{H}(\xi',\xi,t)} + \xi'(F_1+F_2)\tilde{\mathcal{H}}(\xi',\xi,t) - \frac{t}{4M^2}F_2\mathcal{E}(\xi',\xi,t)]\sin\phi$$

- Measure muon-Charge Asymmetry (μCA) (more next slides)



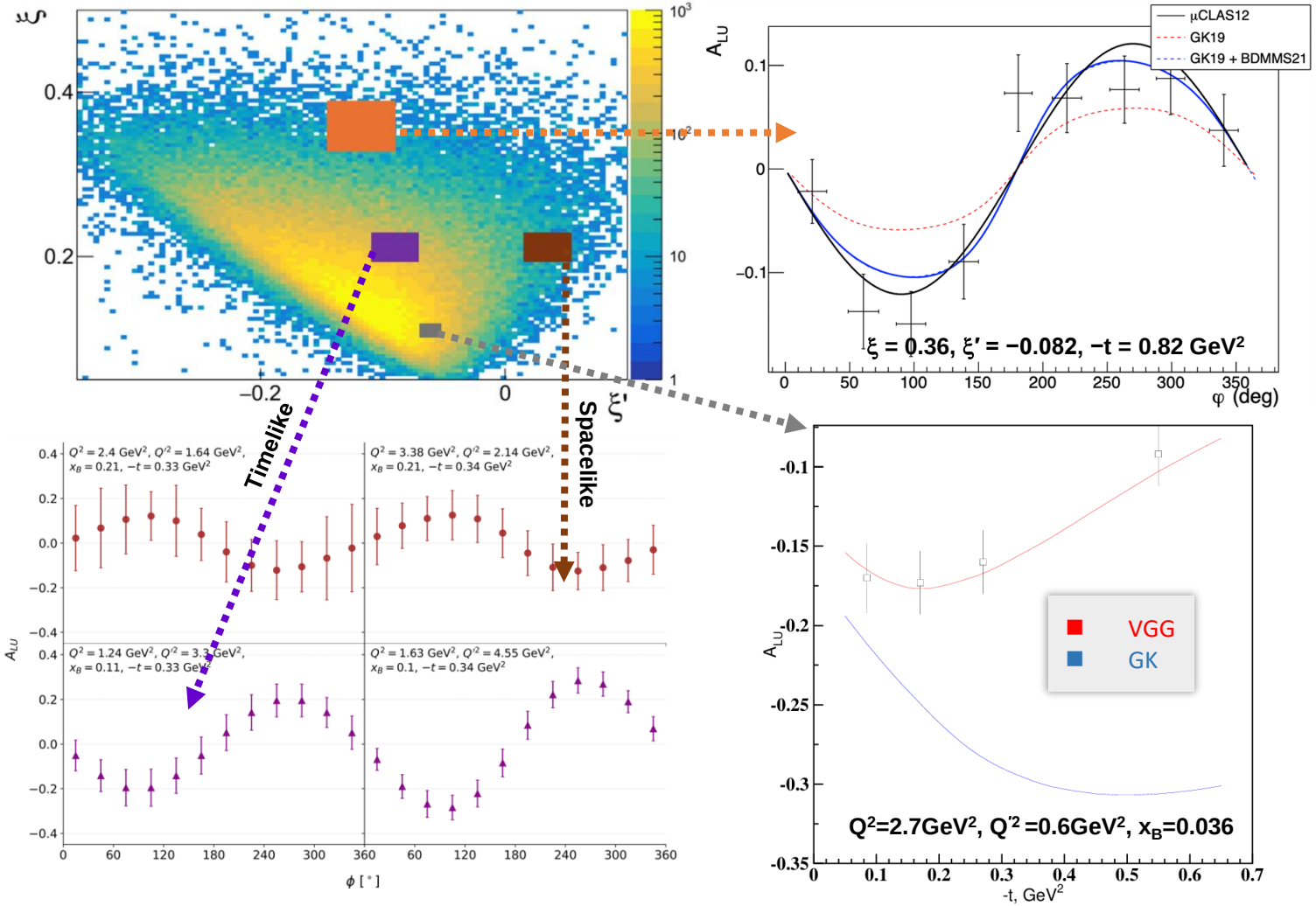
Phys. Rev. Lett. 90, 012001 (2003); Phys. Rev. Lett. 90, 022001 (2003)





Double DVCS: μCLAS12 projections

J. S. Alvarado, M.H., and E. Voutier, . PRC, 111 065205 (2025).
J.S. Alvarado,...,...,... M.H.et al. Eur. Phys. J. A 62, 157 (2026).



- Kinematic regions where it is possible to put limits on SGPD models.
  - 13.6% accuracy
  - Separated at >3 S.D.
- Full separation of SGPD effects will remain unattainable in certain regions of the accessible phase space and for some classes of SGPDs
  - Require more statistics (100 days is not enough)
- Significant model sensitivity
  - Strong constraints on GPD models
- Possibility to clrearly observe the BSA sign change
  - Test of factorization

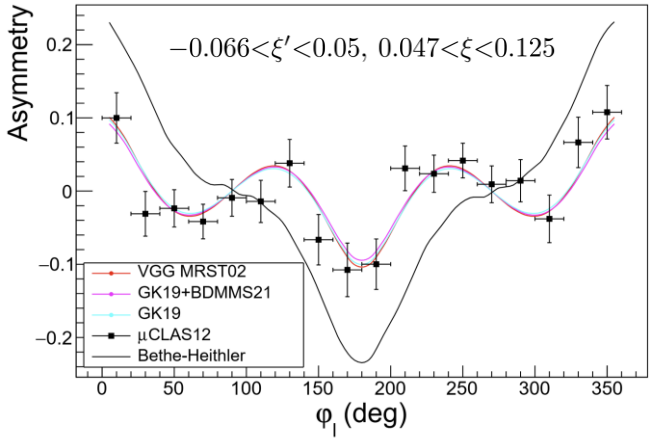
Double DVCS: **μCLAS12** μCA projections

- Measure muon-Charge Asymmetry
- Defined for muons in their center of mass frame: similar to Forward-Backward asymmetry of TCS
  - Redefined as a charge asymmetry over the lepton pair particles (emitted in opposite directions)
  - Modulation diluted with BH contribution (requires good control of systematics)
  - And with detector acceptance effects...
- *Access the same CFF combination of a Beam Charge Asymmetry*

$$A_{UU}^{\mu^\pm}(\varphi_\mu) = \frac{d^5\Sigma_{UU}(\varphi_{\mu^-}) - d^5\Sigma_{UU}(\varphi_{\mu^+})}{d^5\Sigma_{UU}(\varphi_{\mu^-}) + d^5\Sigma_{UU}(\varphi_{\mu^+})}$$

$$A_{UU}^{\mu^\pm}(\varphi_\mu) = \frac{d^5\Sigma_{BH_{12}} + d^5\Sigma_{\mathcal{I}_2}}{d^5\Sigma_{BH_1} + d^5\Sigma_{BH_2} + d^5\Sigma_{DDVCS} + d^5\Sigma_{\mathcal{I}_1}}$$

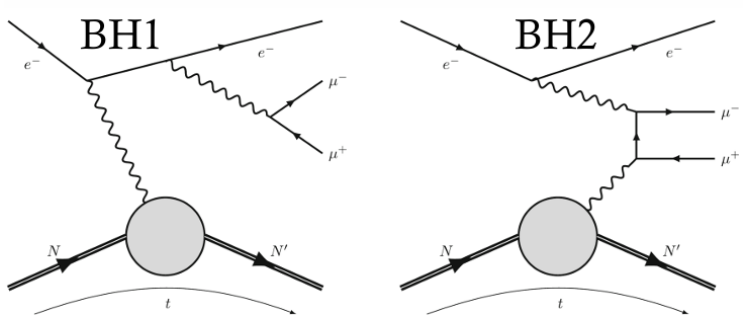
$$d^5\Sigma_{\mathcal{I}_2} \propto \mathfrak{Re}\left[\frac{\xi'}{\xi}\left(F_1\mathcal{H} - \frac{t}{4M_N^2}F_2\mathcal{E}\right) + \xi(F_1+F_2)\tilde{\mathcal{H}}\right]$$



(b) $-0.48<t/\mathrm{GeV}^2<-0.24$

- We demonstrate the possiblity to measure this observable in parallel to BSA measurements

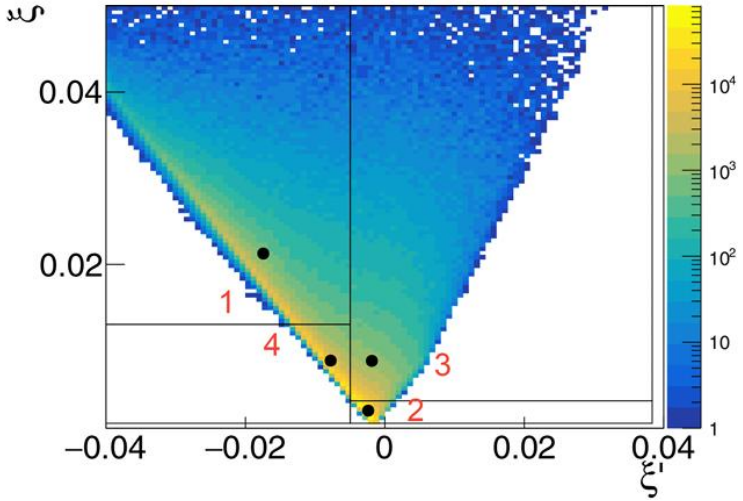
Article draft in preparation

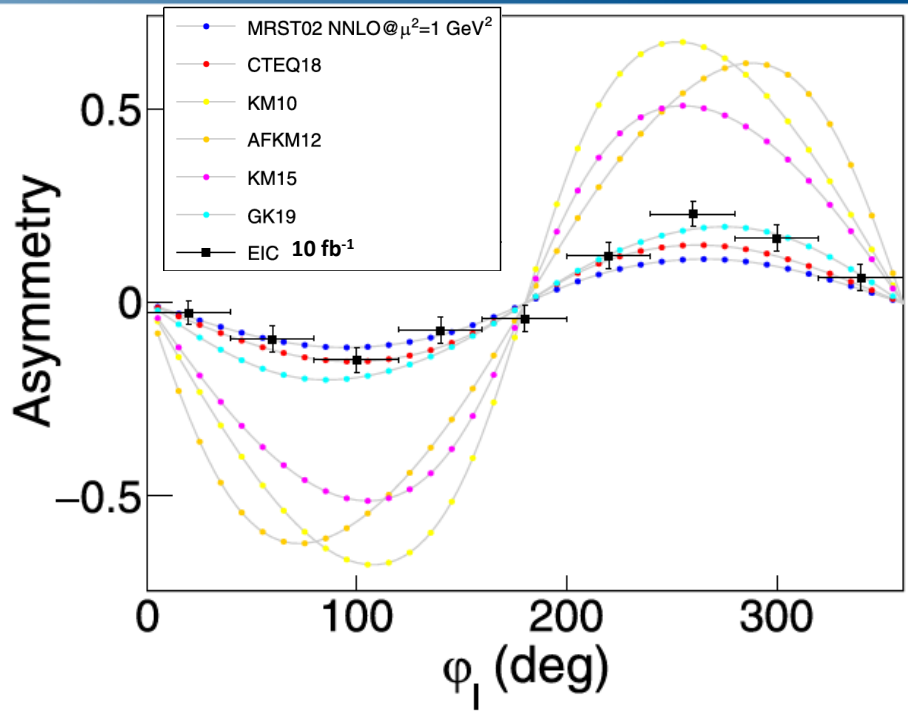


Double DVCS: and at EIC….

J. S. Alvarado, M.H., and E. Voutier, . PRC, 111 065205 (2025).

- EIC kinematics: W~140 GeV leads to {x , ξ', ξ} → 0
- Highly suppressed target-polarized and beam charge observables
  - Very small amplitudes (given existing model predictions)
- Possibility to access BSA dominated by CFF H
  - Measurable after the early science phase
- On the theory side:
  - Missing sea quark and gluon contributions
  - Vanishing valence contributions



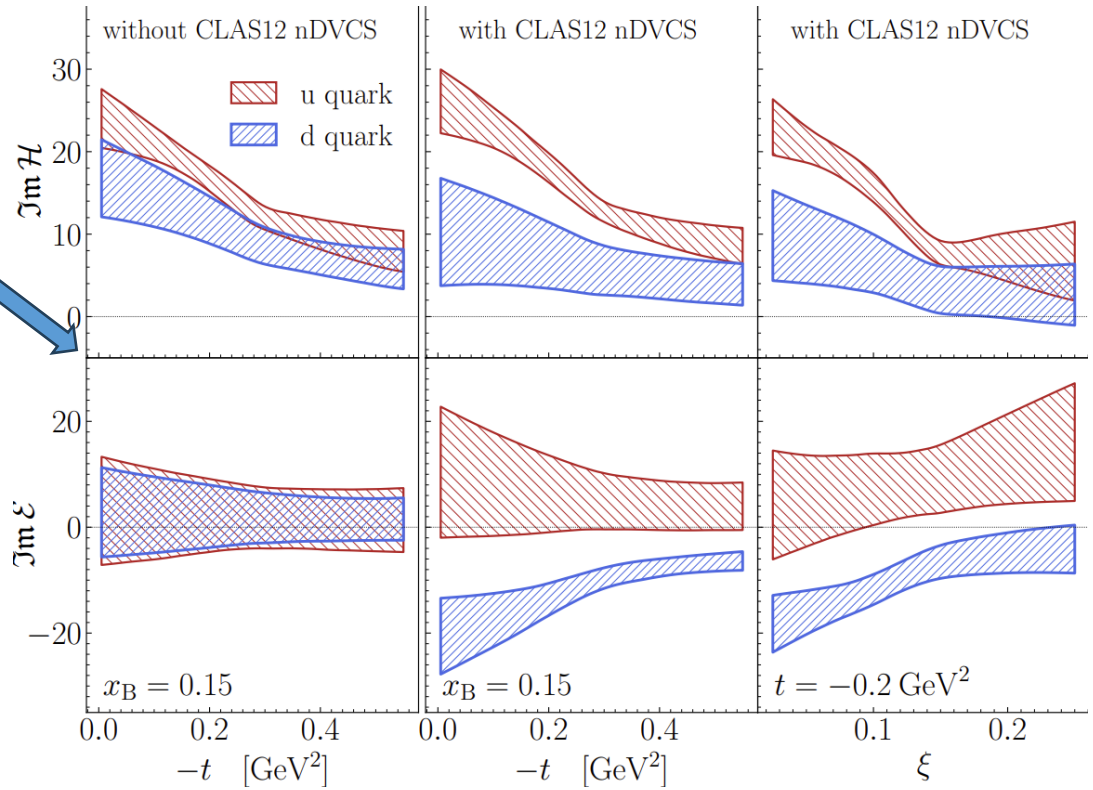


(b) Bin 2: $\xi' > -0.005$ and $\xi < 0.00417$.

- The GPD E is essential for the Ji sum rule

$$\frac{1}{2}\int_{-1}^{1} x dx (H(x,\xi,t=0)+E(x,\xi,t=0)) = J = \frac{1}{2}\Delta\Sigma + \Delta L$$

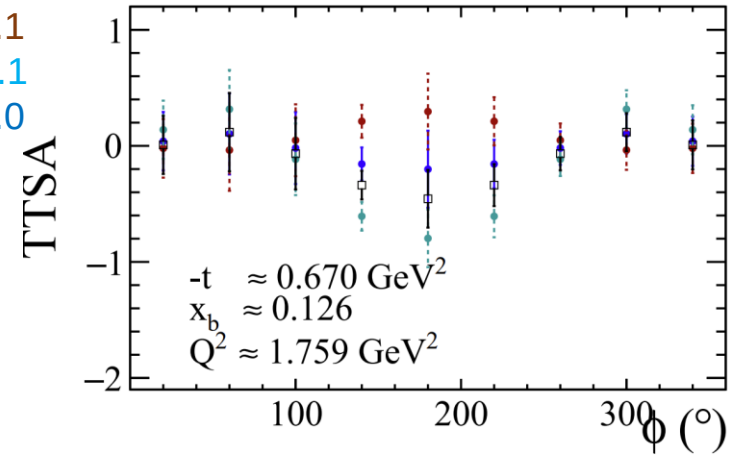
- **nDVCS BSA constrains E**
- Global fits of CFF using neural networks (model-independent)
  - K. Kumericki et al., JHEP 07, 073531 (2011); M. Cuic, K. Kumericki, et al., Phys. Rev. Lett. 533 125, 232005 (2020)).
- Data used:
  - CLAS6 and HERMES pDVCS observables
  - CLAS12 pDVCS BSA and nDVCS BSA
- Same extraction method applied to nDVCS Hall-A data: only separation for ImH

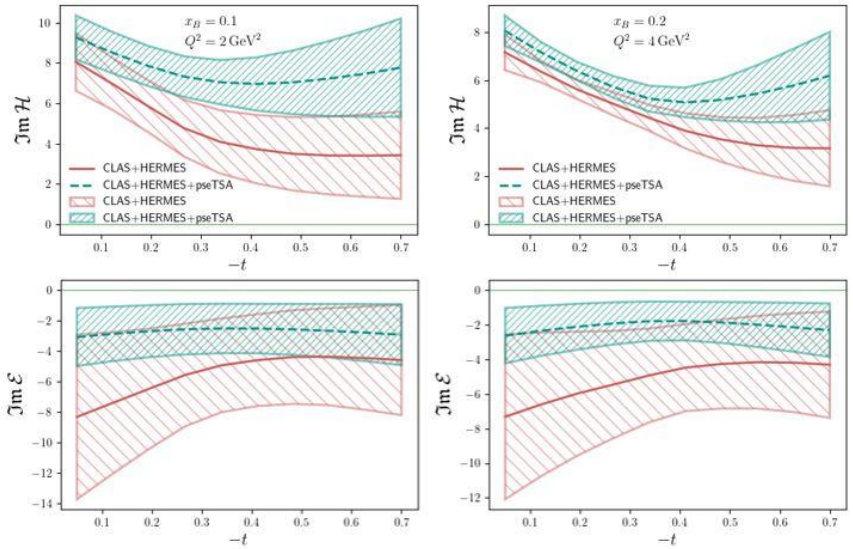


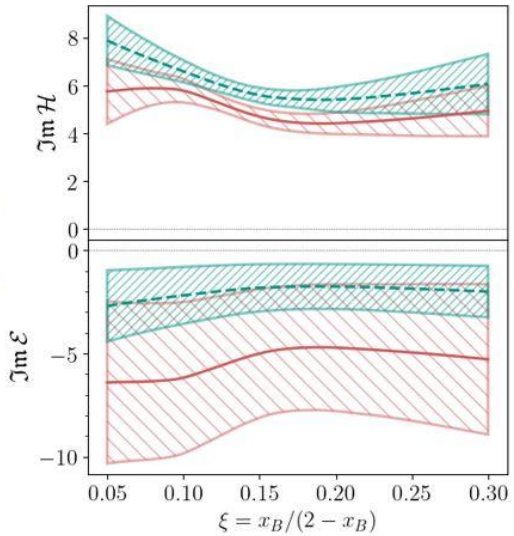
Back to DVCS: and the GPD E from the proton?

- **Transverse polarized proton target**
  - $\Delta\sigma_{UT} \sim \cos(\phi)\,\sin(\phi_s - \phi)\,\Im\{k(F_2\,\boldsymbol{H} - F_1\boldsymbol{E}) + \ \ldots\}$
- Experimental proposal submitted to Jlab PAC
- Experiments are forseen to run in ~2028
- High impact expexted on the extraction of the GPD E

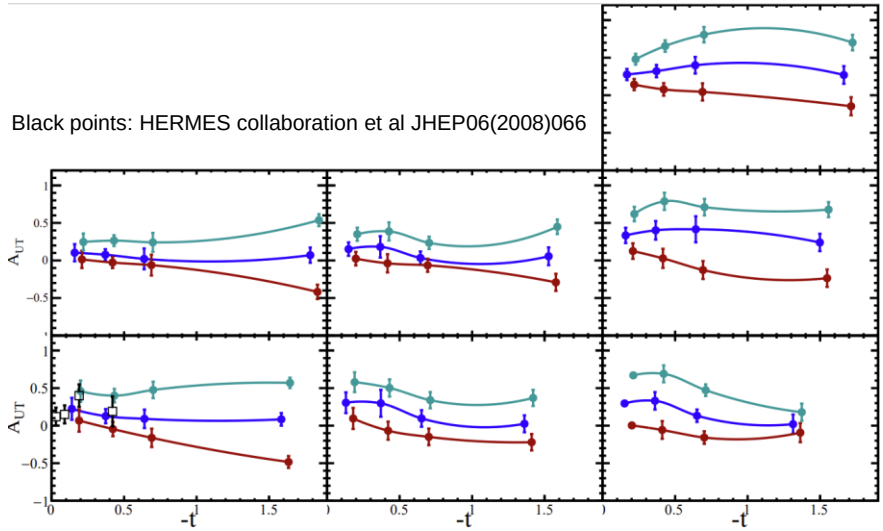
$J_u = 0.5 \quad J_d = 0.1$
$J_u = -0.5 \quad J_d = -0.1$
$J_u = 0.2 \quad J_d = 0.0$







Black points: HERMES collaboration et al JHEP06(2008)066



More on GPD E: AFTER@LHC

Physics Reports 911 (2021)

- Conservation of total angular momentum: off-diagonal TMDs vanish in absence of orbital angular momentum

$$\Delta\lambda=(\Lambda'-\Lambda)-(\lambda'-\lambda)\neq 0$$

Λ : initial target light-front helicity
Λ': final target light-front helicity
λ :initial parton light-front helicity
λ': final parton light-front helicity

- Some of these off-diagonal TMDs appear to be experimentally sizeable

Hermes **Phys. Rev. Lett. 94 (2005) 012002**
COMPASS **Phys. Rev. Lett. 94 (2005) 202002**
PHENIX **Phys. Rev. D 82 (2010) 112008**

- The quark Sivers TMD $f_{1T}^{\perp q}(x,k_\perp^2)$ and the quark GPD $E^q(x,\xi,t)$ could be related by a chromodynamic lensing mechanism

M. Burkardt Phys. Rev. D 66 (2002) 114005 and Nuclear Phys. A 735 (2004)

$$\int d^2k_\perp \frac{\boldsymbol{k}_\perp^2}{2M^2} f_{1T}^{\perp q}(x,\boldsymbol{k}_\perp^2) \propto \int d^2b_\perp \bar{\mathcal{I}}(\boldsymbol{b}_\perp)(\boldsymbol{S}_T \times \boldsymbol{\partial}_{b_\perp})_z \mathcal{E}^q(x,\boldsymbol{b}_\perp^2)$$

Lensing function

Proton transverse spin

$$\mathcal{E}^q(x,\boldsymbol{b}_\perp^2) = \int \frac{d^2\Delta_\perp}{(2\pi)^2} e^{-i\boldsymbol{b}_\perp\cdot\boldsymbol{\Delta}_\perp} E^q(x,0,-\boldsymbol{\Delta}_\perp^2)$$

Bacchetta and Radici Phys. Rev. Lett. 107 (2011) 212001

- The Sivers function could then be used to constrain the GPD E^q and hence the kinetic OAM via the Ji sum rule.

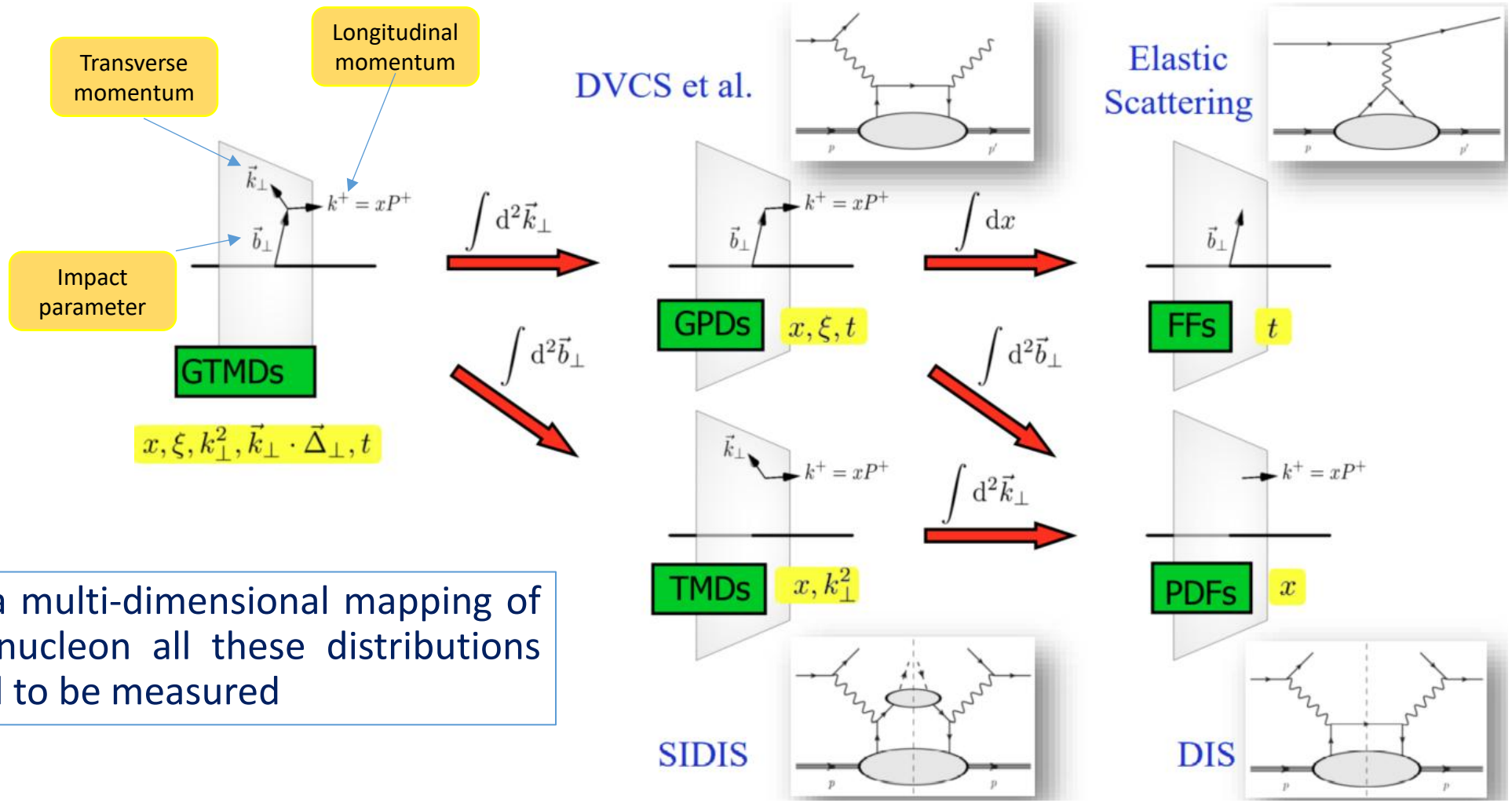
Summary

- GPDs are powerful tool to explore the structure of the nucleons and nuclei
  - Nucleon tomography, quark angular momentum, distribution of forces in the nucleon
- Exclusive reactions can provide important information on nucleon structure
  - DVCS via the extraction of GPDs
- CLAS12 offers a wide kinematical reach over which the GPDs dependence on different kinematical variables can be scanned
  - Data adds constraints on GPDs in unexplored regions of the phase space
  - Possibilities to measure new observables using different experimental configurations
    - Flavor separation of GPDs
- DDVCS is the new avenue
  - At JLab: forseen High-Luminosity upgrade and detector upgrades (μCLAS12 and SoLIDμ)
  - At EIC: measurable after the early science phase and theoretical effort for better modeling
- Constrain the GPD E to better understand the nucleon spin.



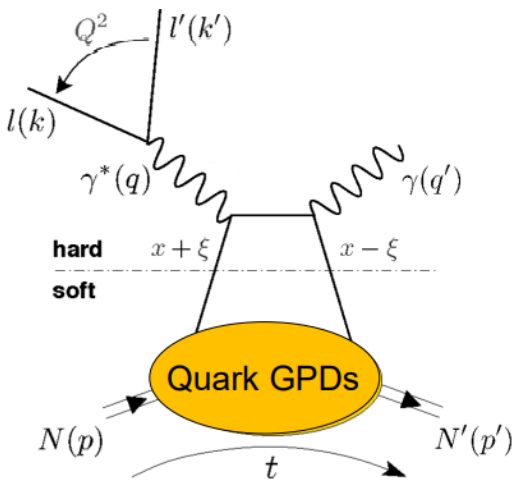
Backups

Multi-dimensional mapping of nucleon structure

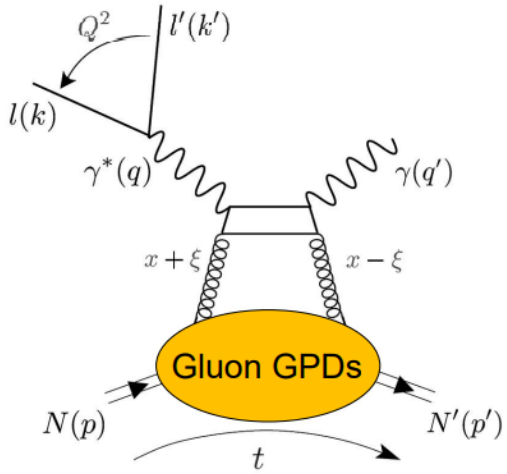


For a multi-dimensional mapping of the nucleon all these distributions need to be measured

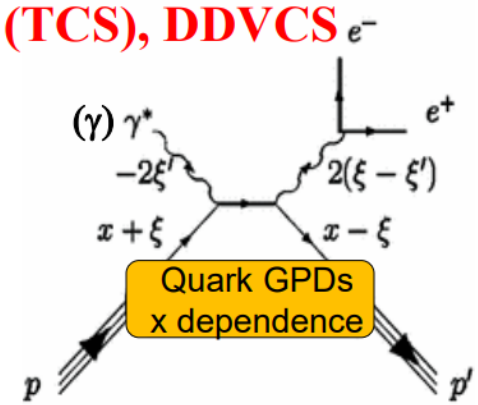
Exclusive reactions giving access to GPDs

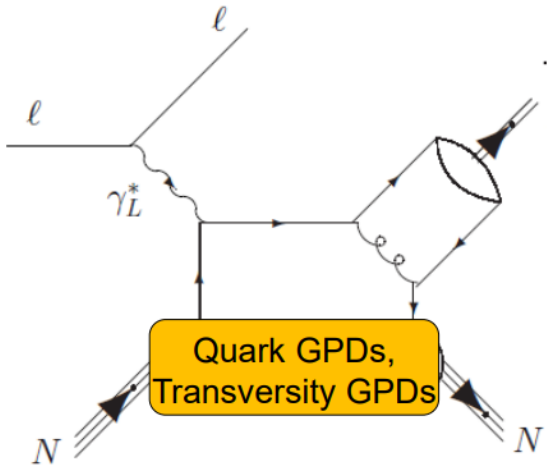


DVCS

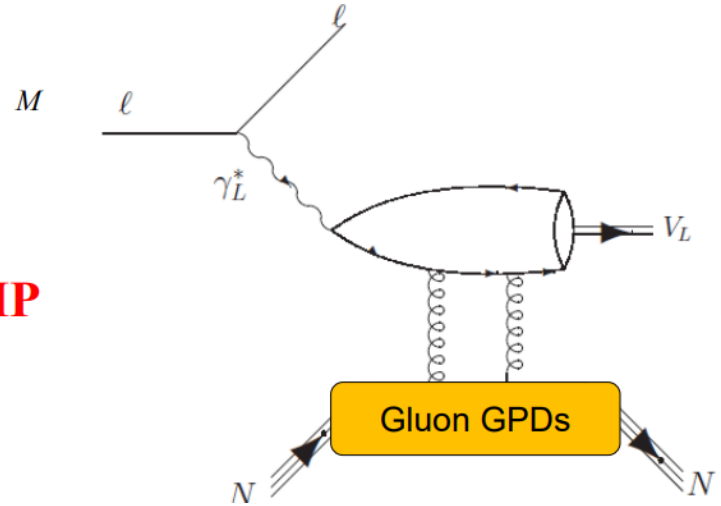


(TCS), DDVCS





DVMP



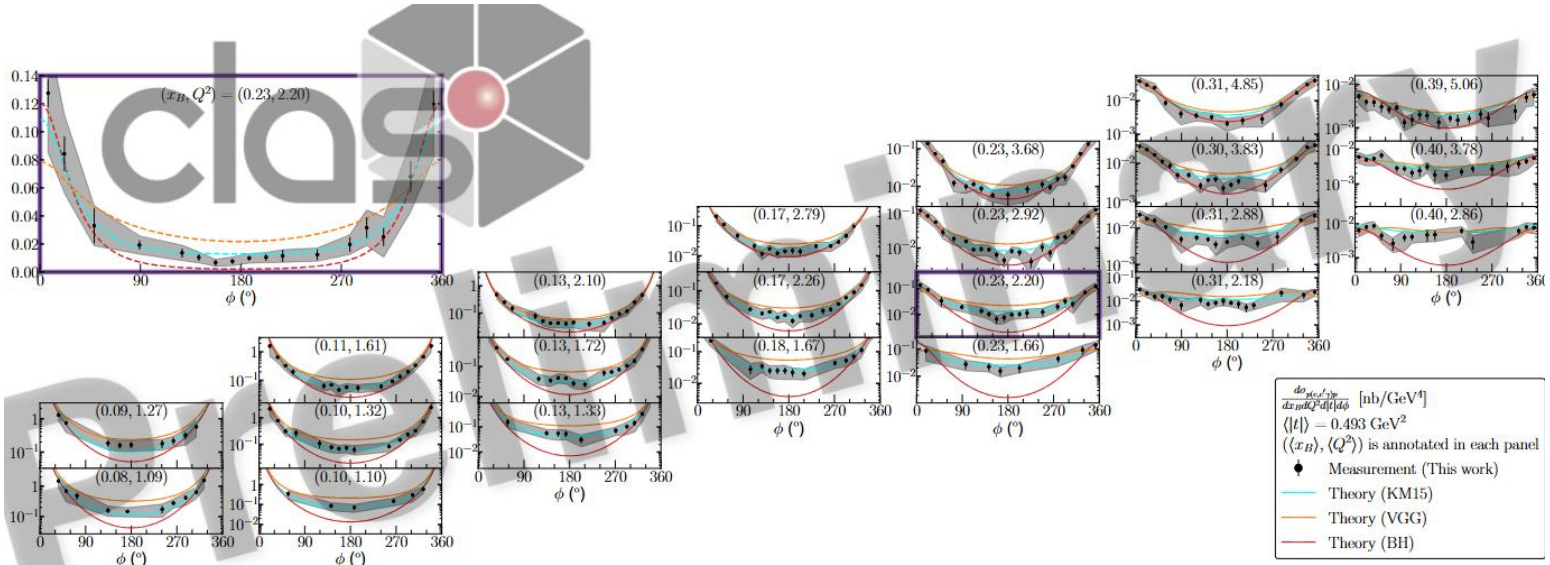
$Q^2 = -(k-k')^2$
$x_B = Q^2/2M\nu$ $\nu = E_e - E_{e'}$
$x+\xi$, $x-\xi$ long. mom. fract.
$t = \Delta^2 = (p-p')^2$
$\xi \cong x_B/(2-x_B)$

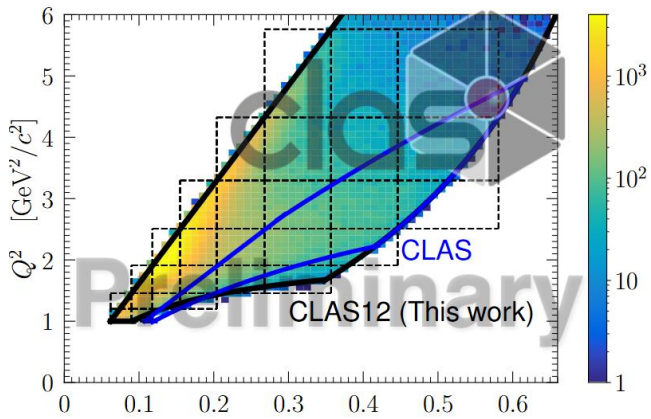
Results not shown in main slides

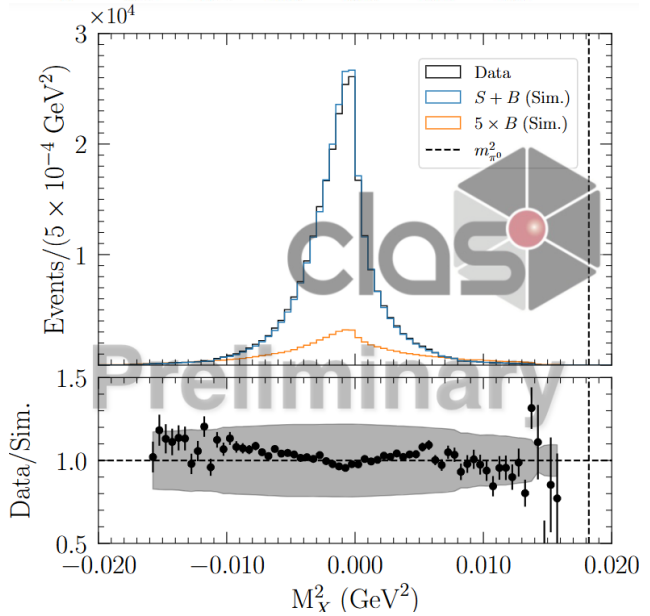
DVCS off proton cross section

Credits: Sangbaek Lee et al.

- preliminary unpolarized cross section results
  - Lever arms of GPD extraction using the universality
  - a significant contribution beyond the Bethe-Heitler process over an extended kinematic range.
  - well described by a theoretical model.
  - This work will enhance the global data sets to study the nucleon structure



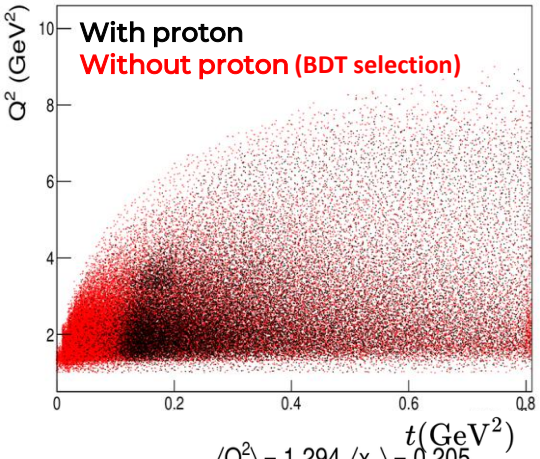


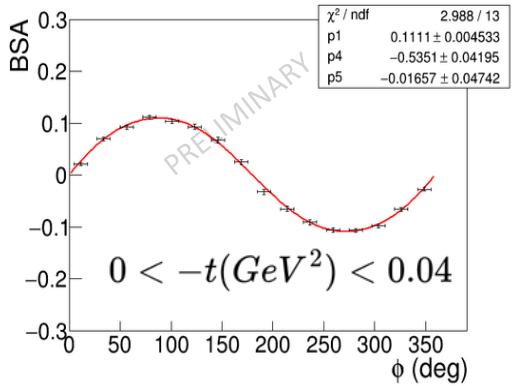


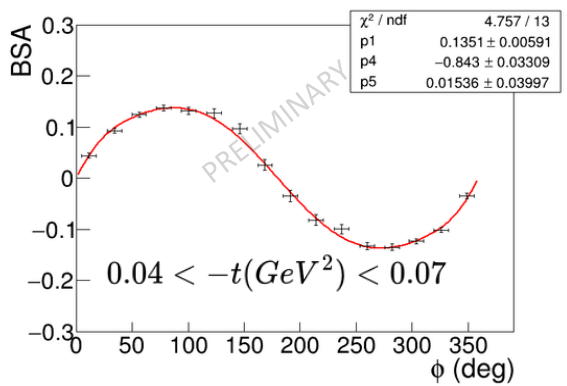
To be published soon.

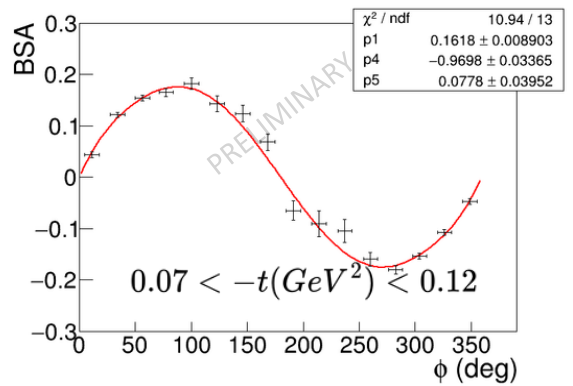
DVCS Beam Spin Asymmetry at small t: update Credits: Sebastian Alvarado

The smaller the t, the better the interpretation in terms of GPDs





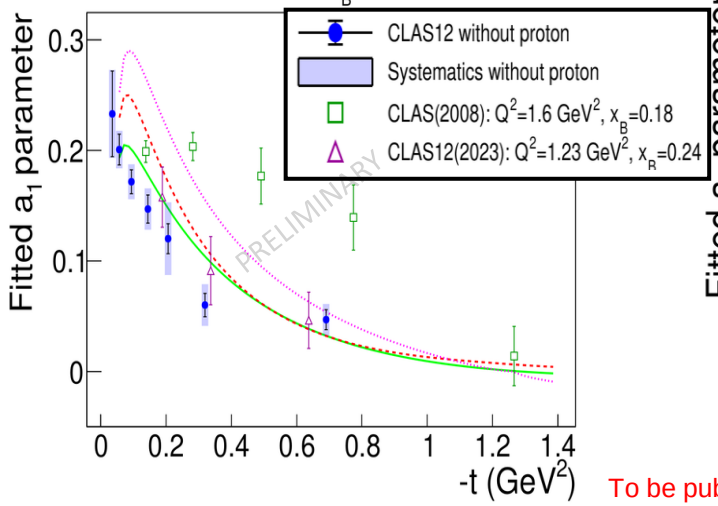


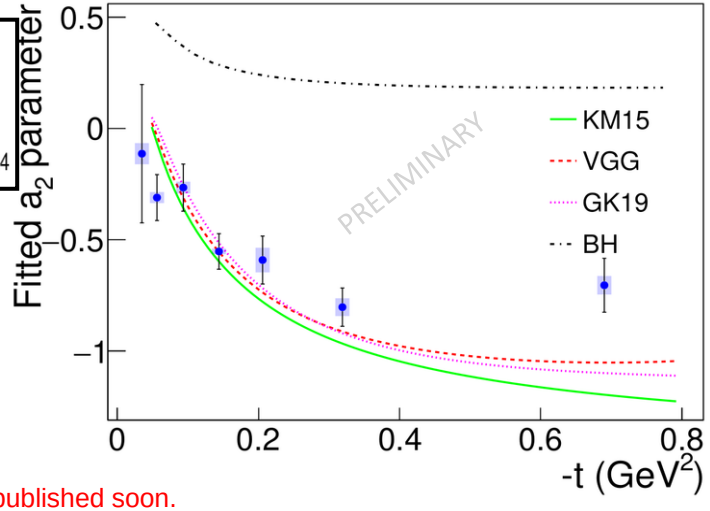


$1.0 < Q^2(\mathrm{GeV}^2) < 1.6$

$0 < x_B < 0.12$

$$BSA \equiv \frac{a_1 \sin(\phi)}{1 + a_2 \cos(\phi)}$$





To be published soon.

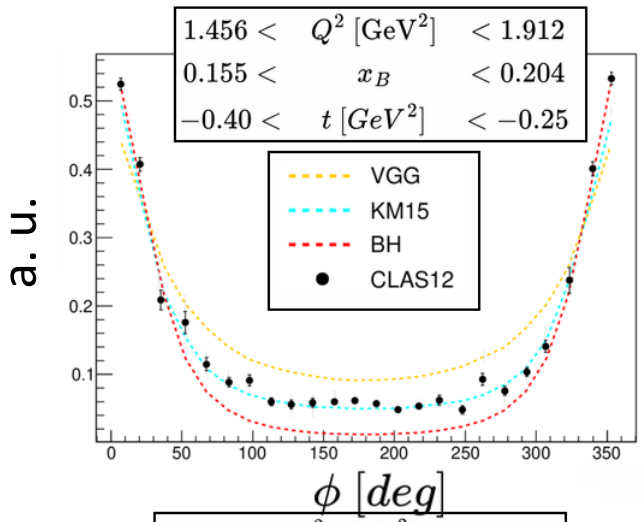
$$a_2 = \frac{2\int_0^{2\pi} d\phi \; cos(\phi)\; \mathcal{P}_1\mathcal{P}_2(\phi) d^5\sigma_{unp}(\phi)}{\int_0^{2\pi} d\phi \; \mathcal{P}_1\mathcal{P}_2(\phi) d^5\sigma_{unp}(\phi)} \qquad a_2 \equiv a_2(\Re\mathfrak{e}[CFFs])$$

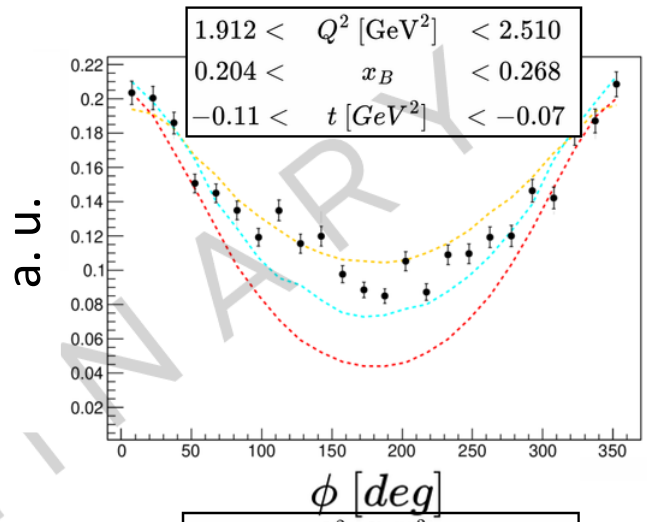
Given the achieved precision on the BSA, constraints on the real part of CFFs can be retrieved from the a2 parameter

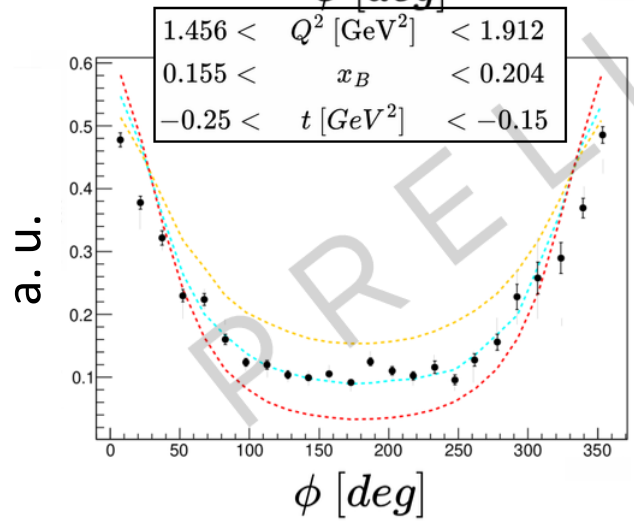
….and DVCS cross-section: update

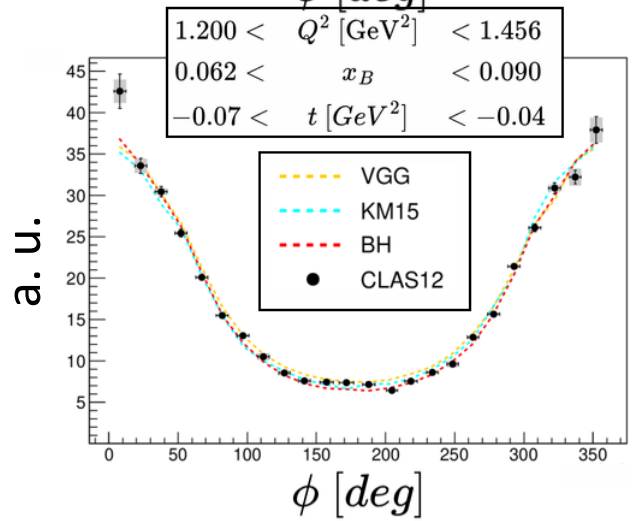
Credits: Sebastian Alvarado

The boost of statistics and extended phase space brought by BDT classification are particularly beneficial for cross section measurements





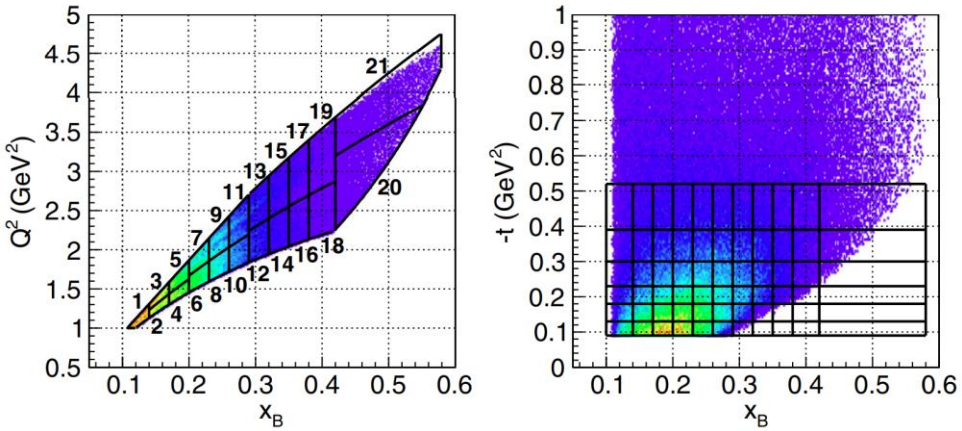




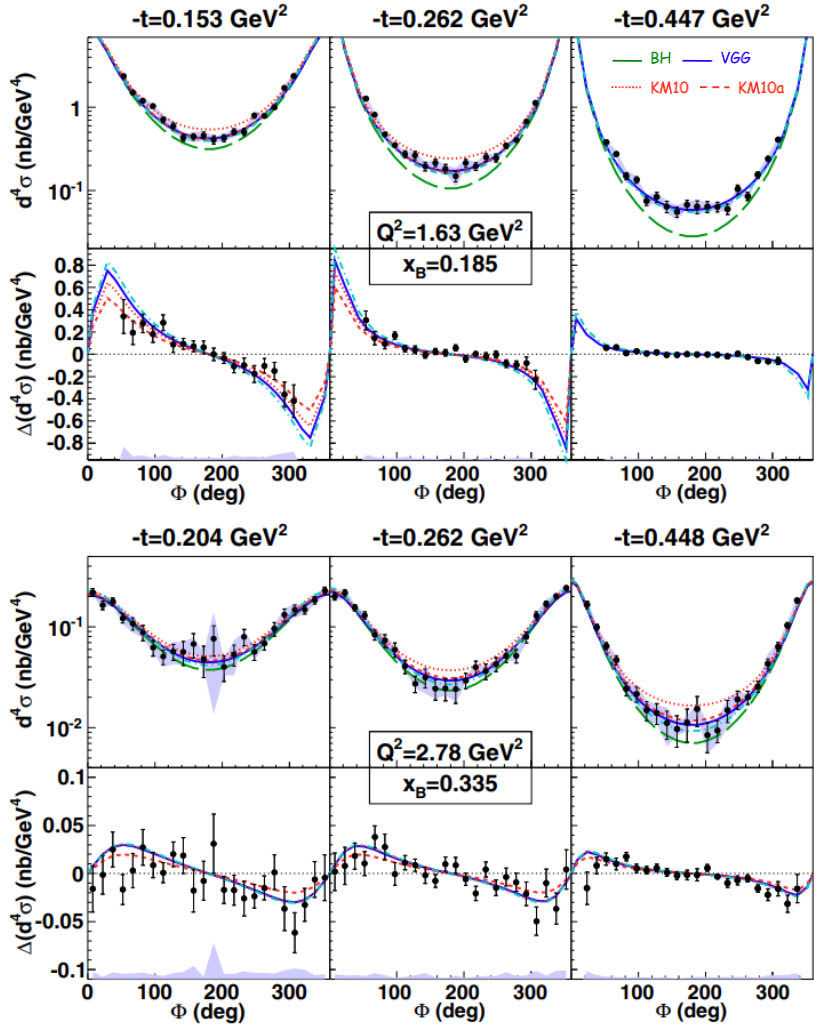
PRELIMINARY

CLAS: unpolarized and beam-polarized cross sections at ~6 GeV

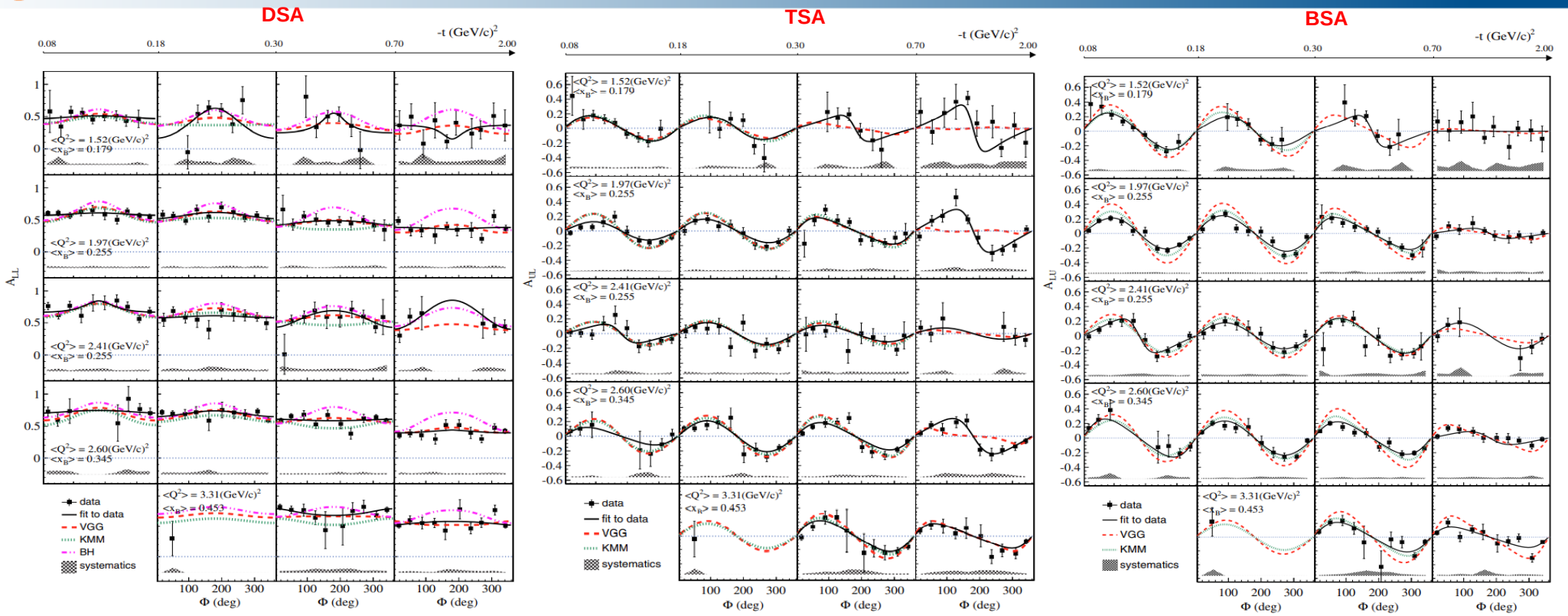
- Beam energy ~ 5.75 GeV
- Beam polarization ~ 80%
- Target LH2
- 110 (Q^2, x_b, t) kinematical bins in total



H.S. Jo et al., PRL 115, 212003 (2015)



CLAS: DVCS on longitudinally polarized target at ~6 GeV



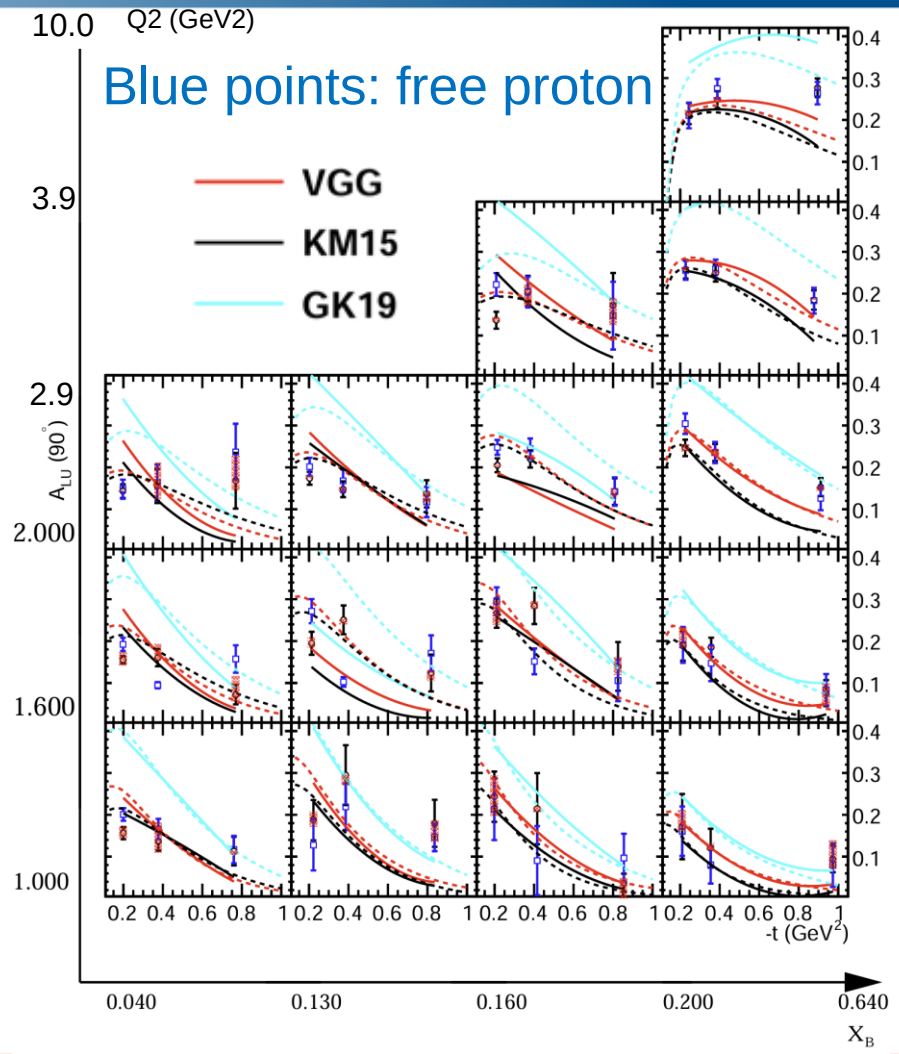
- Beam energy ~5.9 GeV and longitudinally polarized NH3 (P~80%)
- Observables: Beam, Target and double Spin Asymmetries
- Bins: 5 $Q^2 - x_b$ bins, 4 t bins and 10 Φ bins

w.r.t previous pioneering CLAS6 data
Improved statistics x10 at low –t
Extended kinematic coverage

E. Seder et al., PRL 114 (2015) 032001
S. Pisano et al., PRD 91, 052014 (2015)

pDVCS: BSA and t-profile of the $\sin(\phi)$ moment

- Comparison with BSA from free proton shows a very clear compatibility
  - Clearly, medium effects in deuterium are negligible (as expected)
- More to understand with results from data taken on nuclear targets at CLAS12
  - Currenty being analyzed



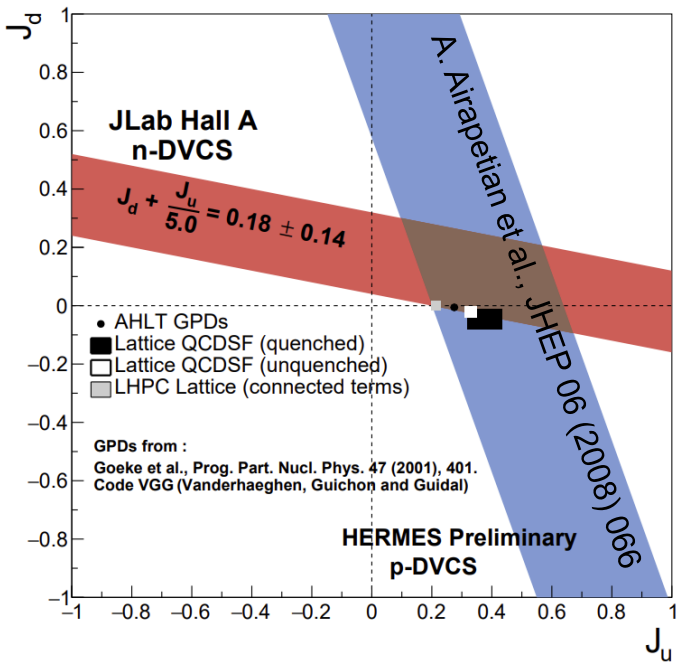
Kumericki, Kresimir and M uller, Dieter, EPJ Web of Conferences 112, 01012 (2016).
S. V. Goloskokov and P. Kroll, EPJC 65, 10.1140 (2009)
M. Vanderhaeghen, P. A. Guichon, and M. Guidal, Phys.Rev. D60, 094017 (1999)

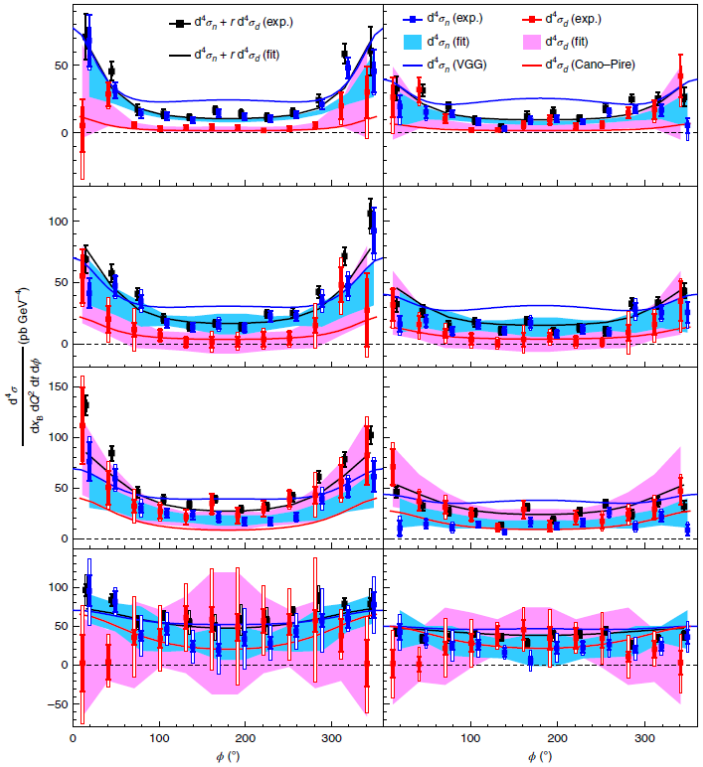
To be published soon.

Previously on DVCS with an unpolarized deuterium target

- Previous pioneering measurement of nDVCS (Jlab Hall A @ 6 GeV)
  - Beam-energy « Rosenbluth » separation of nDVCS CS using an LD2 target and two different beam energies
  - First observation of non-zero nDVCS CS
- No neutron detection

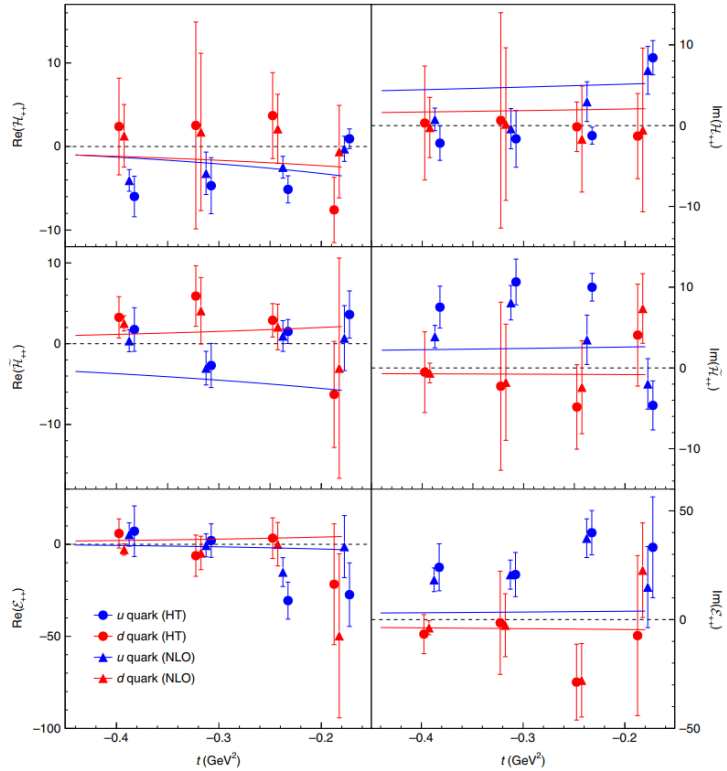
$$D(e,e'\gamma)X - H(e,e'\gamma)X = n(e,e'\gamma)n + d(e,e'\gamma)d + \ldots$$





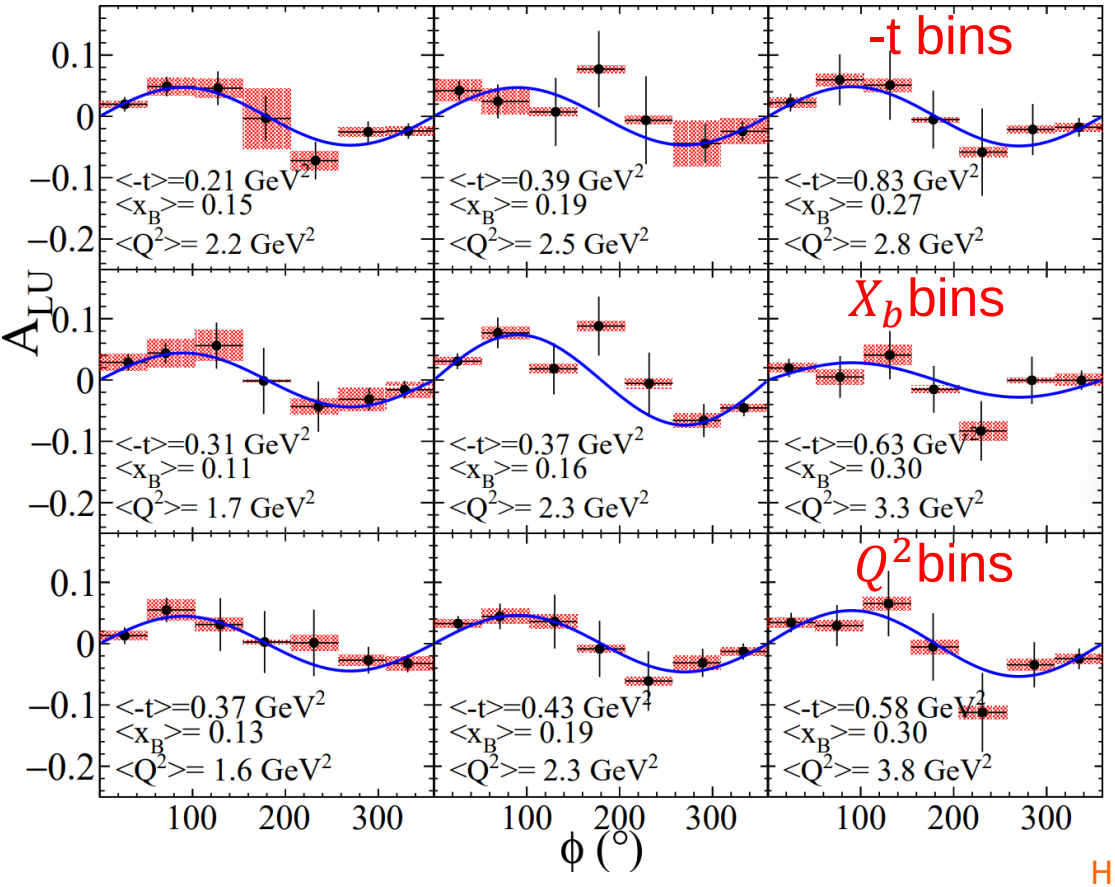
Q^2=1.9 GeV^2 and x_B=0.36

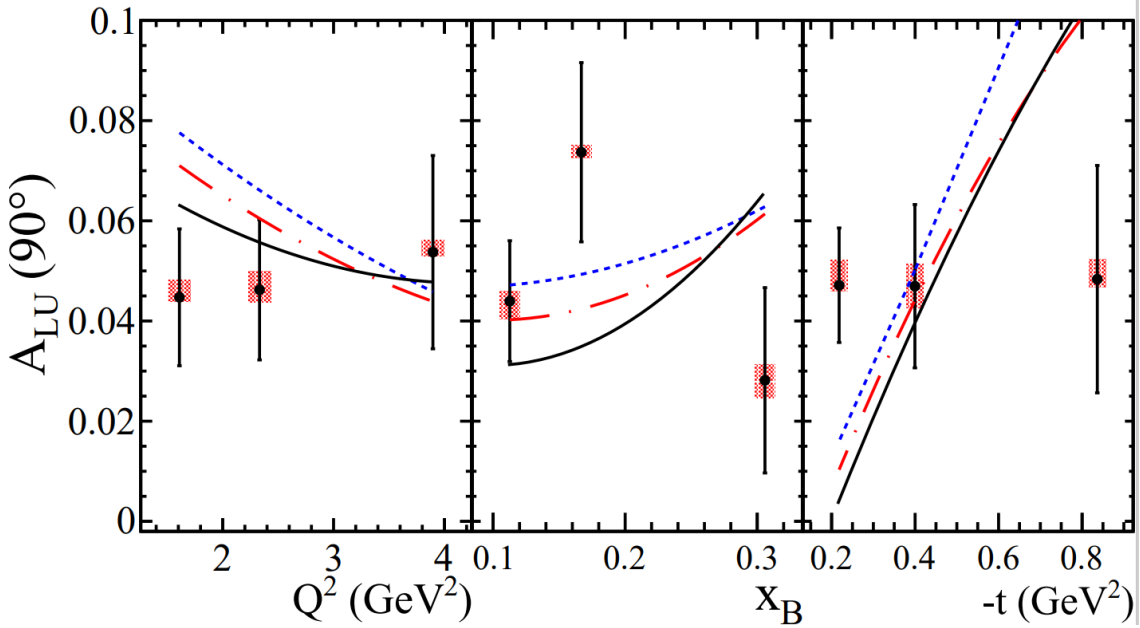
+data from: Mazouz, M. et al. Phys. Rev. Lett. 99, 242501 (2007).



Benali, M., Desnault, C., Mazouz, M. *et al. Nat. Phys.* **16,** 191–198 (2020)

First-time measurement of nDVCS with detection of the active neutron





$$A_{LU} \approx \Im\{F_1 \boldsymbol{H} + \xi(F_1 + F_2)\widetilde{\boldsymbol{H}} - k\, F_2 \boldsymbol{E} + \ldots\}$$

VGG model predictions giving the smallest χ^2

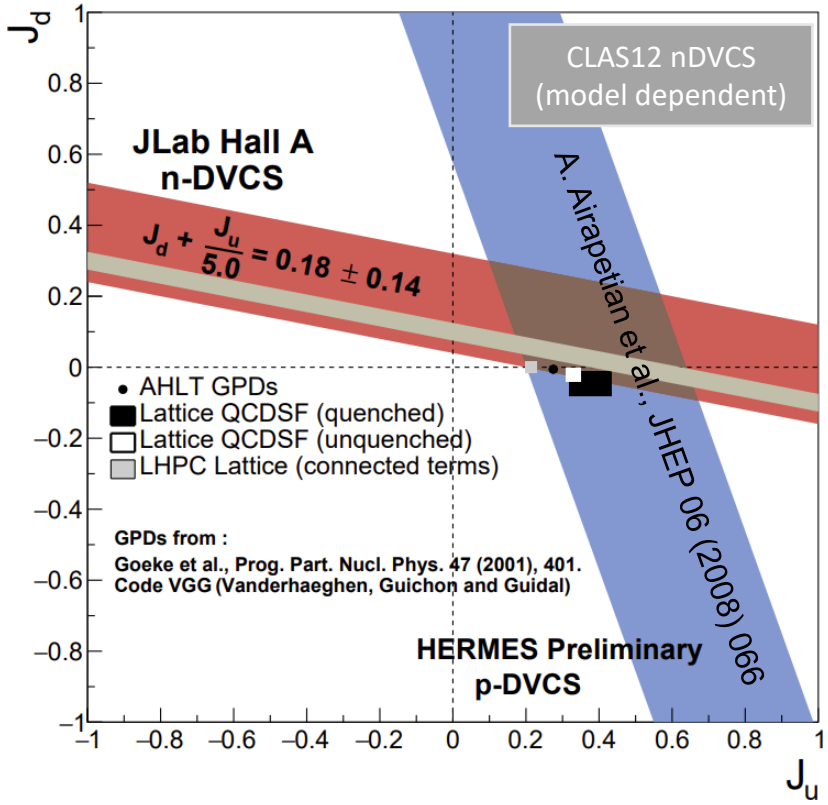
$J_u = 0.35$ $J_d = 0.05$
$J_u = -0.2$ $J_d = 0.15$
$J_u = -0.45$ $J_d = 0.2$

M. Vanderhaeghen, P.A.M. Guichon, and M. Guidal, PRD 60, 094017 (1999)

Hall A @ JLAB: one measured kinematical point at Q^2=1.9 GeV² and x_B=0.36

Impact of nDVCS data from CLAS12

- Model-dependant extraction of J_u and J_d
  - Use VGG model (PRD 60, 094017 (1999)) and generate a set of values for J_u and J_d
  - Look for the 1 standard deviation error ellipse: defined as $\chi^2 - \chi^2_{min} \leq 1$
- Compatible with limits set before by pioneering Hall A measurement
- Compatible with Lattice QCD predictions
- Shortcomings:
  - none of the considered sets of J_u and J_d reproduce correctly the distributions
  - VGG has problems in reproducing proton data
- Closest-to-truth model-dependent representation of data.

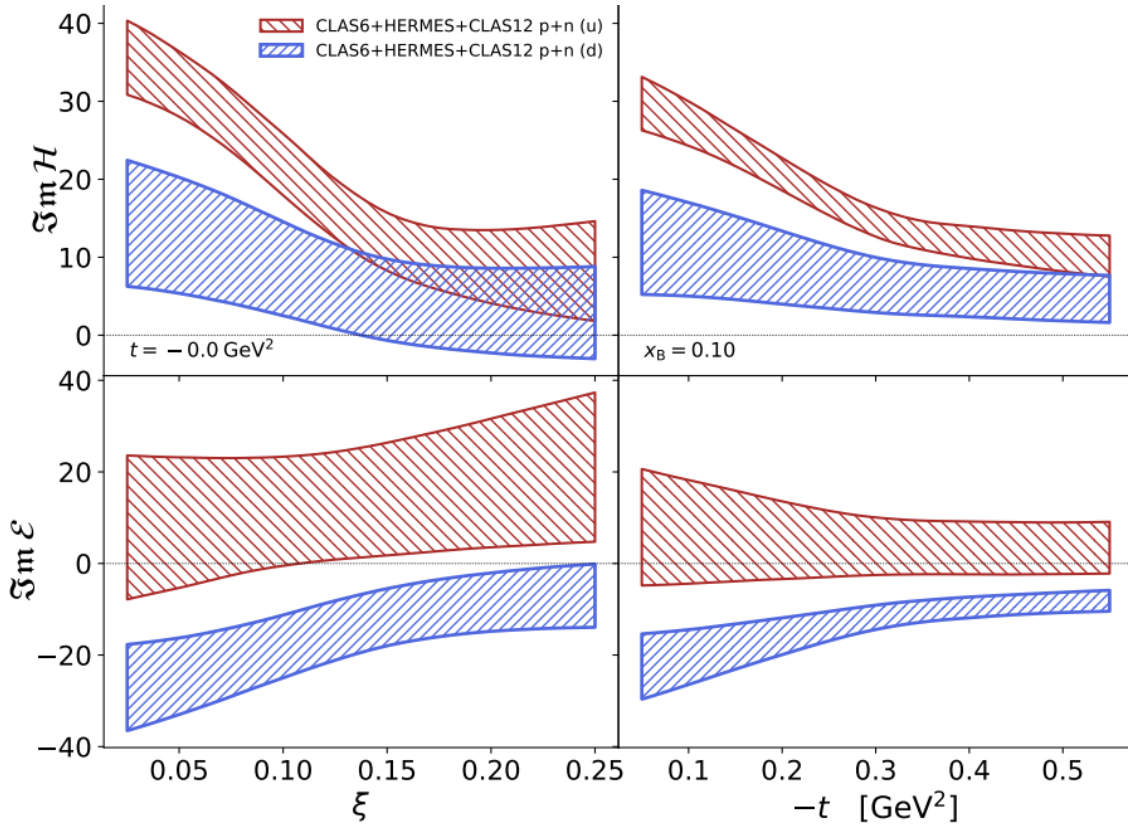


CFF extraction and flavor separation!

- Global fits of CFF using neural networks (model-independent)
  - K. Kumericki et al., JHEP 07, 073531 (2011); M. Cuic, K. Kumericki, et al., Phys. Rev. Lett. 533 125, 232005 (2020)).
- Data used:
  - CLAS6 and HERMES pDVCS observables
  - CLAS12 pDVCS BSA and nDVCS BSA
- Same extraction method applied to nDVCS Hall-A data, only separation for ImH

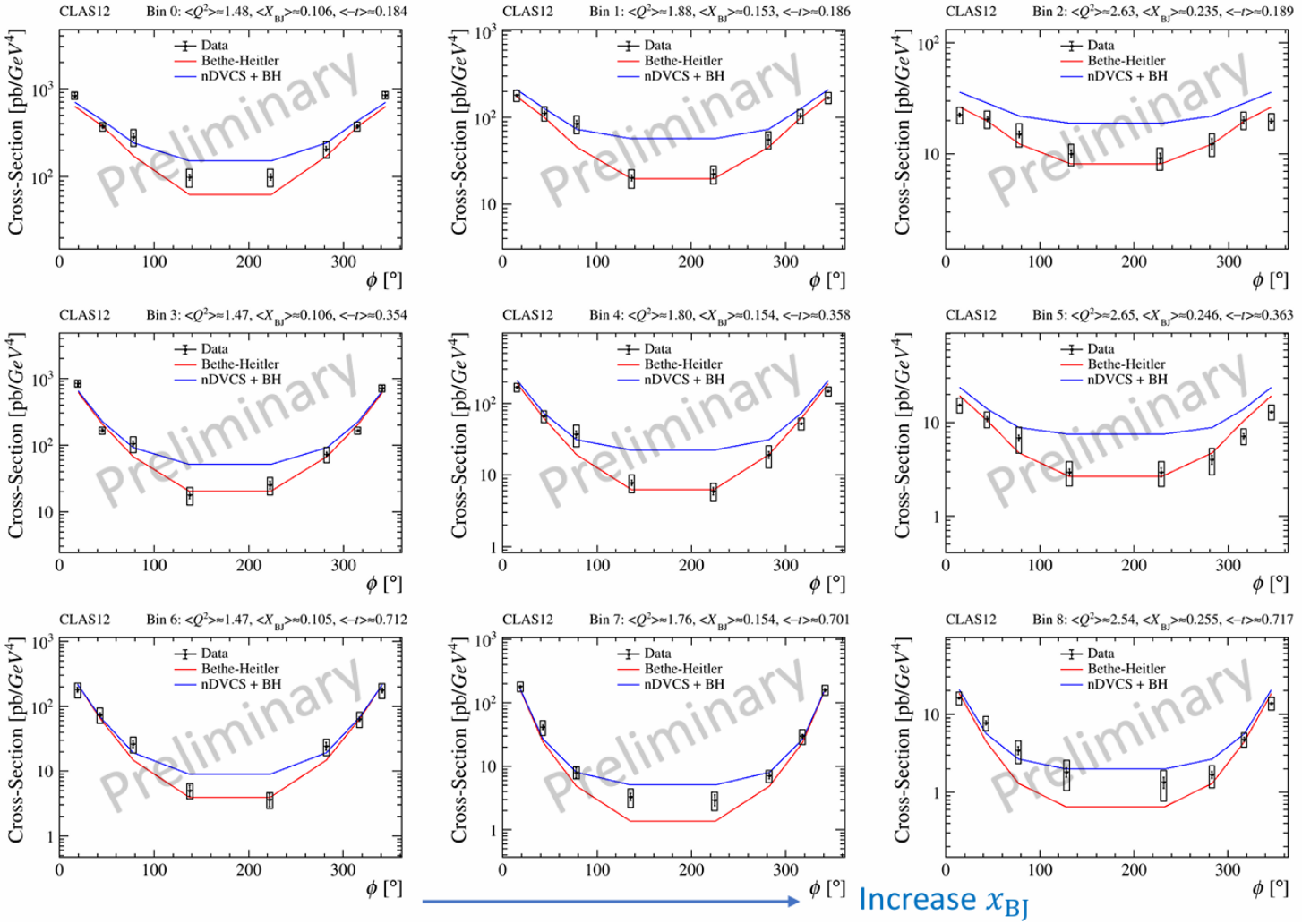
Clear quark-flavor separation of both ImH and ImE thanks to CLAS12 nDVCS data

Results extrapolated to t=0 GeV^2



Unpolarized nDVCS cross section

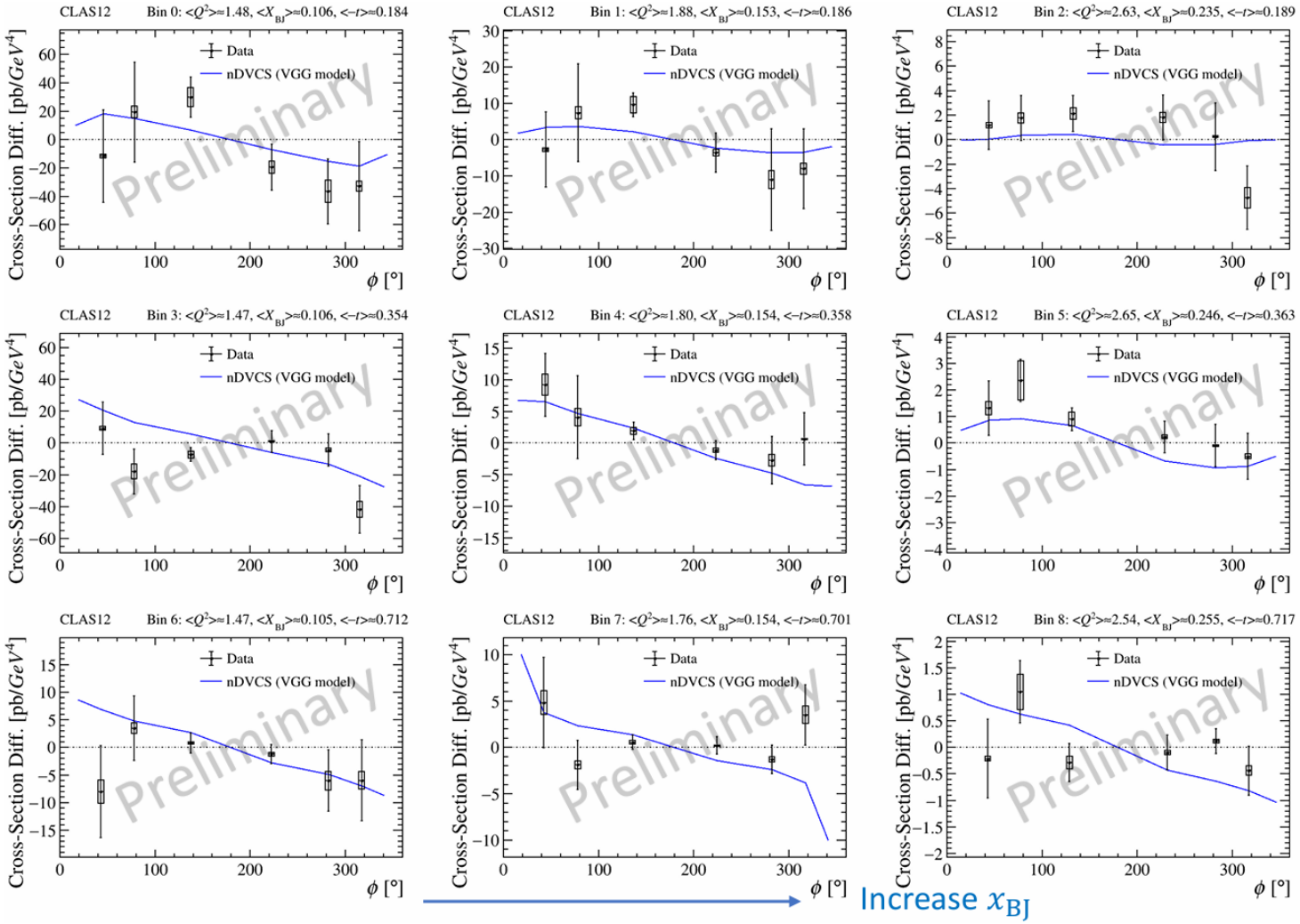
Credits: Li Xu



- Linked mainly to the real CFF of GPD E
- Error bars: statistical
  Boxes: systematic
- The data are compatible with the BH calculations at ϕ edges
- nDVCS+BH predictions: VGG model with $J_u = 0.3$ and $J_d = 0.1$
- Predictions overshoot the data in the central-ϕ region, indicating the real CFF of E is not correctly parametrized in the VGG model

Polarized nDVCS cross-section difference

Credits: Li Xu



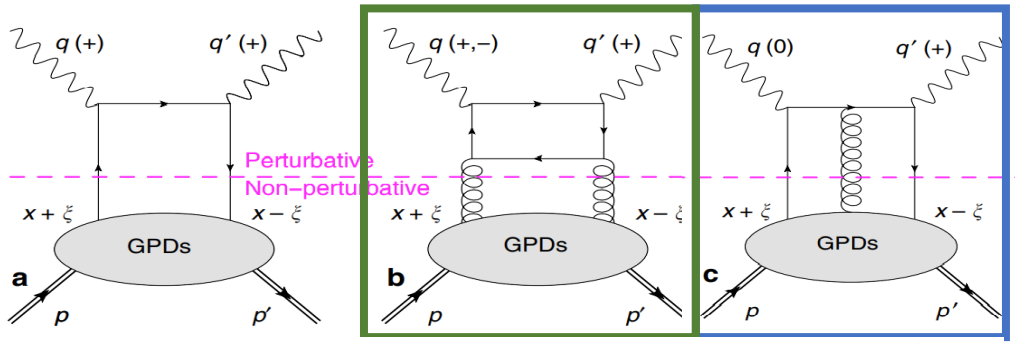
- Linked to the imaginary CFF of GPD E
- Error bars: statistical
  Boxes: systematic
- Predictions are provided at the mean values of $(Q^2, x_{\mathrm{BJ}}, -t, \phi)$, which vary with ϕ
- nDVCS predictions: VGG model with particular parameters $J_u = 0.3$ and $J_d = 0.1$
- The data are consistent with the predictions given the large statistical uncertainties

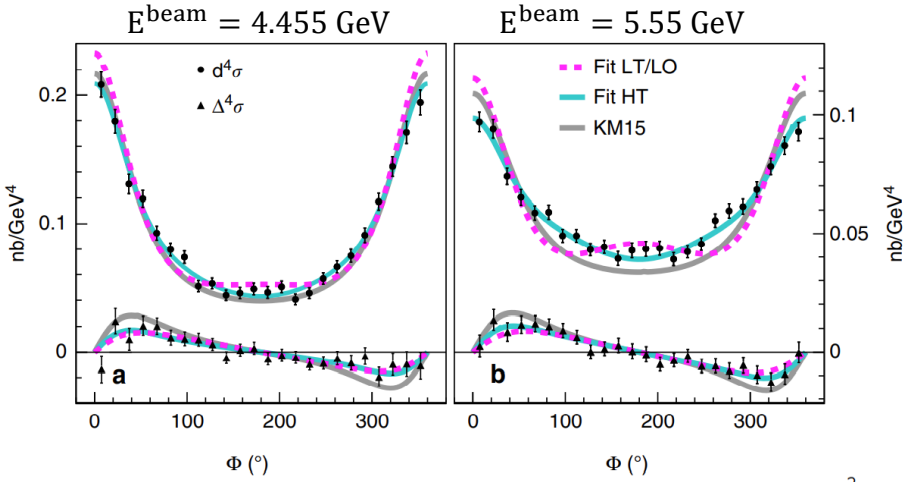
Hall A: High-precision DVCS at 6 GeV

M. Defurne et al., Nature Communications 8, 1408 (2017)

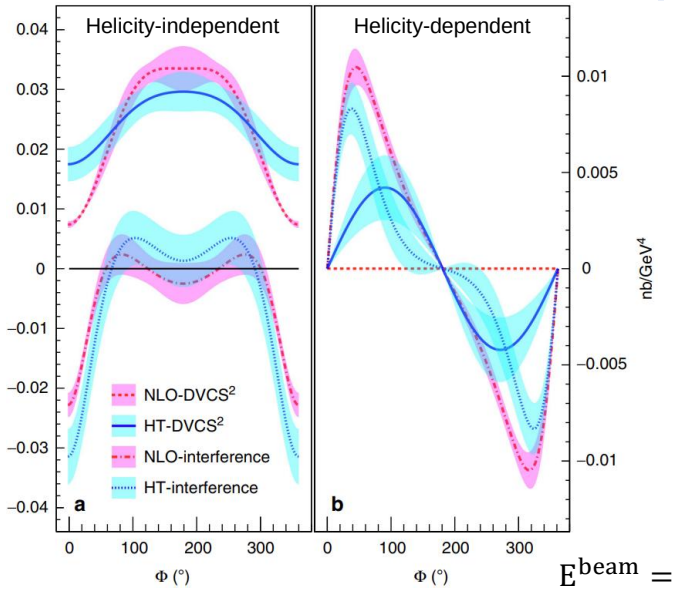
- Quantify the sensitivity to LT-NLO contributions or higher twist (HT) (gluon exchange)

- Different beam energies used to separate BH-DVCS interference and $DVCS^2$ contributions





$Q^2 = 1.75\ \text{GeV}^2$, $x_B = 0.36$, and $t = -0.30\ \text{GeV}^2$



$E^{beam} = 5.55\ \text{GeV}$

First observation of Timelike Compton Scattering

Phys. Rev. Lett. 127, 262501 (2021)

- Test of universality of GPDs: direct comparison between DVCS and TCS results
- Real part of CFFs and D-term: TCS unpolarized cross section is sensitive to $\Re\{H\}$
- D-term can be related to the mechanical properties of the nucleon.

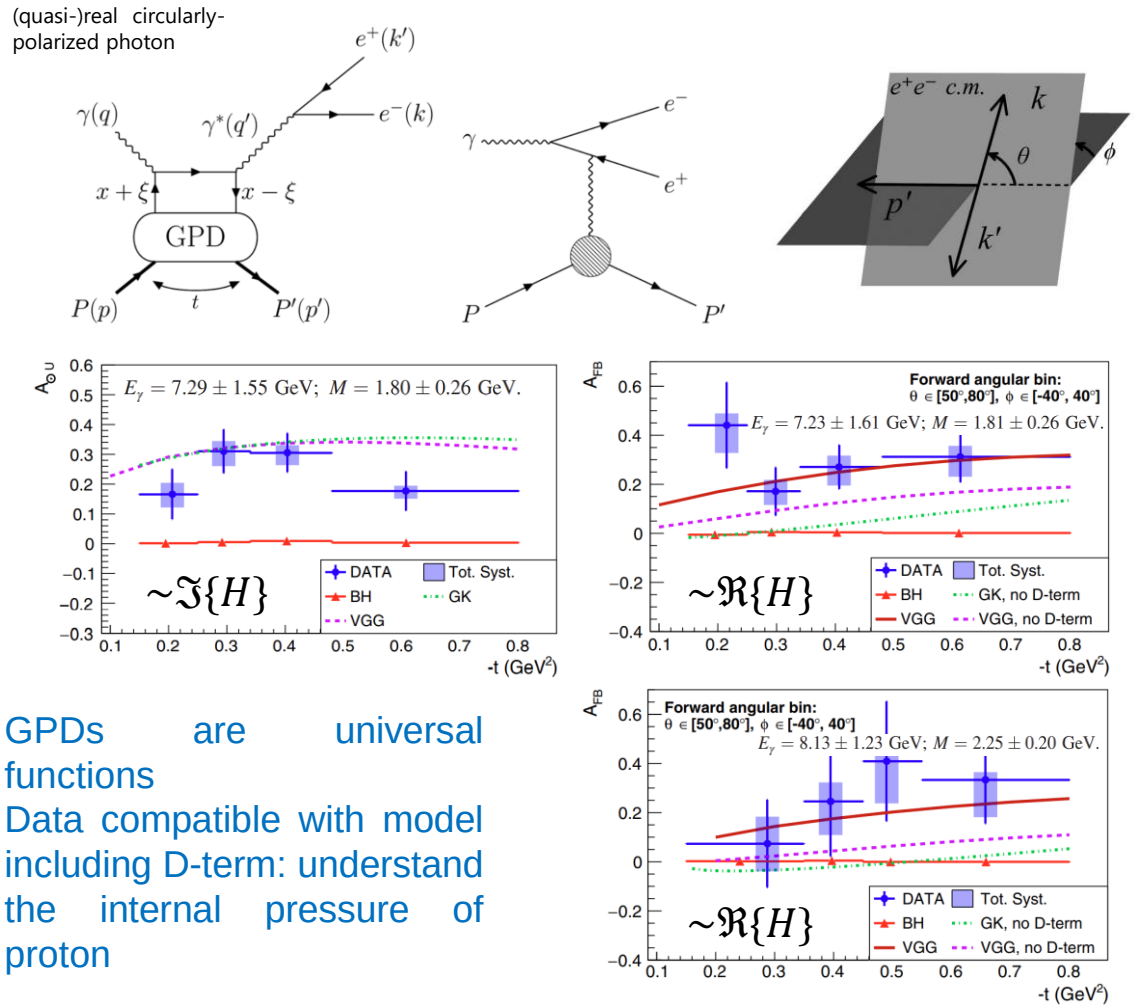
$$\mathrm{Re}\mathcal{H}(\xi,t) \overset{\mathrm{lo}}{=} D(t) + \mathcal{P}\int_{-1}^{1} \mathrm{d}x \left(\frac{1}{\xi - x} - \frac{1}{\xi + x}\right) \mathrm{Im}\mathcal{H}(x,t)$$

$$D(t) = \frac{1}{2}\int_{-1}^{1} \frac{D(z,t)}{1-z}\mathrm{d}z \qquad D(z,t) = (1-z^2)\left[d_1(t) C_1^{3/2}(z) + \cdots\right]$$

Measured observables:

- Beam helicity asymmetry: $\Im\{H\}$
- Forward-backward asymmetry: $\Re\{H\}$

S. V. Goloskokov and P. Kroll, EPJC 65, 10.1140 (2009)
M. Vanderhaeghen, P. A. Guichon, and M. Guidal, Phys.Rev. D60, 094017 (1999)



- GPDs are universal functions
- Data compatible with model including D-term: understand the internal pressure of proton

DV π^0P : the chiral odd GPD

Phys. Lett. B 849 (2024) 138459

- The BSA of DVπ^0P is sensitive to the chiral odd GPD $\bar{E}_T$

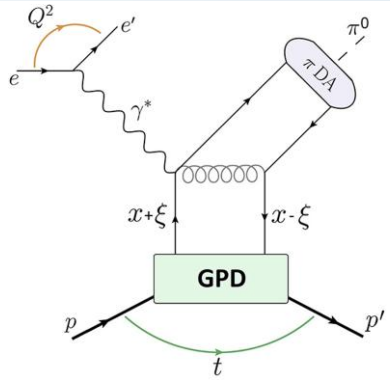
$$\bar{E}_T^q = 2\tilde{H}_T^q + E_T^q$$

  - Access quark transverse spin densities in polarized and unpolarized nucleons
  - Nucleon transverse anomalous magnetic moment

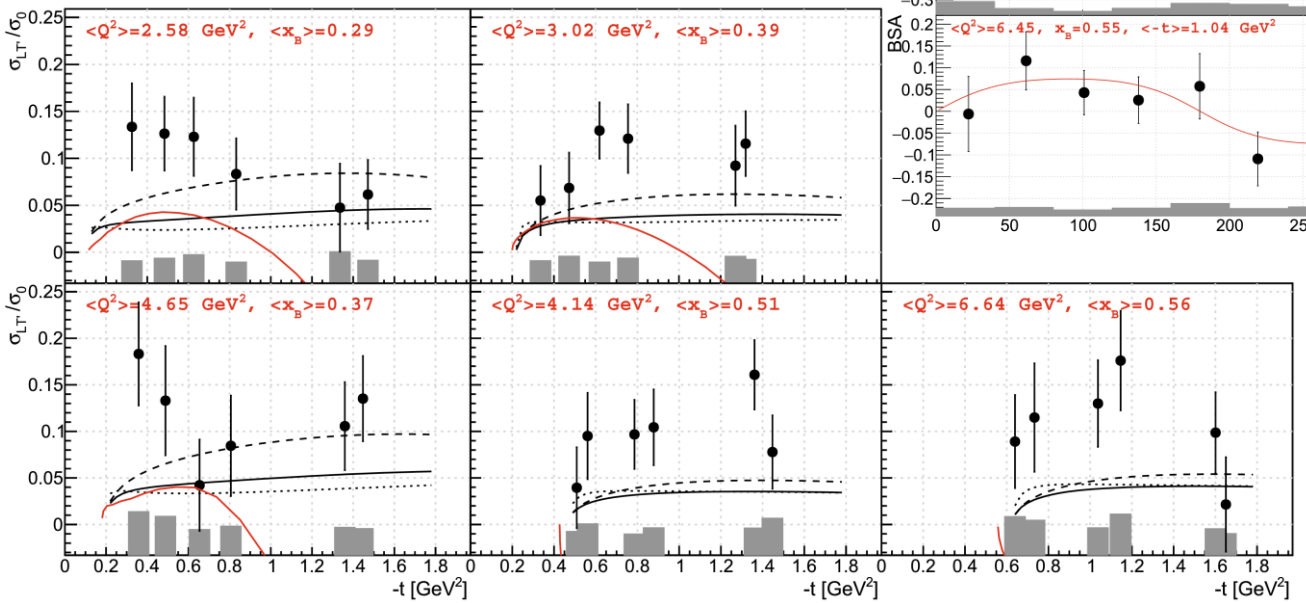
$$\kappa_T^u = \int dx \bar{E}_T^u(x,\xi,t=0)$$
$$\kappa_T^d = \int dx \bar{E}_T^d(x,\xi,t=0)$$

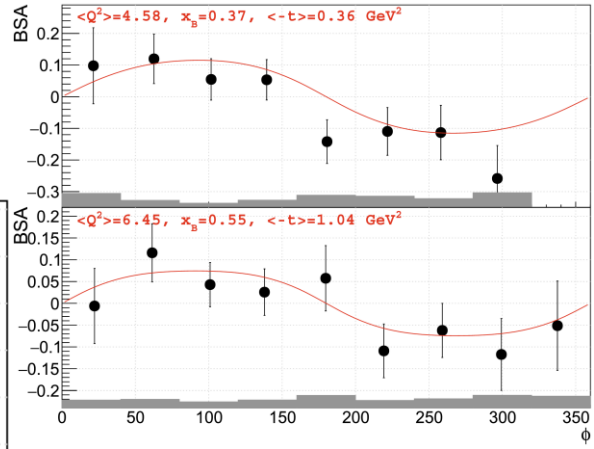
  - Proton tensor charge

$$\delta_T^u = \int dx H_T^u(x,\xi,t=0)$$
$$\delta_T^d = \int dx H_T^d(x,\xi,t=0)$$



$$BSA = \frac{\sqrt{2\epsilon(1-\epsilon)}\frac{\sigma_{LT'}}{\sigma_0}\sin\phi}{1+\sqrt{2\epsilon(1+\epsilon)}\frac{\sigma_{LT}}{\sigma_0}\cos\phi+\epsilon\frac{\sigma_{TT}}{\sigma_0}\cos 2\phi}$$

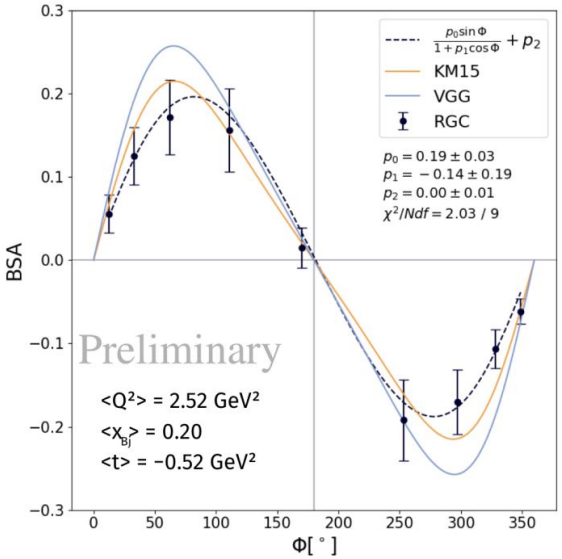


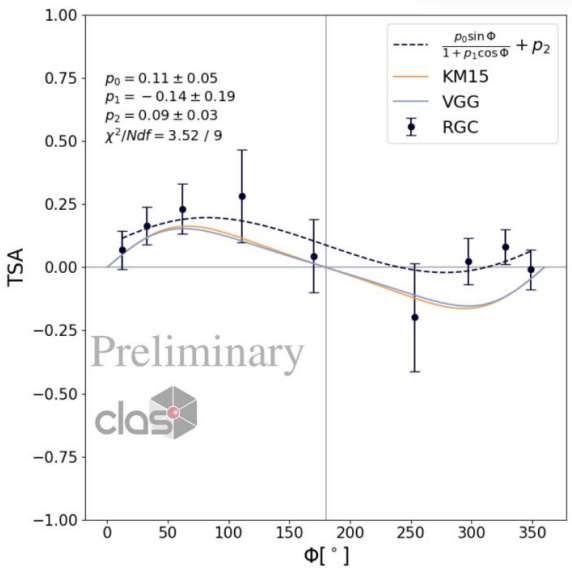


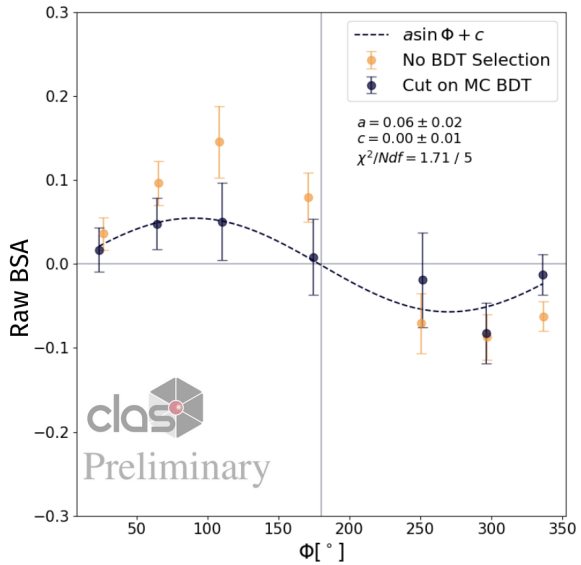
DVCS on longitudinally polarized target

Credits: Noémie Pilleux

- First time CLAS12 uses a polarized target
- Asymmetries on the proton:
  - BSA is for **bound protons in ND_3**
  - TSA is for protons in **D** only
  - They are corrected for π^0 DVMP
- BSA on the neutron:
  - BSA is for **bound neutrons in ND_3**
  - Not corrected for π^0 DVMP



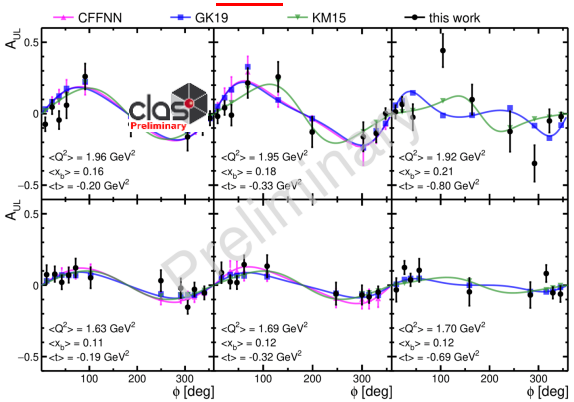


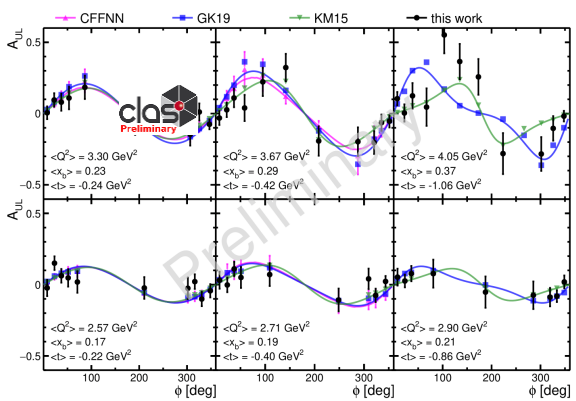


DVCS on longitudinally polarized target

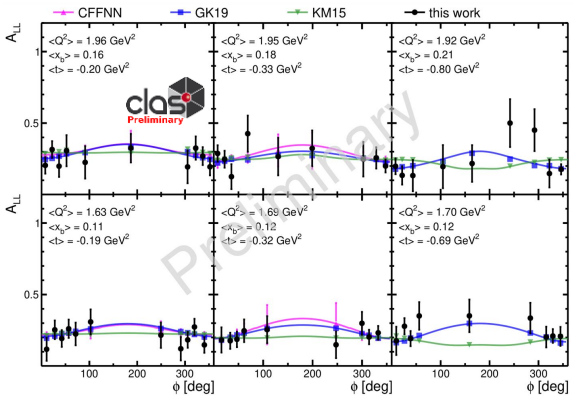
Credits: Samy Polcher Rafael

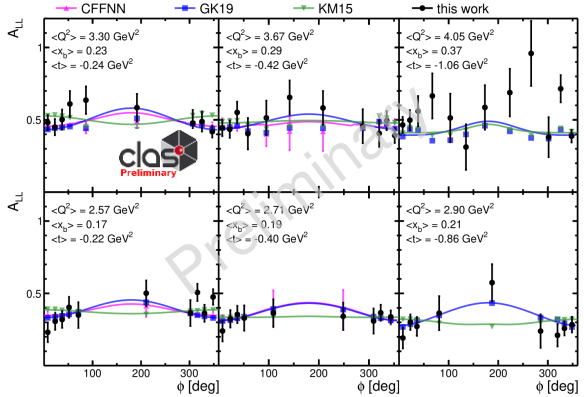
- First time CLAS12 uses a polarized target
- Asymmetries on the proton in NH_3 :
  - **TSA**



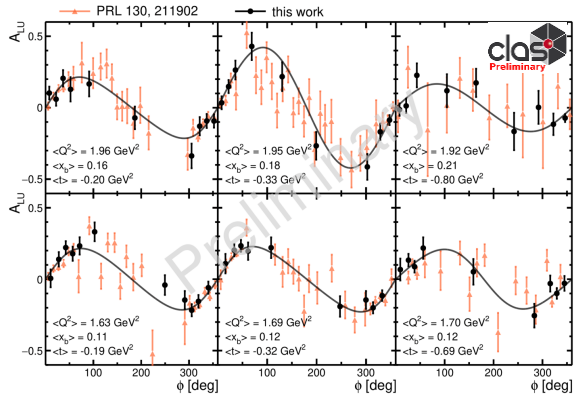


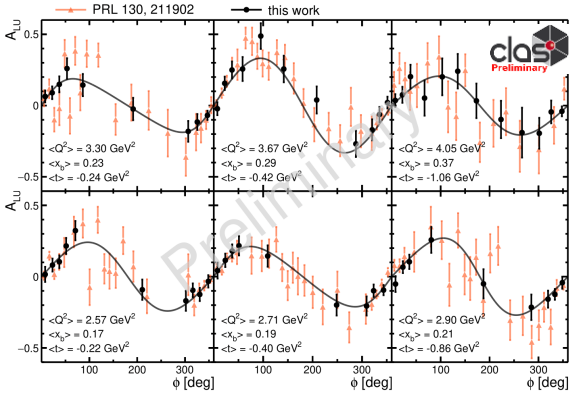
  - **DSA**





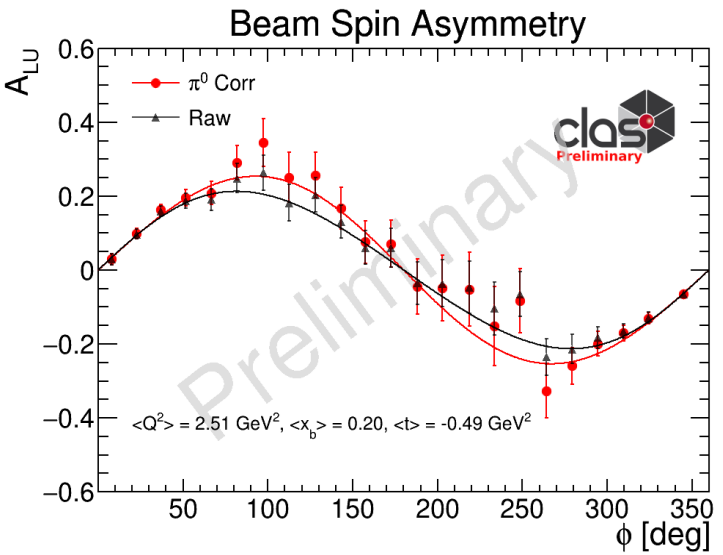
BSA

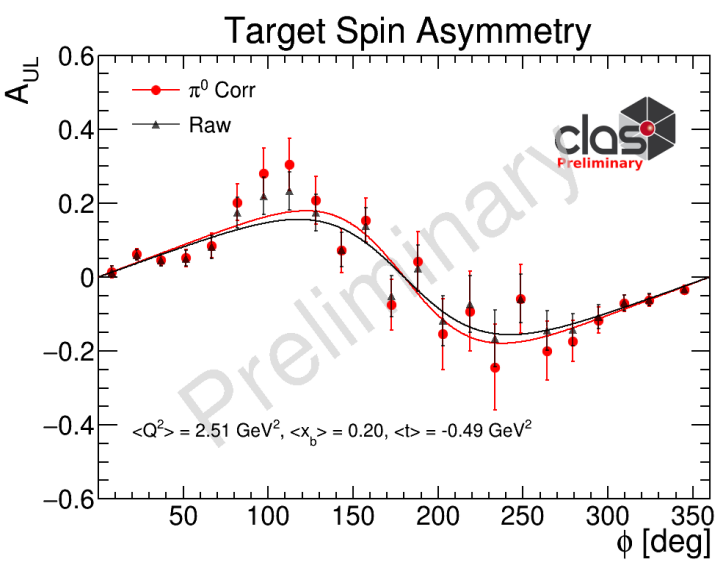


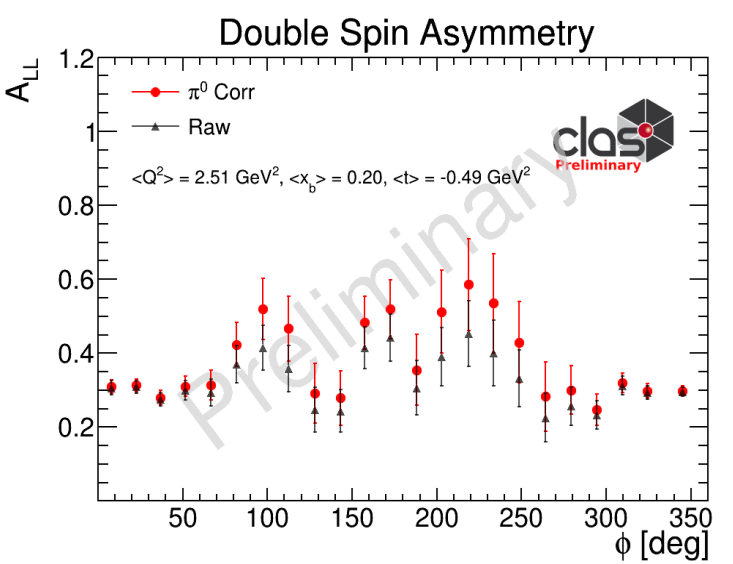


Integrated asymmetries

- Only statistical uncertainties are included
- For display only, the BSA and TSA are interpolated with: $$f(\phi) = \frac{a \sin(\phi)}{1 + c \cos(\phi)}$$
- The π^0 subtraction enhances the asymmetry
-



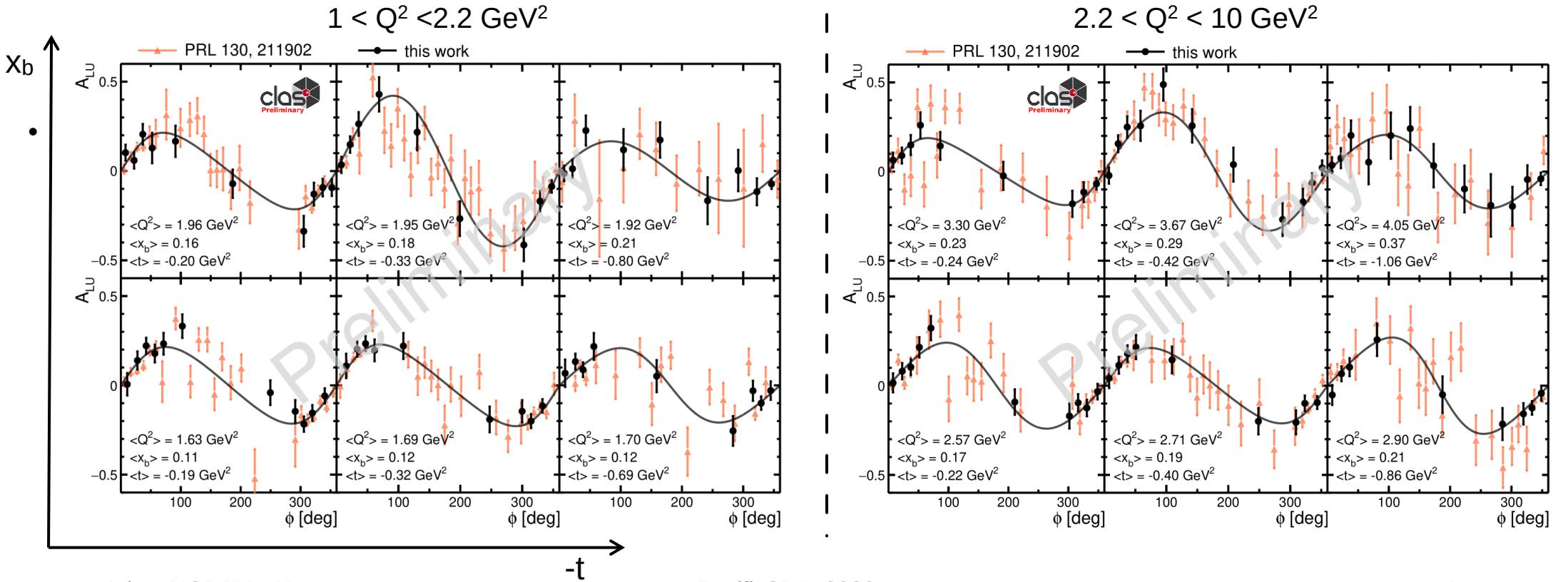




Comparison to CLAS12 BSA on unpolarised proton

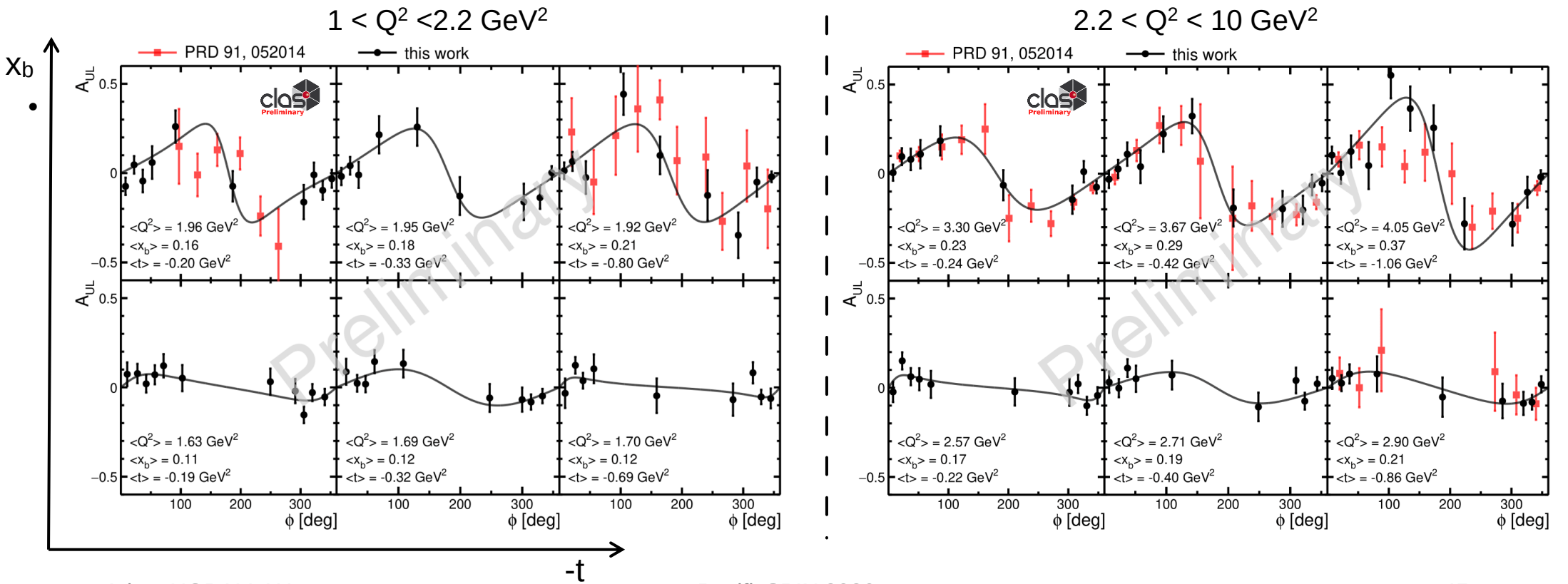
- CLAS12 BSA measurement on a liquid hydrogen target, [Phys. Rev. Lett. 130, 211902]
  - Same kinematic reach and no nuclear background → Good cross check

- The published results include systematic uncertainties and this work only includes statistical uncertainties



Comparison to CLAS6 TSA

- CLAS6 TSA measurement [Phys. Rev. D 91, 052014] at JLab 6GeV → Different beam energy and kinematic reach
- The published results include systematic uncertainties and this work only includes statistical uncertainties



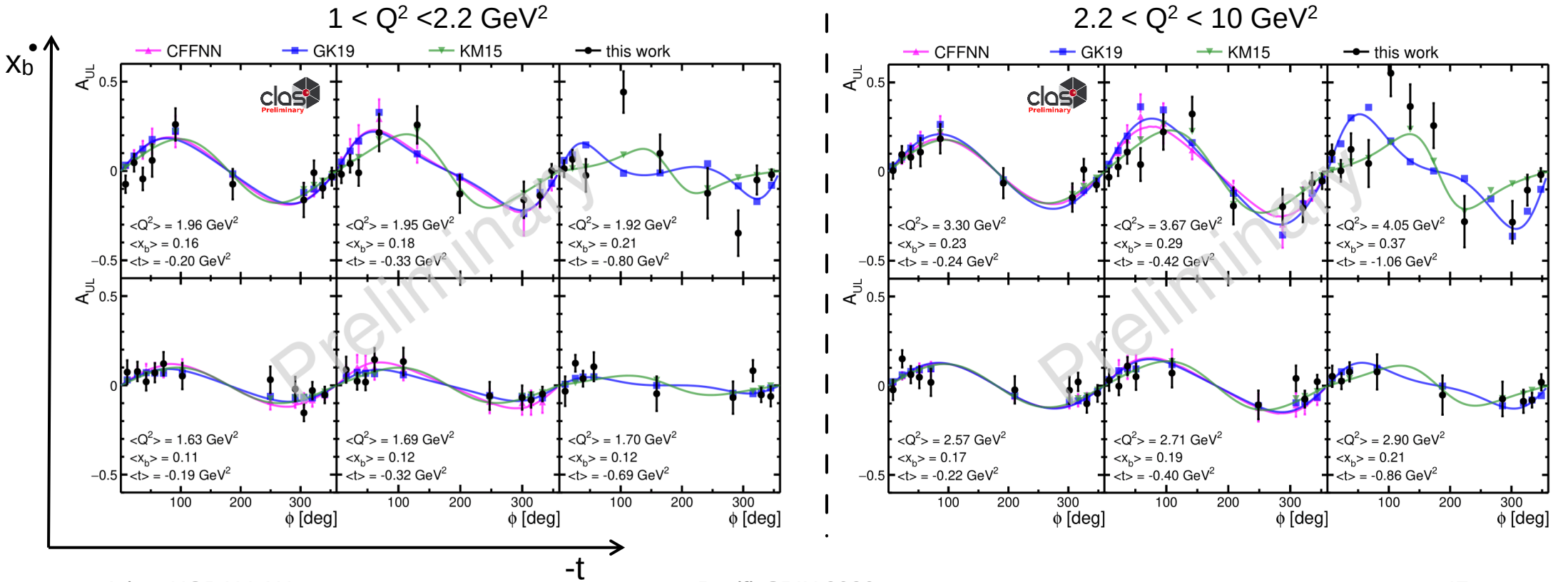
Comparison to models

- In the next slides the asymmetries are compared to models from the Partons and Gepard libraries
- Three models/fits are compared:
  - KM15 implemented in Gepard
  - GK19 implemented in Partons
  - CFFNN, 2019 CFF fit with a neural network parametrisation implemented in Partons. The comparison is restricted to bins with $-t/Q^2 < 0.2$, where the fit is constrained
- The model points are computed at the average kinematics of each ϕ bin, and over 100 ϕ points at the average kinematics of the Q^2, x_b, t bin to have a continuous line.
-

Thanks to K. Kumerički and P. Sznajder for their help !

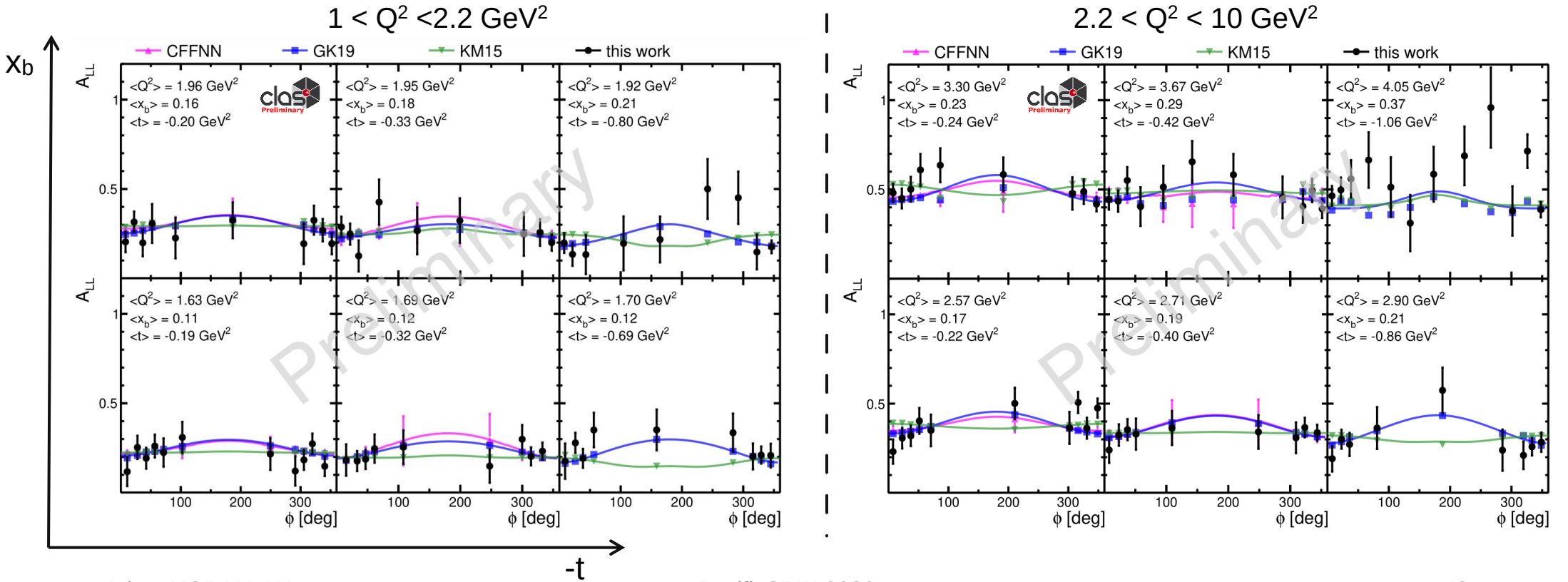
Comparison to models, TSA

- The model points are computed at the average kinematics of each specific phi bin, and the model line is computed at the average kinematics of the whole Q^2, x_b, t bin



Comparison to models, DSA

- The model points are computed at the average kinematics of each specific phi bin, and the model line is computed at the average kinematics of the whole Q^2, x_b, t bin



- First time CLAS12 uses a polarized target!
- Target polarization from analysis of elastic events:
  - $24 \pm 4\%$ for the positively polarized target,
  - $17 \pm 5\%$ for the negatively polarized target

All results use a third of the accumulated data, from the summer of 2022.

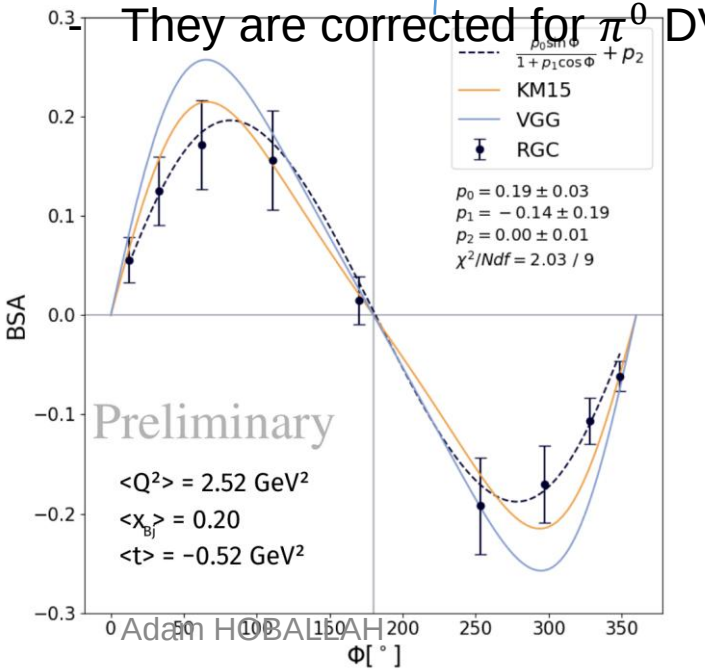
The remainder of the dataset is being analyzed now!

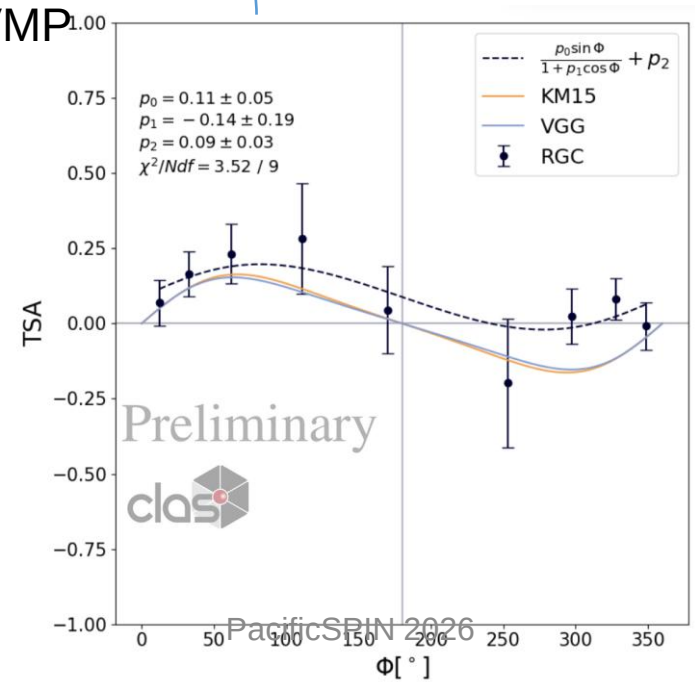
Asymmetries on the proton:

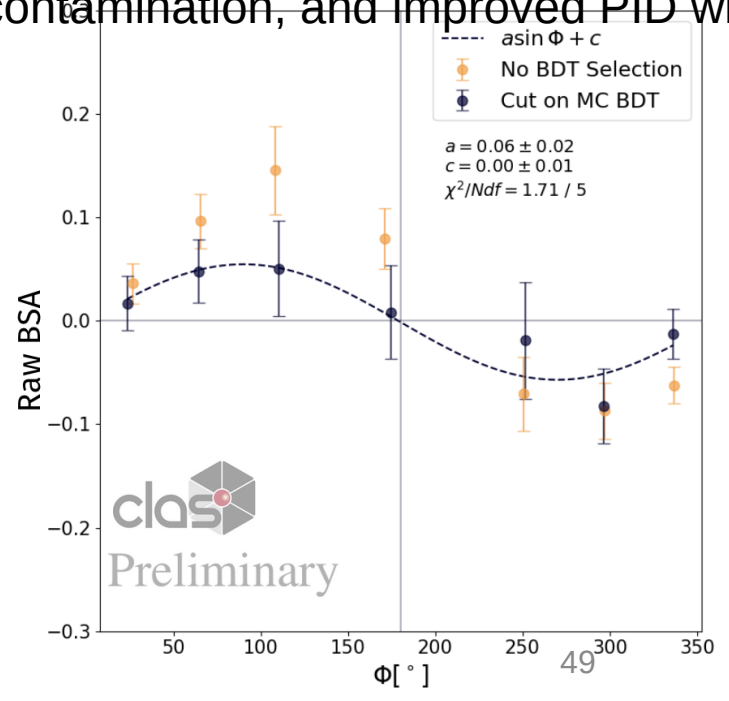
- BSA is for **bound protons in ND_3**
- TSA is for protons in **D** only, shape/shift is under investigation
- They are corrected for π^0 DVMP

BSA on the neutron:

- BSA is for **bound neutrons in ND_3**
- Not corrected for π^0 DVMP
- Comparing standard PID with proton contamination, and improved PID with

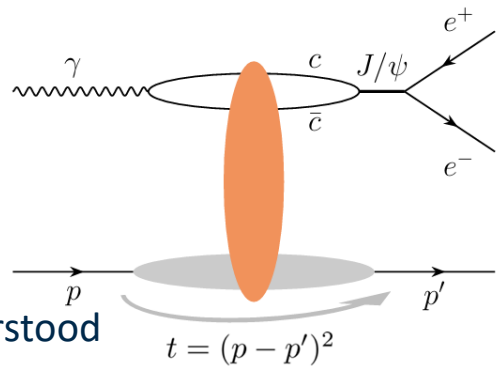






Near-threshold J/ψ photoproduction: gluonic GPDs

Phys. Rev. D 106, 086004, 2022 (Holographic QCD)
Phys. Rev. D 103, 096010, 2021 (GPDs)



- J/ψ Photoproduction explained either through Holographic QCD or GPD models
- GPD models: QCD factorization in terms of gluon GPDs is valid in the threshold region
  - Probe the gluonic Gravitational Form Factors of the proton: gluon contributions to mass and spin and internal forces.
  - However: open-charm meson channels and potential pentaquark production must understood
- Differential cross section $\frac{d\sigma}{dt} = \frac{\alpha_{\rm EM} e_Q^2}{4(W^2 - M_N^2)^2} \frac{(16\pi\alpha_S)^2}{3M_V^3} |\psi_{\rm NR}(0)|^2 |G(t,\xi)|^2$ expressed in terms of gluon GPDs
- With $G(t,\xi) = \frac{1}{2\xi}\int_{-1}^{1} {\rm d}x \mathcal{A}(x,\xi) F_g(x,\xi,t)$. Expanding the hard kernel $\mathcal{A}(x,\xi)$ in x having $\xi \sim 1$

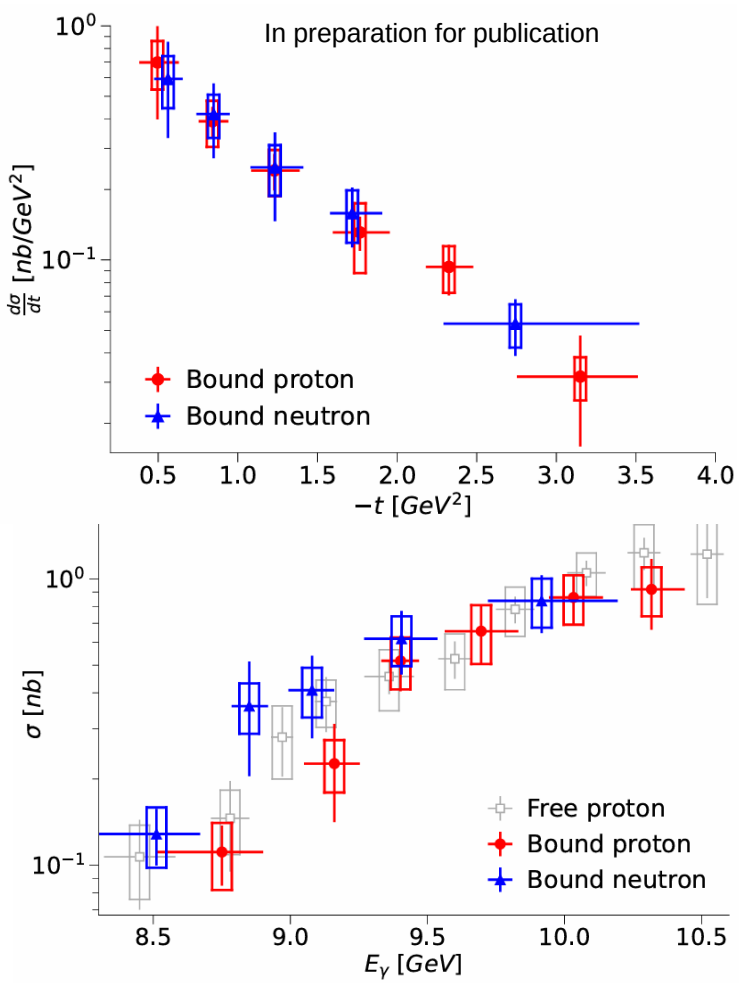
$$G(t,\xi) = \frac{1}{2\xi^2 (\bar{P}^+)^2} \langle P'|T_g^{++}|P\rangle$$

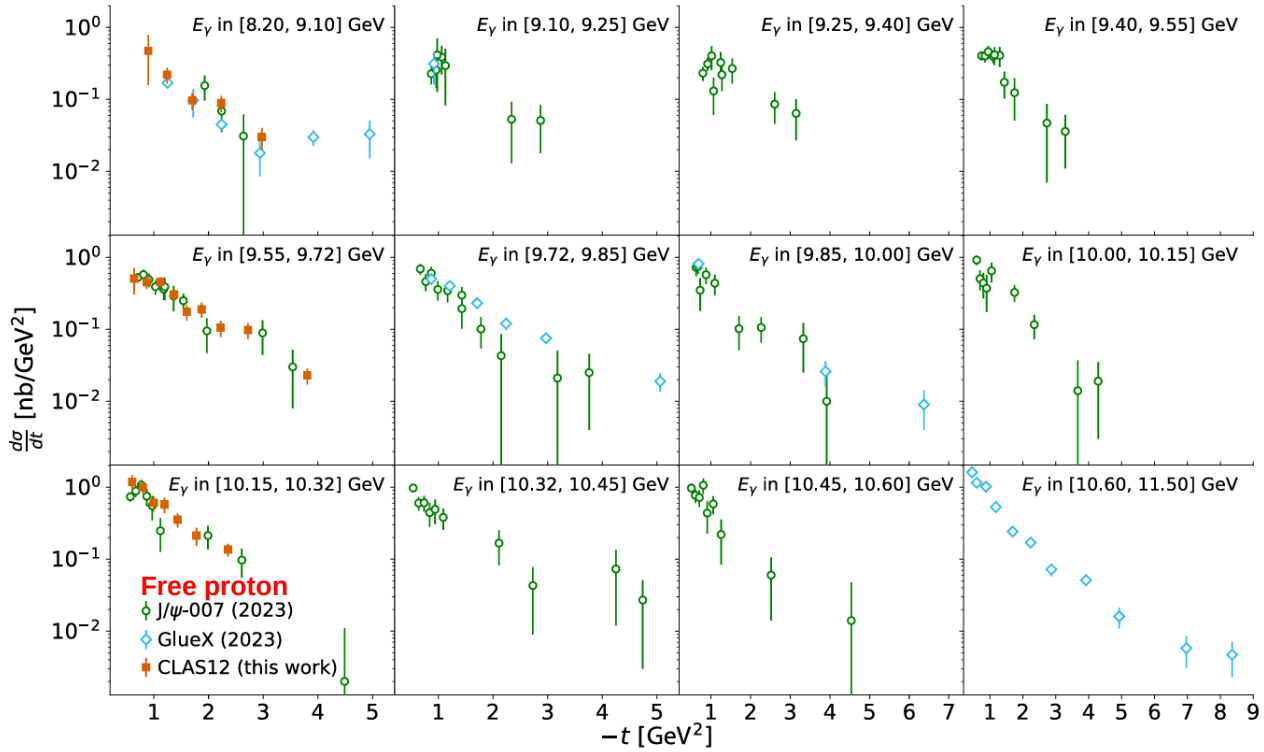
- Rewrite the cross section in terms of the GFFs encoded in the matrix element of the gluon EMT

$$\langle P'|T_{q,g}^{\mu\nu}|P\rangle = \bar{u}(P')\left[A_{q,g}(t)\gamma^{(\mu}\bar{P}^{\nu)} + B_{q,g}(t)\frac{\bar{P}^{(\mu} i\sigma^{\nu)\alpha}\Delta_\alpha}{2M_N} + C_{q,g}(t)\frac{\Delta^\mu\Delta^\nu - g^{\mu\nu}\Delta^2}{M_N} + \bar{C}_{q,g}(t) M_N g^{\mu\nu}\right] u(P)$$

Near-threshold J/ψ photoproduction: CLAS12 results

PHYSICAL REVIEW C 113,065203 (2026)



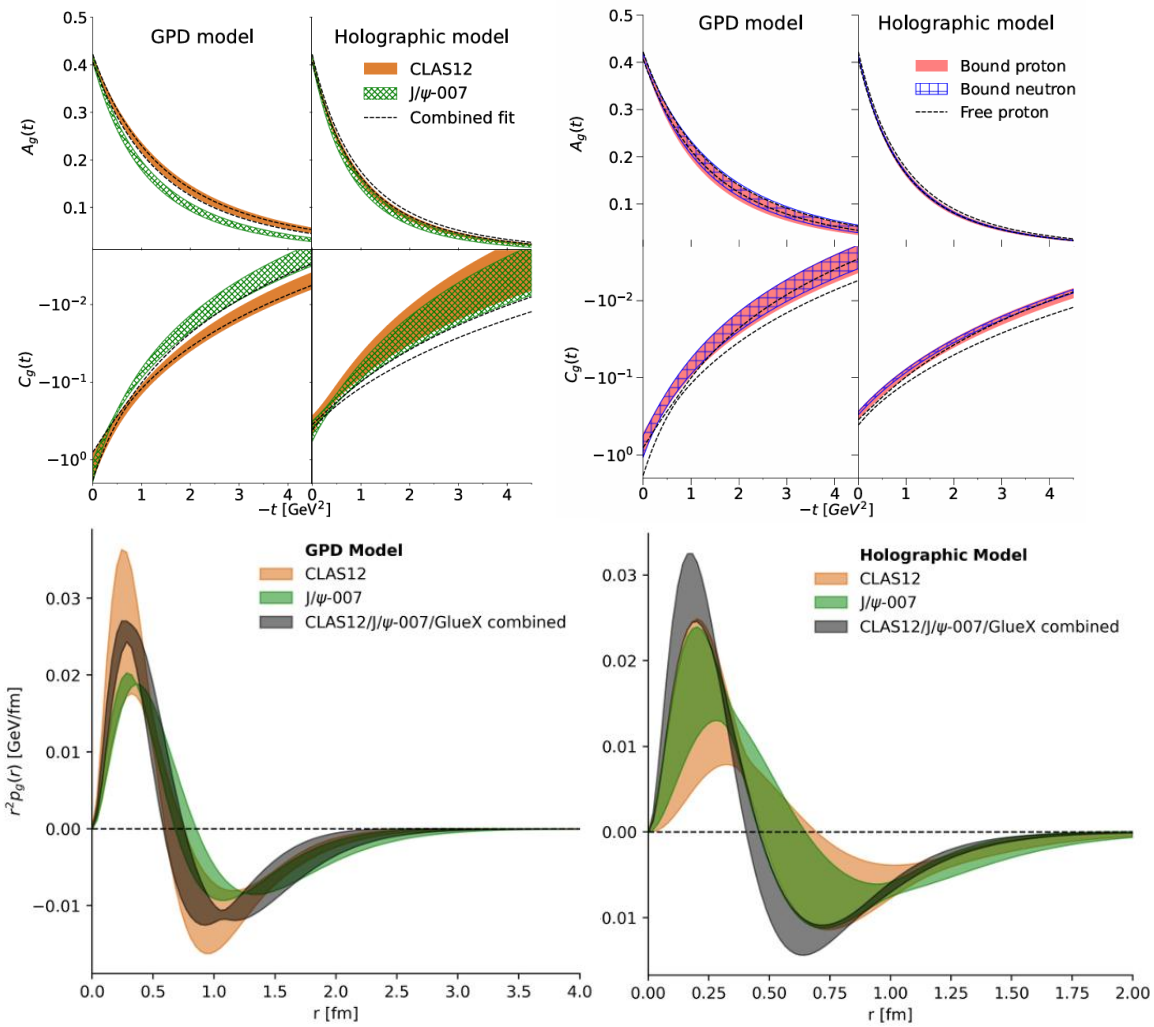


Near-threshold J/ψ photoproduction: CLAS12 results

- Extraction of mass and scaler radii from slopes of the GFFs

Radius	Target	VMD	GPD	Holo.
Mass [fm]	Bound Proton	0.48±0.08	0.83 ± 0.11	0.67 ± 0.01
	Bound Neutron	0.48±0.07	0.83 ± 0.10	0.66 ± 0.01
	Bound Nucleon	0.48±0.05	0.81 ± 0.08	0.67 ± 0.01
	Free Proton	0.52±0.02	1.00 ± 0.17	0.70 ± 0.02
Scalar [fm]	Bound Proton	N/A	1.31 ± 0.20	0.92 ± 0.04
	Bound Neutron	N/A	1.31 ± 0.18	0.90 ± 0.01
	Bound Nucleon	N/A	1.28 ± 0.15	0.91 ± 0.02
	Free Proton	N/A	1.64 ± 0.31	0.99 ± 0.03

- And a glimps on the gluon contribution to the internal pressure of the proton
  - Fourier transform of $C_g(t)$



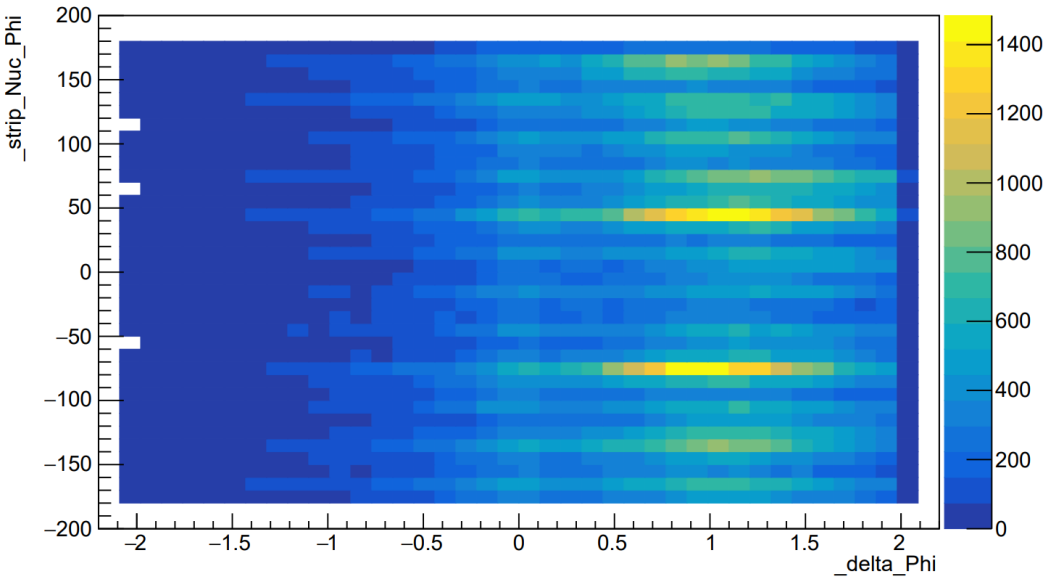
- Published:
  - TCS **Phys. Rev. Lett. 127, 262501 (2021)**
  - DVCS **Phys. Rev. Lett. 130 (21) 211902 (2023)**
  - nDVCS **Phys. Rev. Lett. 133, 211903 (2024)**
  - DV π^0 P **Phys. Lett. B 849 (2024) 138459**
  - J/ψ production off proton **Phys.Rev.C 113 (2026) 6, 065203** (gluon GPDs)
  - hard exclusive π+ electro-production off protons **Phys.Lett.B 839 (2023) 137761 (chiral odd GPDs)**
  - pi-Delta++ electroproduction **Phys. Rev. Lett. 131, 021901 (2023) (transition GPDs)**
- Analysis approved to be published soon:
  - pDVCS cross section from hydrogen (S. Lee)
  - pDVCS from deuterium
  - pDVCS from hydrogen: improved selection using ML techniques; no proton detection, BSA (S. Alvarado)
  - J/ψ production off proton and neutron from deuterium (R. Tyson) (gluon GPDs)
- Analysis ongoing:
  - pDVCS from hydrogen: cross section improved selection using ML techniques; no proton detection (S. Alvarado)
  - Longitudinal target: BSA TSA (proton) and BSA (neutron) ND3 (N. Pilleux)
  - Longitudinal target: BSA TSA DSA (proton) NH3 (S. Polcher)
  - Sullivan DVCS: BSA (https://agenda.infn.it/event/47074/contributions/289139/) (E. Ferrand)
  - Phi electroproduction off proton (M. Ronayette)
  - DVCS at multiple beam energies (Yijie Wang)
  - Pi0 cross section (https://agenda.infn.it/event/47074/contributions/289135/) (I. Korover)
  - phi cross section (B. Singh)
  - pi+pi- BSA (T. Hayward)

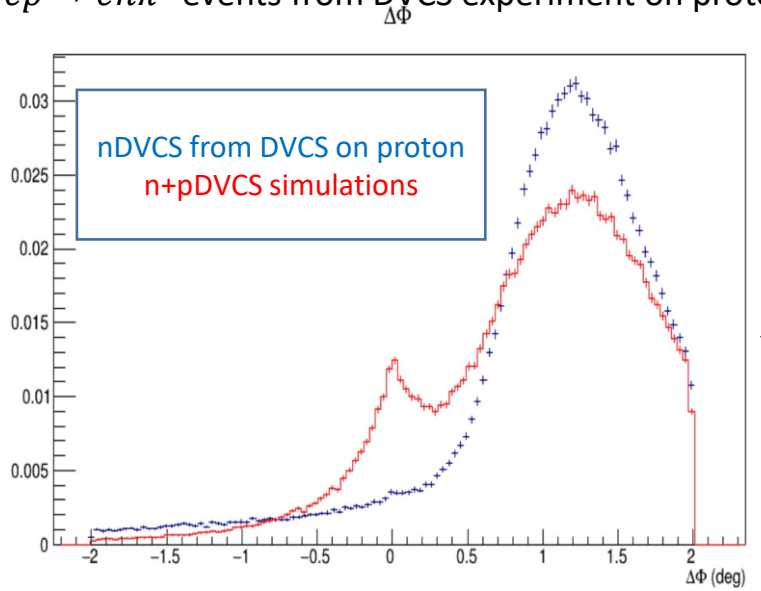


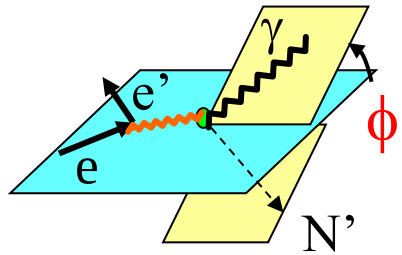
Analysis details

Improving the neutron selection with ML techniques

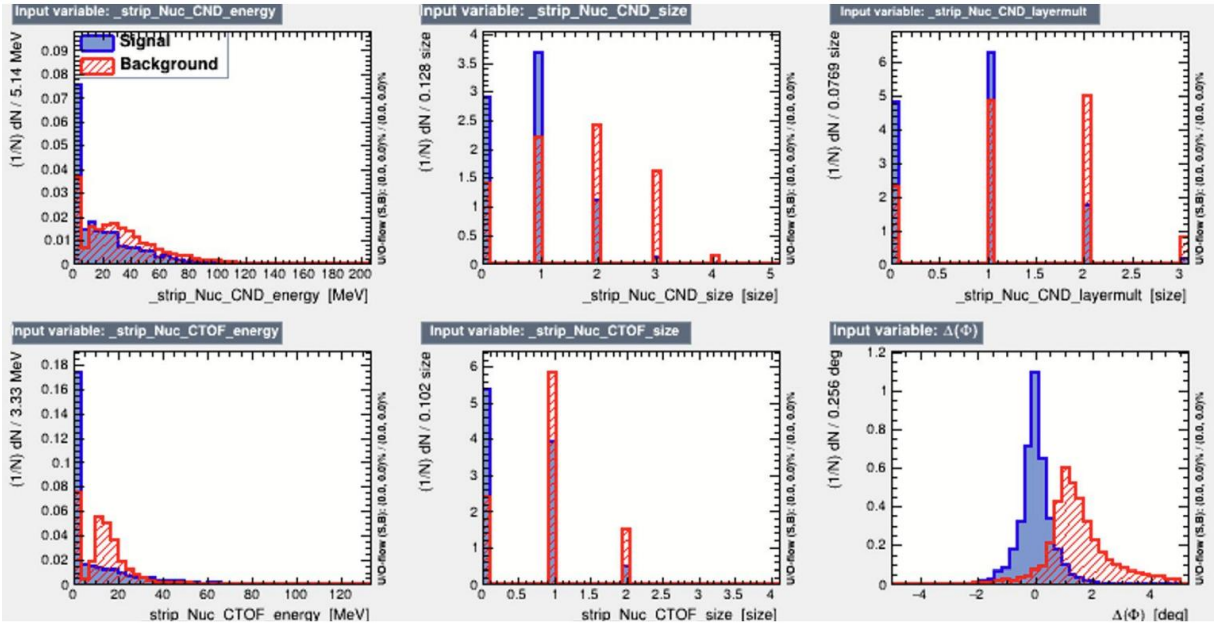
- The tracking of the CVT is neither 100% efficient nor uniform
- In the dead regions of the CVT protons have no associated track and thus can be misidentified as neutrons
- Protons roughly account for more than >40% contamination in the “nDVCS” signal sample Current approach, based on Machine Learning & Multi-Variate Algorithms:
  - We reconstruct nDVCS from DVCS experiment on proton requiring neutron PID : selected neutron are misidentified protons
  - We use this sample to determine the characteristics of fake neutrons in low- and high-level reconstructed variables
  - Based on those characteristics we subtract the fake neutrons contamination from nDVCS
  - As a « signal » sample in the training of the ML we use $ep \rightarrow en\pi^+$events from DVCS experiment on proton

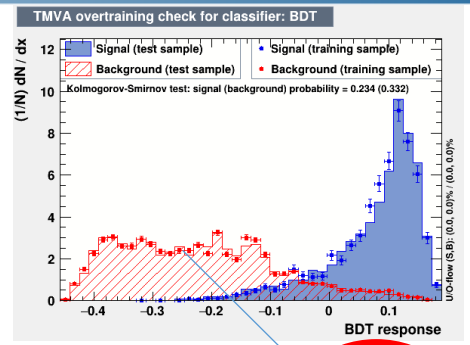


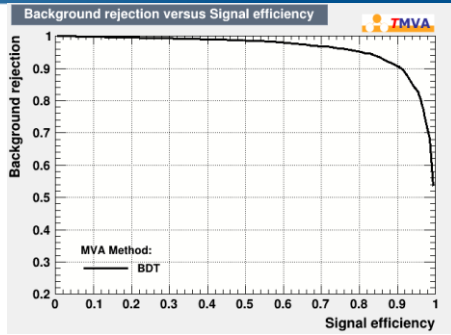


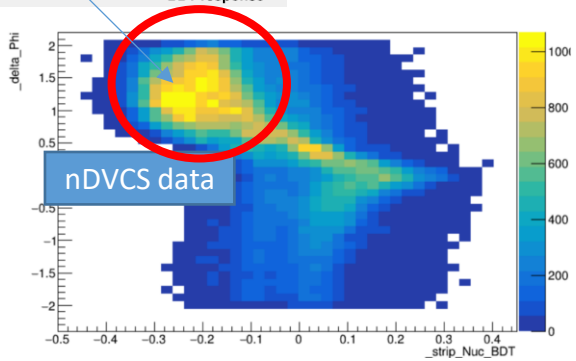


Improving the neutron selection with ML techniques

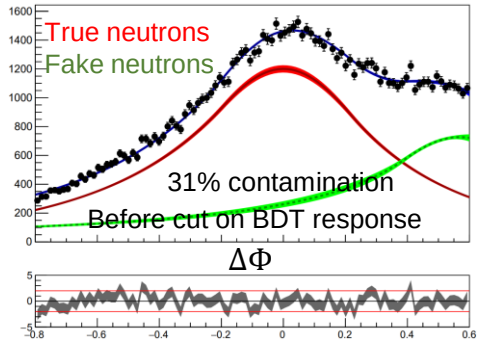


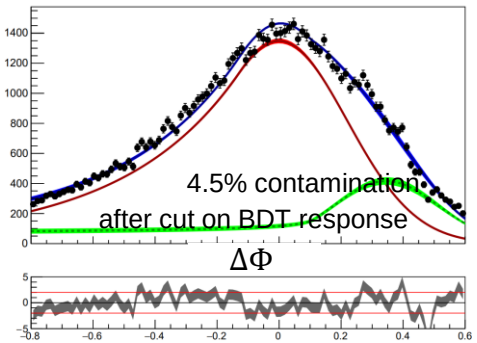






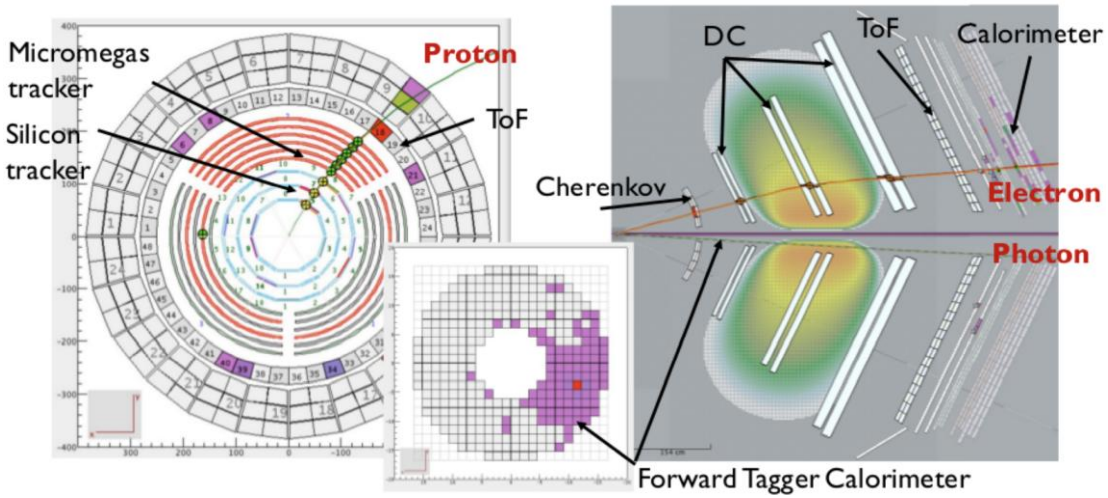
- Using detector variables (CTOF and CND) and one exclusivity variable (ΔΦ)
- Directly trained on data
- Better optimization of signal to background ratio than straight cuts
- Few percent irreducible contamination corrected for in the final BSA





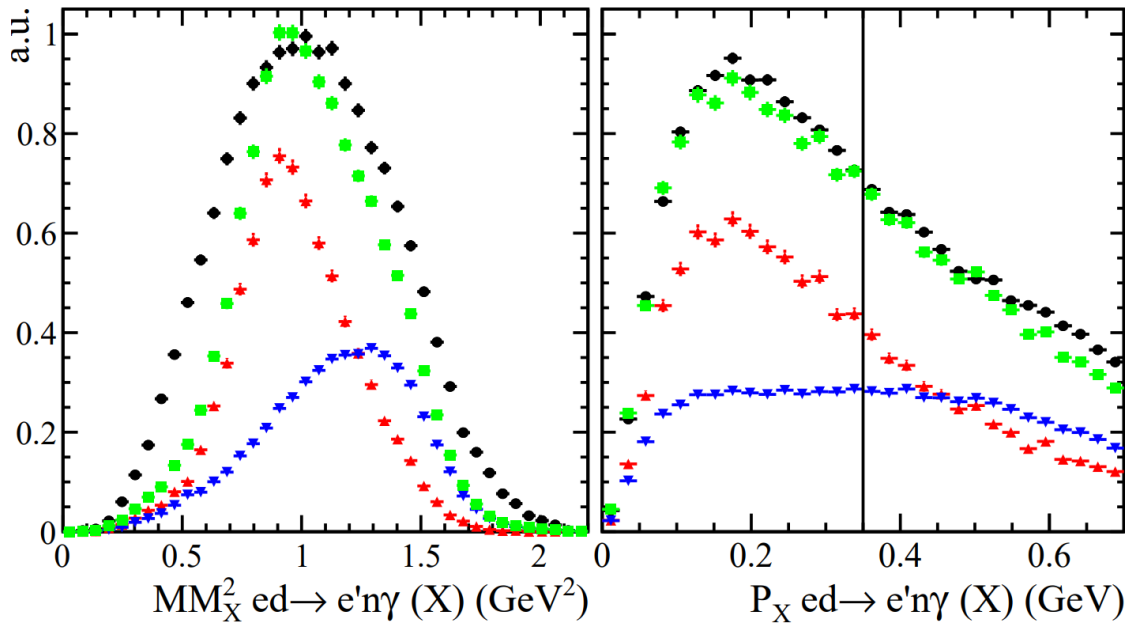
CLAS12: DVCS with an unpolarized deuterium target

- A 10.6/10.4/10.2 GeV electron beam
  - With an average polarization of 86%
  - Scattering off an unpolarized Liquid Deuterium target of 5 cm length
- The exclusivity of the event is insured by:
  - Electron detection: Cerenkov detector, drift chambers and electromagnetic calorimeter
  - Photon detection: sampling calorimeter or a small PbWO4-calorimeter close to the beamline
  - Proton detection: Silicon and Micromegas detector OR Neutron detection: Central Neutron Detector
- For Neutron Detection:
  - Machine Learning techniques are applied to improve the Identification and reduce charged particle contamination



CLAS12: DVCS with an unpolarized deuterium target

- The nDVCS (pDVCS) final state is selected with the following exclusivity criteria: (N:nucleon)
  - Missing mass
    - e d → e N γ X
    - e N → e N γ X
    - e N → e N X
  - Missing momentum
    - e d → e N γ X
  - ΔΦ, Δt, θ(γ,X)
    - Difference between two ways of calculating Φ and t
    - Cone angle between measured and reconstructed photon



nDVCS simulation

π^0 simulation

Sum of simulations

Data with π^0 contamination

π^0 background contamination is estimated using simulations

π^0 background subtraction

- Subtraction using simulations of the background channel
  - Monte Carlo simulations:
    - GPD-based event generator for DVCS/pi0 on deuterium
    - DVCS amplitude calculated according to the BKM formalism
    - Fermi-motion distribution evaluated according to Paris potential

1. Estimate the ratio of partially reconstructed eN π^0(1 photon) decay to fully reconstructed eN π^0 decays in MC
2. This is done for each kinematic bin to minimize MC model dependence
3. Multiply this ratio by the number of reconstructed eN π^0 in data to get the number of eN π^0(1 photon) in data
4. Subtract this number from DVCS reconstructed decays in data per each kinematical bin

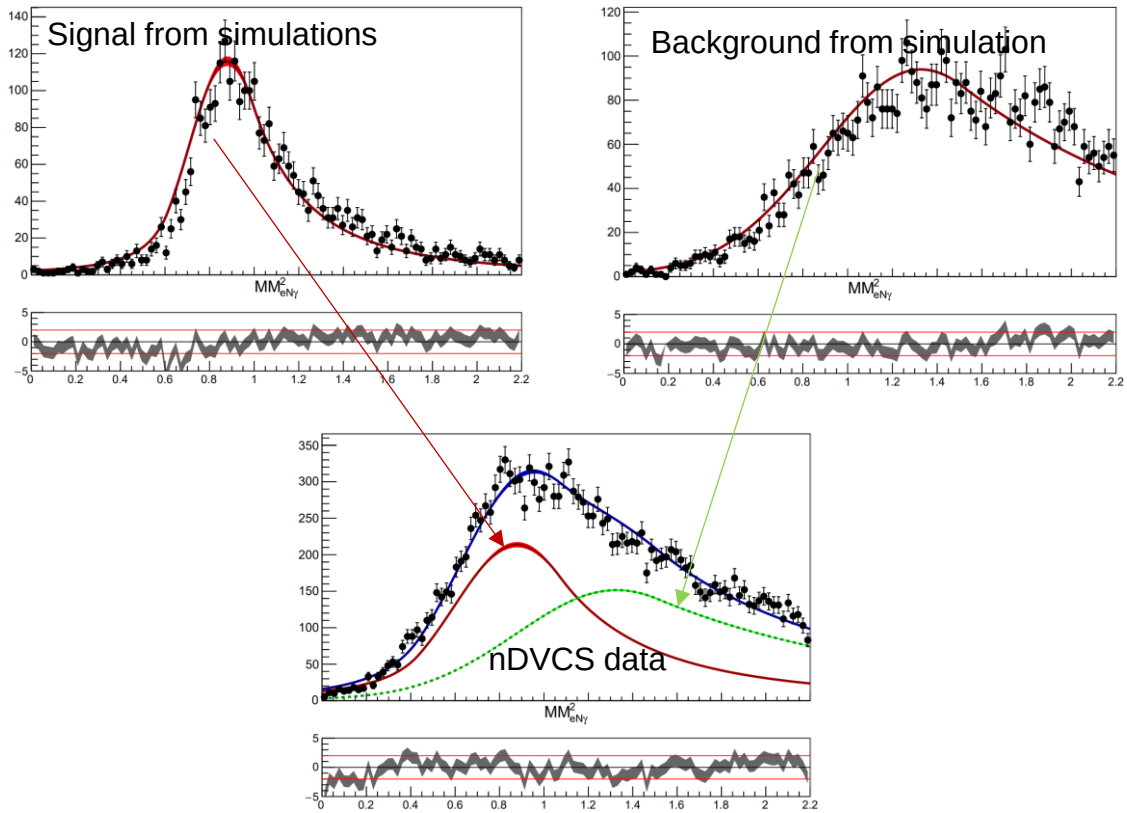
$$\text{Simulations: R} = \frac{\text{N}\left(eN\pi^0_{1\gamma}\right)}{N(eN\pi^0)}$$

$$\text{Data: } N\left(eN\pi^0_{1\gamma}\right) = R * N\left(eN\pi^0\right)$$

$$N(DVCS) = N(DVCS_{recon}) - N(eN\pi^0_{1\gamma})$$

- π^0 background subtraction is also performed by statistical unfolding of contribution to the missing mass spectrum

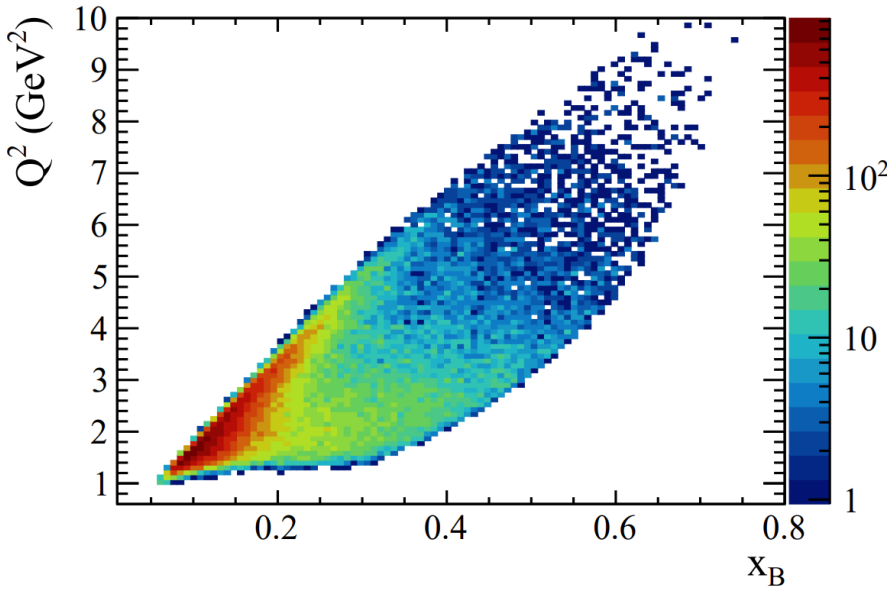
M. Pivk and F.R. Le Diberder, NIMA 555 1 2005



The difference between the estimations of background from both methods is considered as a systematic

CLAS12: nDVCS with an unpolarized deuterium target

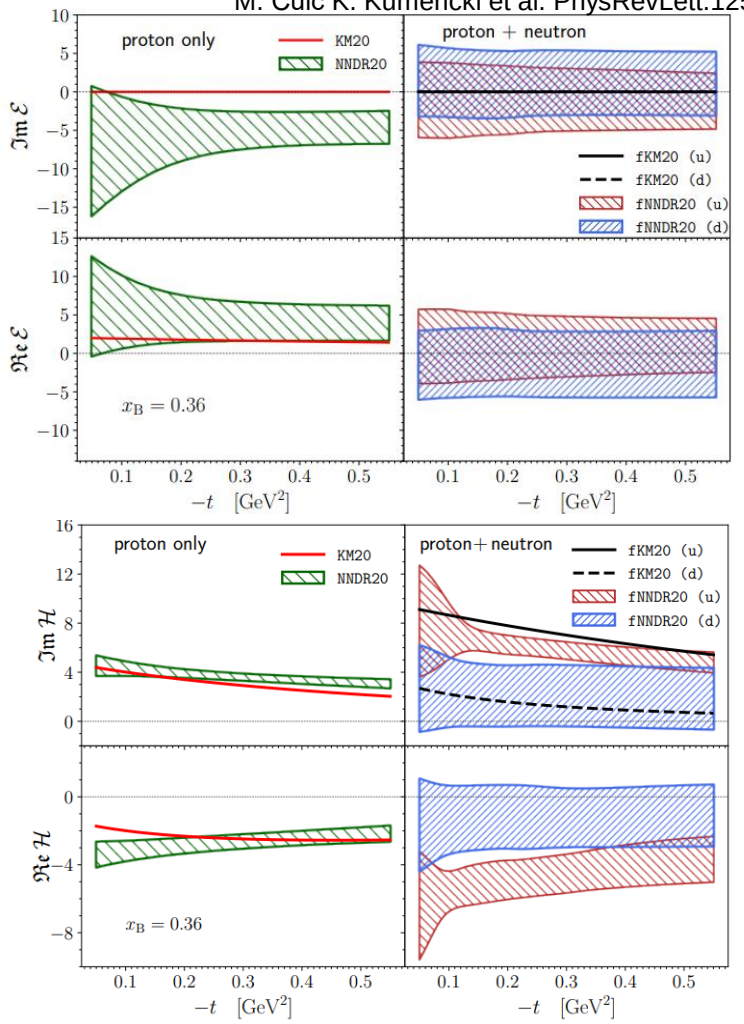
- Observation of positive BSA for nDVCS
- Systematic errors include:
  - Error due to beam polarization
  - Error due to selection cuts
  - Error due to residual proton contamination
  - Error due to merging of data sets with different energies
- Statistics is expected to double with remaining schedualed beam time and improvements with reconstruction software



Previously on CFF extraction and flavor separation!

- Use of Neural Networks (NN) to perform a model-independent CFF evaluations
- Input are measurements of spin-dependent observables and cross section values
  - Proton and neutron data from Jlab (clas6 and Hall A)
- The presence of CLAS6 neutron data allows a flavor separation
  - Up and down contributions to CFF H separated
  - CFF E flavors are not separated, a significant sign ambiguity remains

M. Čuić K. Kumericki et al. PhysRevLett.125.232005





Perspective

More on DVCS at CLAS12

- Deuteron DVCS
  - Physics observable to extract is Beam Spin Asymmetry (BSA)

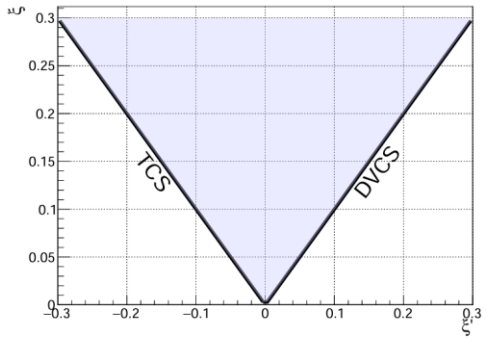
$$\Delta\sigma_{LU} \sim \sin(\phi)\,\Im\left\{\frac{2G_1\boldsymbol{H_1} + (G_1 - \tau G_3)(\boldsymbol{H_1} - 2\tau\boldsymbol{H_3}) + \frac{2}{3}\tau G_3\boldsymbol{H_5}}{2G_1^2 + (G_1 - 2\tau G_3)^2}\right\}$$

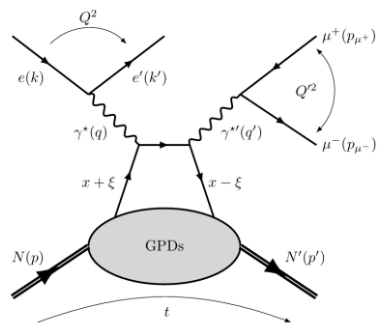
  - Spin 1: 9 GPDs for each quark flavor
    - BSA of DVCS off deuterium is sensitive to 3 of them

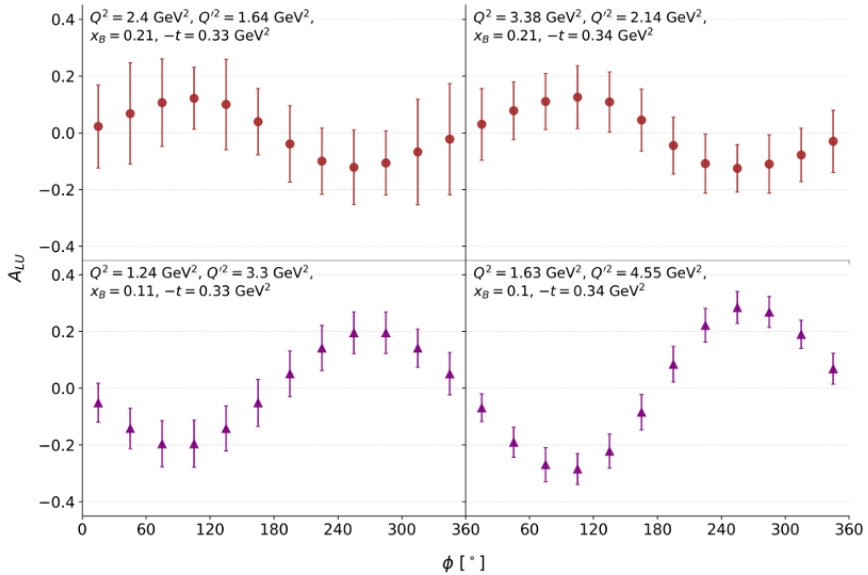
Beyond DVCS: Double DVCS with μCLAS12

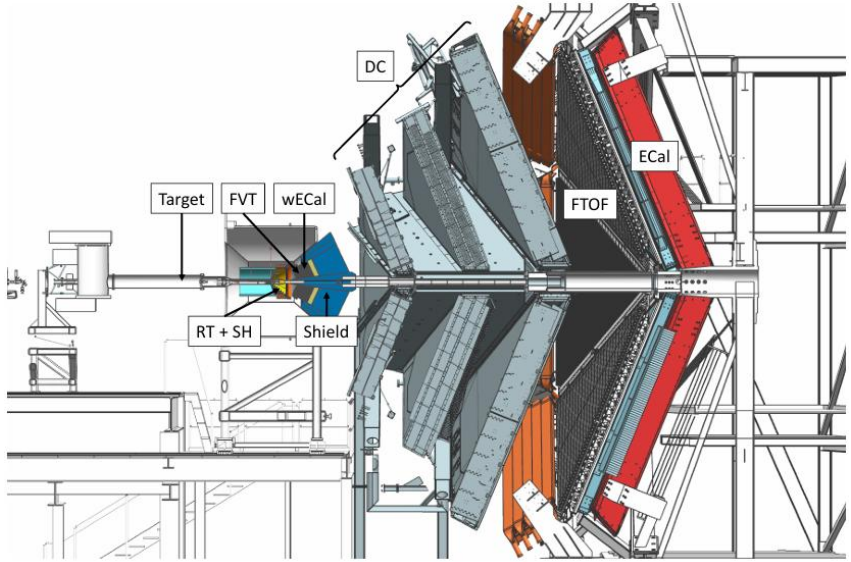
Phys. Rev. C **111**, 065205 (2025)
arXiv:2605.11690

- Thanks to the virtuality of the final photon, Q'2, DDVCS allows a unique direct access to GPDs at x ≠ ±Xi,
- Experimental challenges:
  - Small cross section (300 times less than DVCS)
  - Need to detect muons
- CLAS12 upgrade:
  - "µCLAS12" for DDVCS and J/ψ
  - ep→e'p'µ+µ- at L~1037 cm-2s-1
  - New tracker, calorimeter, shielding









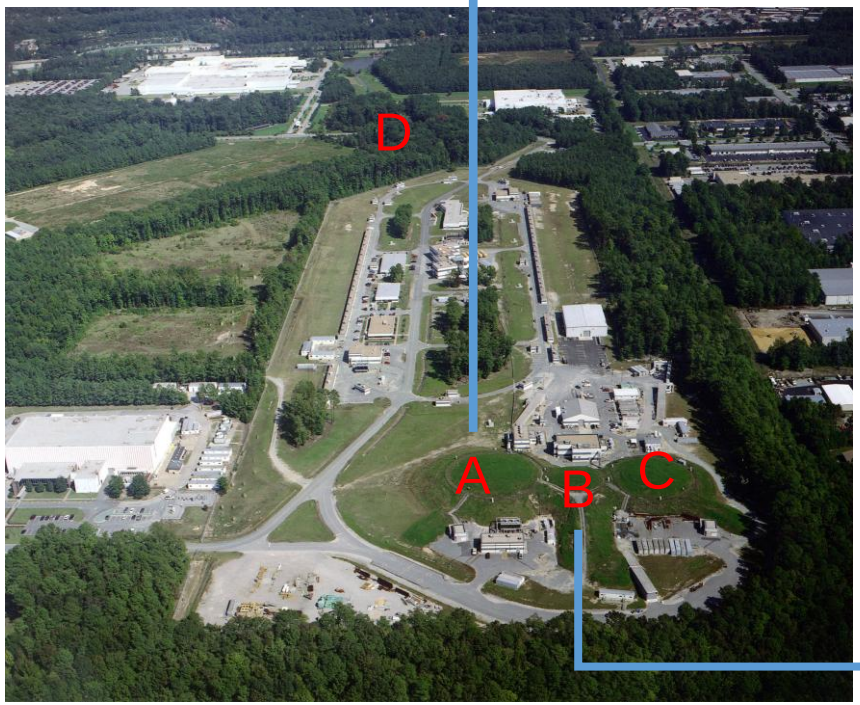


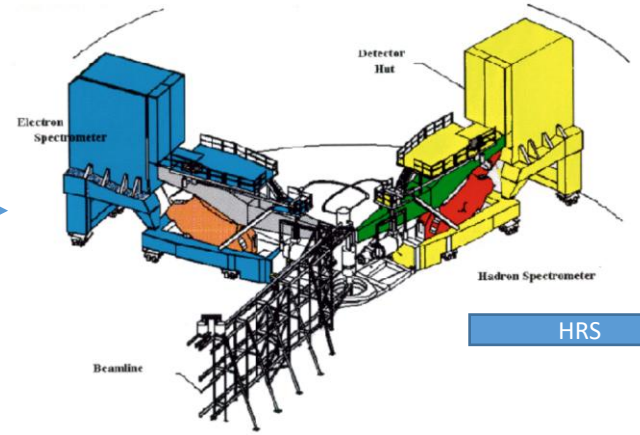
Other

The CEBAF at Jefferson Laboratory

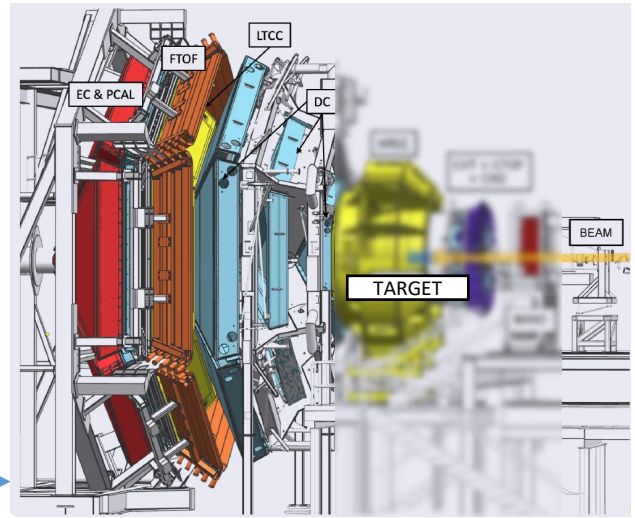
Continuos Electron Beam Accelerator Facility

- Up to 12 GeV electrons
- Two anti-parallel linacs, with recirculating arcs on both ends
- 4 experimental halls





HRS

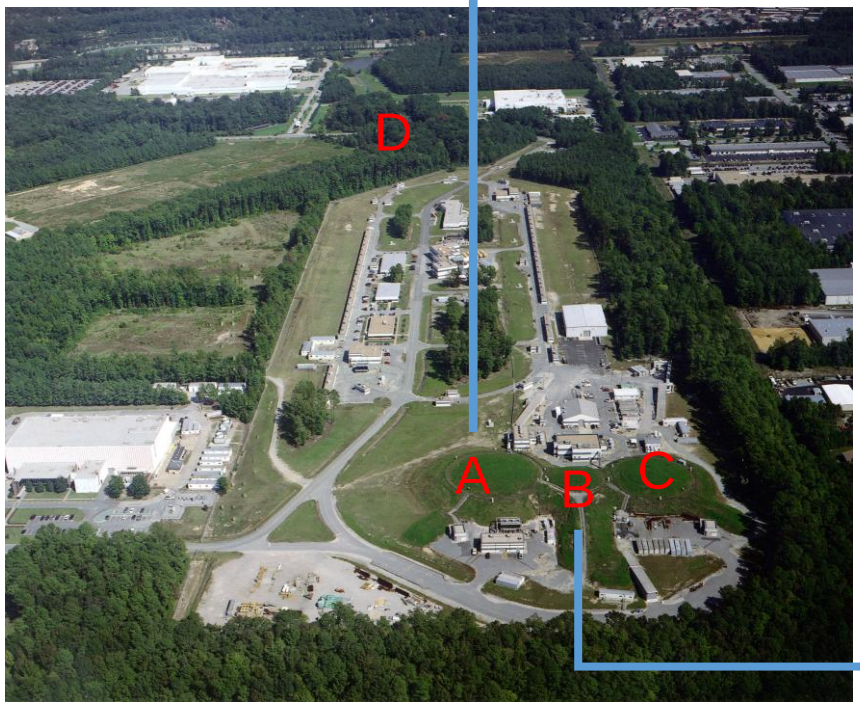


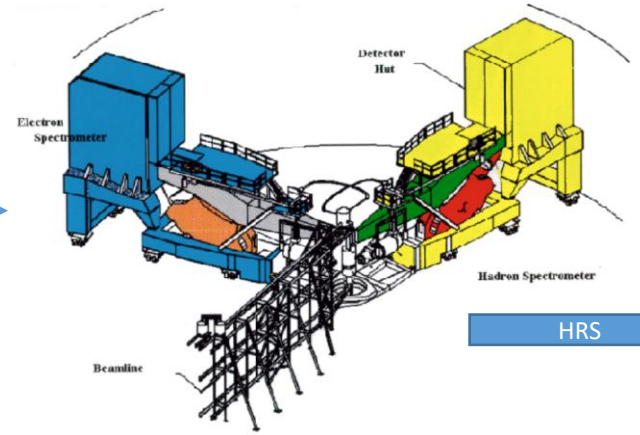
CLAS

The CEBAF at Jefferson Laboratory

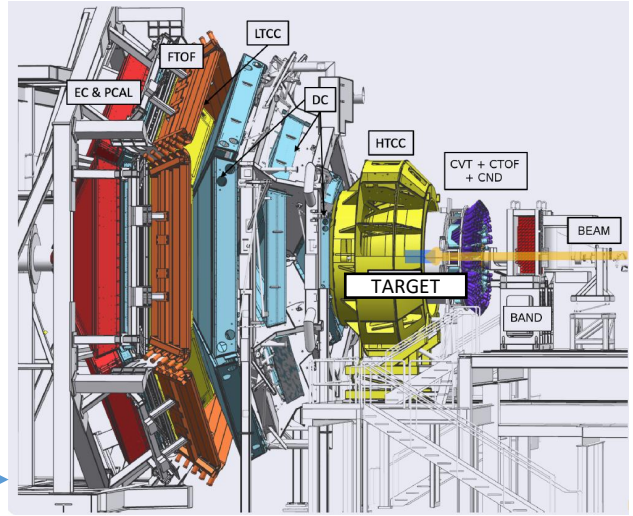
Continuos Electron Beam Accelerator Facility

- Up to 12 GeV electrons
- Two anti-parallel linacs, with recirculating arcs on both ends
- 4 experimental halls





HRS



CLAS12

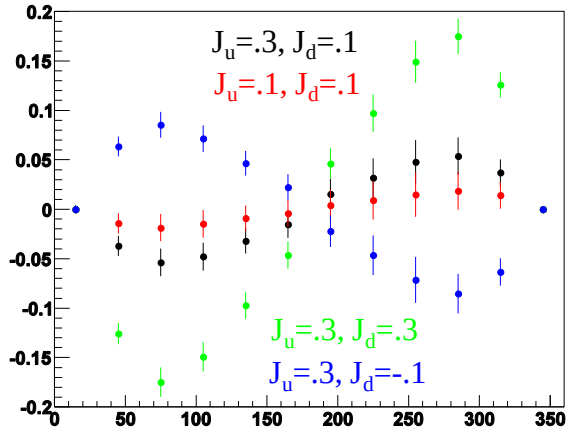
The GPD E: a missing piece in the puzzle

- **GPD E, one of the least constrained GPD**
- **DVCS with an unpolarized deuterium target :**
  - Scattering off neutron (nDVCS): GPD **E**
    - Determination of Ji sum rule
    - A step closer to being model independent
  - Scattering off proton (pDVCS): GPD **H**
    - Quantify medium effects: essential for the extraction of BSA of a "free" neutron (de-convoluting medium effect via comparison with DVCS on hydrogen target)
- To get a clear understanding of the GPD E: the BSA for nDVCS is
  - complementary to the TSA for pDVCS on transverse target, aiming at *E*
  - depends strongly on the kinematics → wide coverage needed
  - is smaller than for pDVCS → more beam time needed to achieve reasonable statistics

Different contributions from F_1 and F_2 for the different nucleons

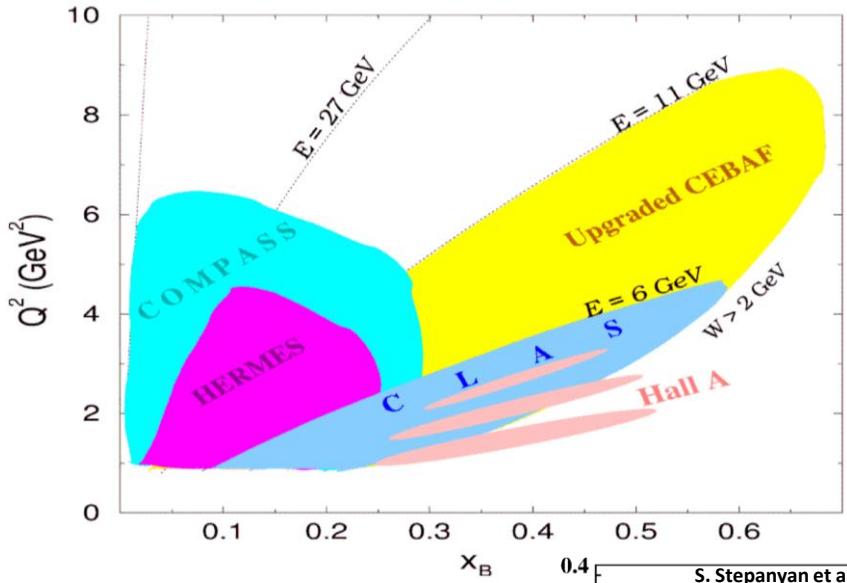
Observable	Proton	Neutron
$\Delta\sigma_{LU}$	$\Im\{\boldsymbol{H_p}, \widetilde{H}_p, E_p\}$	$\Im\{H_n, \widetilde{H}_n, \boldsymbol{E_n}\}$
$\Delta\sigma_{UL}$	$\Im\{\boldsymbol{H_p}, \boldsymbol{\widetilde{H}_p}\}$	$\Im\{\boldsymbol{H_n}, E_n\}$
$\Delta\sigma_{LL}$	$\Re\{\boldsymbol{H_p}, \boldsymbol{\widetilde{H}_p}\}$	$\Re\{\boldsymbol{H_n}, E_n\}$
$\Delta\sigma_{UT}$	$\Im\{\boldsymbol{H_p}, \boldsymbol{E_p}\}$	$\Im\{\boldsymbol{H_n}\}$

Model predictions (VGG) for different values of quarks' angular momentum



GPD-aimed experiments worldwide

- JLAB
  - Hall A: cross sections and beam-polarised cross section differences measurements
  - Hall B (CLAS/CLAS12): beam and target spin asymmetries + cross section measurements over large phase-space acceptance
  - Hall C (NPS): Spin-dependent observables + cross section measurements
- DESY
  - HERMES: low-x_b low-Q^2 moments of spin asymmetries measurements
  - ZEUS: cross section measurements
- CERN
  - COMPASS: low-x_b high-Q^2 cross section measurements



$ep \rightarrow epX$, from CLAS data: First observation of DVCS-BH interference

